TECHNISCHE UNIVERSITÄT MÜNCHEN

TUM School of Life Sciences

Lehrstuhl für Analytische Lebensmittelchemie

Investigations of changes of the metallome and metabolome as a cause for neurodegeneration: Application of combines speciation and metabolomics techniques

Desiree Willkommen

Vollständiger Abdruck der von der TUM School of Life Sciences der Technischen Universität München zur Erlangung des akademischen Grades eines

Doktors der Naturwissenschaften

genehmigten Dissertation.

Vorsitzender: Prof. Dr. Erwin Grill

Prüfer der Dissertation:

1. apl. Prof. Dr. Philippe Schmitt-Kopplin

2. Prof. Dr. Wilhelm Windisch

Die Dissertation wurde am 18.01.2021 bei der Technischen Universität München eingereicht und durch die TUM School of Life Sciences am 19.06.2021 angenommen.

"Der aus Büchern erworbene Reichtum fremder Erfahrung heißt Gelehrsamkeit.

Eigene Erfahrung ist Weisheit."

Gotthold Ephraim Lessing

Danksagung

Diese Arbeit wäre ohne die Hilfe und Unterstützung vieler wichtiger Personen nicht möglich gewesen.

Zu aller erst möchte ich mich bei meinem Doktorvater Prof. Dr. Bernhard Michalke bedanken für die unglaubliche Möglichkeit mich mit diesem spannenden Forschungsgebiet beschäftigen zu dürfen. Ihre stetige und wertvolle Betreuung, sowie die Menge an Wissen, die Sie mir vermittelt haben, haben mich während der gesamten Arbeit motiviert.

Bei Prof. Philippe Schmitt-Kopplin möchte ich mich für die Aufnahme in diese tolle Arbeitsgruppe bedanken, für die gute Betreuung, die Ideen und Anregungen während der Thesis Committees und die fröhliche, gemeinschaftliche Atmosphäre, die Sie kreiert haben.

Ein riesengroßer Dank richtet sich an Marianna. Dein unglaubliches statistisches Wissen hat mir immer geholfen. Diese Arbeit wäre ohne deine unermüdliche Mitarbeit und Unterstützung in sämtlichen statistischen Belangen nicht möglich gewesen.

Ebenfalls danken möchte ich Ali Sigaroudi, Univ.-Prof. Dr. Michael Schroeter, Prof. Dr. Uwe Fuhr und Malaz Gazzaz für die Bereitstellung der Proben, der Extraktion von Patientendaten und Ihre Unterstützung und Ratschläge beim Schreiben der Veröffentlichungen.

In unserer kleinen Arbeitsgruppe *Zentrale Analytik* möchte ich mich bei Bärbel, Heidi und Peter bedanken, die mich herzlich aufgenommen haben.

Als drittes Mitglied meines Thesis Committees möchte ich mich herzlich bei Prof. Dr. Tanja Schwerdtle bedanken. Deine engagierte Arbeitsweise wird mir weiterhin Vorbild sein.

Zusätzlich möchte ich mich bei Basem, Constanze, Franco, Sara und allen BGC´lern für Ihre Unterstützung bei verschiedenen Projekten, die angenehme Atmosphäre und die gemeinsame Zeit bedanken.

Mama, Papa, Juli. Danke, dass ihr mich auf dem Weg immer unterstützt und begleitet habt. Die Zeit mit euch hat mir die nötigen Auszeiten und das Durchatmen verschafft, die ich während dieser Zeit brauchte.

Ohne die Kraft und Unterstützung, die aufmunternden Worte an schweren Tagen und die immerwährende Fröhlichkeit meines Mannes Marcel wäre es sehr viel schwerer gewesen diese Arbeit abzuschließen. Du hast mich immer unterstützt, an mich geglaubt und mir die Kraft gegeben, diese Arbeit schlussendlich abzuschließen.

Summary

Parkinson´s disease is the second most common neurodegenerative disease. The incidence of Parkinson´s increases significantly with age which is why the importance especially raises in the aging society. The underlying mechanisms of the disease are not yet completely decoded; especially the initial phase with non-specific symptoms is of great interest in investigations.

In the following work, the goal was to identify disease-relevant changes in Parkinson´s patients compared to controls. In focus of the analyses were on the one hand essential trace elements and on the other hand metabolites. Finally, the systematically investigation was meant to establish a potential explanatory approach for development of Parkinson´s disease. The analyses were carried out in human cerebrospinal fluid. The concentration of the trace elements Cu, Fe, Mn, and Zn measured by ICP-MS, indicated insignificant changes. A detailed investigation of these trace elements was performed with species characterization by SEC-ICP-MS. This showed especially for Cu significant changes in size fractions. However, these results were not only considered separately, but also in relation to each other. Numerous unbalanced size ratios between the individual trace elements turned out. In particular the Cu amino acid fraction crystallized out to be extremely interesting. Furthermore, a Se-speciation as well as a speciation of the redox forms of Fe were carried out. Both studies indicated unspecific changes for the corresponding species. Due to the special position of the amino acid fraction in the results of SEC-ICP-MS, the amino acids were extensively investigated. When examining with AAA-direct method, an increase of serine was observed in comparison to the controls. Amino acid fractions were also analyzed for their content of Cu, Fe, Mg, Mn, Ni, Sr, and Zn by ICP-MS. In the process several differing concentrations in amino acid fractions could be measured. Since amino acids occur in the enantiomeric forms D and L, these have also been investigated by UPLC-QqTOF-MS. An increase in the D-alanine concentration was identified. In addition, a non-targeted study with FT-ICR-MS revealed changes in different metabolic pathways indicating increased oxidative stress and neuro-inflammation. The results of trace element-based and metabolic-based studies were subsequently analyzed using data integration to uncover connections between metallomics and metabolomics.

In summary, changes in Cu-amino acid-species, changes in amino acid balance and changes in metabolism could be demonstrated by these investigations. These changes suggest oxidative stress and neuroinflammation in Parkinson´s patients. The comparative analysis of Parkinson´s and control patients has proven to be a very effective examination method, since even smaller changes and disturbed size ratios of metal species can be detected.

Zusammenfassung

Die Erkrankung Parkinson ist die zweithäufigste neurodegenerative Krankheit. Die Inzidenz von Parkinson steigt mit dem Alter deutlich an und hat daher eine zunehmende Wichtigkeit in der alternden Gesellschaft. Die zugrundeliegenden Mechanismen der Krankheit sind noch nicht komplett entschlüsselt, v.a. die Anfangsphase mit unspezifischen Symptomen ist daher in Untersuchungen von großem Interesse.

Ziel der vorliegenden Arbeit war es krankheitsrelevante Änderungen von Parkinson-Patienten im Vergleich zu Kontroll-Patienten zu eruieren. Hierbei standen einerseits essentielle Spurenelemente und anderseits Verbindungen des Stoffwechsels im Fokus der Untersuchungen. Die systematische Untersuchung sollte letztendlich einen möglichen Erklärungsansatz für die Entwicklung der Parkinson Krankheit etablieren Die Analysen wurden in Human-Cerebrospinalflüssigkeit (Liquor) durchgeführt. Die Konzentration der Spurenelemente Cu, Fe, Mn und Zn, die mit Hilfe von ICP-MS gemessen wurden, zeigten keine signifikanten Änderungen des Konzentrationsprofiles an. Eine detaillierte Untersuchung dieser Spurenelemente erfolgte durch eine Speziescharakterisierung mit SEC-ICP-MS. Dabei zeigten sich v.a. bei Cu deutliche Änderungen der Größenfraktionen. Diese Ergebnisse wurden nicht nur gesondert voneinander betrachtet, sondern auch im Verhältnis zueinander. Dabei zeigten sich zahlreiche unausgewogene Größenverhältnisse zwischen den einzelnen Spurenelementen. Im speziellen kristallisierte sich die Cu-Aminosäure-Fraktion als besonders interessant heraus. Weiterhin wurden sowohl eine Se-Speziation, als auch eine Speziation der Redoxformen von Fe durchgeführt. Beide Untersuchungen zeigten nicht-spezifische Änderungen der entsprechenden Spezies an. Aufgrund der besonderen Stellung der Aminosäure-Fraktion bei den Ergebnissen der SEC-ICP-MS wurden die Aminosäuren umfassend untersucht. Bei der Untersuchung mit der Methode AAA-direct konnte eine Erhöhung von Serin im Vergleich zu den Kontrollen beobachtet werden. Fraktionen der Aminosäuren wurden außerdem mit Hilfe von ICP-MS auf ihren Gehalt an Cu, Fe, Mg, Mn, Ni, Sr und Zn untersucht. Dabei konnten sechs signifikant unterschiedliche Konzentrationen in unterschiedlichen Aminosäurefraktionen gemessen werden. Da Aminosäuren in den enantiomeren Formen D und L auftreten, wurden auch diese mit Hilfe von UPLC-QqTOF-MS untersucht. Es konnte ein Anstieg der D-Alanin Konzentration ermittelt werden. Zudem zeigte eine nicht-zielgerichtete Untersuchung mit FT-ICR-MS Änderungen in verschiedenen Stoffwechselwegen, welche auf erhöhten oxidativen Stress und Neuroinflammation hindeuten. Die Ergebnisse der Spurenelementbasierten und Stoffwechselbasierten Untersuchungen wurden anschließend anhand von Datenintegration untersucht, um Zusammenhänge zwischen *Metallomics* und *Metabolomics* aufzudecken.

Zusammenfassend konnten durch diese Untersuchungen Änderungen von Cu-Aminosäure-Spezies, Änderungen im Aminosäure-Haushalt und Änderungen im Stoffwechsel nachgewiesen werden. Diese Änderungen deuten auf oxidativen Stress und Neuroinflammation bei Parkinson-Patienten hin. Die vergleichende Analyse von Parkinson- und Kontroll-Patienten hat sich als sehr wirkungsvolle Untersuchungsmethode herausgestellt, da auch kleinere Änderungen und gestörte Größenverhältnisse von Metallspezies aufgedeckt werden können.

List of publications

The importance of speciation analysis in neurodegeneration research

B. Michalke, <u>D. Willkommen</u>, E. Drobyshev and N. Solovyev

TrAC Trends in Analytical Chemistry, 2018, 104: 160-170

DOI: https://doi.org/10.1016/j.trac.2017.08.008.

Species fractionation in a case-control study concerning Parkinson´s disease: Cu-amino acids discriminate CSF of PD from controls

<u>D. Willkommen</u>, M. Lucio, P. Schmitt-Kopplin, M. Gazzaz, M. Schroeter, A. Sigaroudi and B. Michalke

Journal of Trace Elements in Medicine and Biology, 2018, 49: 164-170.

DOI: https://doi.org/10.1016/j.jtemb.2018.01.005.

Manganese causes neurotoxic iron accumulation via translational repression of Amyloid Precursor Protein (APP) and H-Ferritin

V. Venkataramani, T. R. Doeppner, <u>D. Willkommen</u>, C. M. Cahill, Y. Xin, G. Ye, Y. Liu, A. Southon, A. Aron, H. Yu Au-Yeung, X. Huang, D. K. Lahiri, F. Wang, A. I. Bush, G. G. Wulf, P. Ströbel, B. Michalke, J. T. Rogers

Journal of Neurochemistry, 2018, 147(6):831-848.

DOI: https://doi.org/10.1111/jnc.14580

Metabolomic investigations in cerebrospinal fluid of Parkinson´s disease

<u>D. Willkommen</u>, M. Lucio, F. Moritz, S. Forcisi, B. Kanawati, K. S. Smirnov, M. Schroeter, A. Sigaroudi, P. Schmitt-Kopplin, B. Michalke

PLoS One, 2018; 13(12)

DOI: https://doi.org/10.1371/journal.pone.0208752

Iron Redox Speciation Method Using Capillary Electrophoresis coupled to Inductively Coupled Plasma Mass Spectrometry (CE-ICP-MS)

B. Michalke, <u>D. Willkommen</u>, V. Venkataramani

Frontiers in Chemistry, 2019; 7: 136.

DOI: https://doi.org/10.3389/fchem.2019.00136

Selenium speciation analysis in the cerebrospinal fluid of patients with Parkinson's disease

F. Maass, B. Michalke, <u>D. Willkommen</u>, C. Schulte, L. Tönges, M. Börger, I. Zerr, M. Bähr, P. Lingor

Journal of Trace Elements in Medicine and Biology, 2020, 126412.

DOI: https://doi.org/10.1016/j.jtemb.2019.126412

Assessment of copper, iron, zinc and manganese status and speciation in patients with Parkinson's disease: a pilot study in Russia

O. P. Ajsuvakova, A. A. Tinkov, <u>D. Willkommen</u>, A. A. Skalnaya, A. B. Danilov, A. A. Pilipovich, B. Michalke, A. V. Skalny, M. G. Skalnaya

Journal of Trace Elements in Medicine and Biology, 2020, 59:126423.

DOI: https://doi.org/10.1016/j.jtemb.2019.126423.

Integrative metabolomic and metallomic analysis in a case control cohort with Parkinson´s disease

M. Lucio, <u>D. Willkommen</u>, M. Schroeter, A. Sigaroudi, P. Schmitt-Kopplin, B. Michalke

Frontiers in Aging Neuroscience, 2019, 11, 331.

DOI: https://doi.org/10.3389/fnagi.2019.00331

Setup of Capillary Electrophoresis-Inductively Coupled Plasma Mass Spectrometry (CE-ICP-MS) for Quantification of Iron Redox Species (Fe(II), Fe(III))

B. Michalke, <u>D. Willkommen</u>, V. Venkataramani

Journal of Visualized Experiments, 2020, 159, e61055.

DOI: https://doi.org/10.3791/61055 (2020)

Poster and oral presentations

Speciation analysis in a case control study concerning Parkinson´s disease: Strong changes in correlations with Cu-binding species as possible marker. (poster)

Desiree Willkommen, Marianna Lucio, Phillippe Schmitt-Kopplin, Bernhard Michalke
at 32. Jahrestagung der GMS 2016, Berlin, Germany

Metallomics investigation in Parkinson´s disease. The importance of speciation analysis. (poster)

Desiree Willkommen, Marianna Lucio, Phillippe Schmitt-Kopplin, Bernhard Michalke
at 13th International Conference on Alzheimer's and Parkinson's Diseases, 2017, Vienna, Austria

Metals and metabolites in Cerebrospinal Fluid of Parkinson´s disease patients. (poster)

Desiree Willkommen, Marianna Lucio, Basem Kanawati, Sara Forcisi, Ali Sigaroudi, Michael Schroeter, Uwe Fuhr, Philippe Schmitt-Kopplin, Bernhard Michalke
at 33. Jahrestagung der GMS, 2017, Aachen, Germany

Metals and metabolites in Cerebrospinal Fluid of Parkinson´s disease patients. (oral presentation)

Desiree Willkommen, Marianna Lucio, Basem Kanawati, Sara Forcisi, Ali Sigaroudi, Michael Schroeter, Uwe Fuhr, Philippe Schmitt-Kopplin, Bernhard Michalke
at 33. Jahrestagung der GMS, 2017, Aachen, Germany

Selenium speciation in neurodegeneration (oral presentation)

Desiree Willkommen, Bernhard Michalke
at ESAS & CANAS, 2018, Berlin, Germany

Metabolomics investigation in cerebrospinal fluid of Parkinson´s disease (poster)

Desiree Willkommen, Marianna Lucio, Franco Moritz, Sara Forcisi, Basem Kanawati, Ali Sigaroudi, Michael Schroeter, Philippe Schmitt-Kopplin, Bernhard Michalke
at 13th EFTMS Workshop and the 2nd EFTMS School

Content

List of Abbreviations

AA	amino acid
AAS	atom absorption spectrometry
AChE	acetylcholinesterase
AD	Alzheimer´s disease
AEC	anion exchange chromatography
Ala	alanine
ALS	amyotrophic lateral sclerosis
ANCOVA	analysis of covariance
ARA	arachidonic acid
Arg	arginine
BBB	blood brain barrier
BCB	blood cerebrospinal fluid barrier
BER	balanced error rate
CE	capillary electrophoresis
CEC	cation exchange chromatography
CGE	capillary gel electrophoresis
Cit	citrate
CNS	central nervous system
CSF	cerebrospinal fluid
CTR	control
Cys	cysteine
CZE	capillary zone electrophoresis
DAAO	D-amino acid oxidase
DG	diacylglycerol

DGLA	dihomo-γ-linoleic acid
DLB	dementia with Lewy bodies
DMT	divalent metal transporter
DRC	dynamic reaction cell
ELISA	enzyme-linked immunosorbent assay
ESI	electrospray ionization
FAD	flavin adenine dinucleotide
FI	flow injection
FT	Fourier transformation
GABA	gamma-aminobutyric acid
GC	gas chromatography
GLM	general linear model
Gln	glutamine
Glu	glutamic acid
Gly	glycine
GPx	glutathione peroxidase
GSH	glutathione
GSSG	glutathione disulfide
HILIC	hydrophilic interaction liquid chromatography
His	histidine
HMDB	Human Metabolome Database
HMM	high molecular mass
HPLC	high pressure liquid chromatography
HRP	horseradish peroxidase
HSA	human serum albumin

IBDC	isobutyryl-D-cysteine
ICP	inductively coupled plasma
ICR	ion cyclotron resonance
IEC	ion exchange chromatography
Ile	isoleucine
IOS	inorganic species
IPAD	integrated pulsed amperometric detection
IRP	iron regulatory protein
KED	kinetic energy discrimination
KEGG	Kyoto Encyclopedia of Genes and Genomes
LB	Lewy body
LC	liquid chromatography
Leu	leucine
LMM	low molecular mass
LN	Lewy neurite
LOD	limit of detection
Lys	lysine
MDA	malondialdehyde
MDEA	mass difference enrichment analysis
MECC	micellar electrophoretic capillary chromatography
MEKC	micellar electrokinetic chromatography
MeOH	methanol
Met	methionine
MS	mass spectrometry
MSA	multiple system atrophy

MT	metallothionein
MW	molecular weight
m/z	mass-to-charge ratio
NAC	non-amyloid β-component
Nle	norleucine
NMDA	N-methyl-D-aspartate
NMR	nuclear magnetic resonance
NPV	negative predictive value
O.D.	optical density
OES	optical emission spectrometry
OPA	o-phthalaldehyde
OPLS-DA	Orthogonal Projections to Latent Structures-Discriminant Analysis
PC	phosphatidylcholine
PD	Parkinson´s disease
PDA	photodiode array
PE	phosphatidylethanolamine
Phe	phenylalanine
PPE	protein precipitation extraction
PPV	positive predictive value
Pro	proline
PSP	progressive supranuclear palsy
PUFA	polyunsaturated fatty acid
Q	quadrupole
QC	quality control
RF	radiofrequency

RNA	ribonucleic acid
ROC	receiver operating characteristic
ROS	reactive oxygen species
RPLC	reversed phase liquid chromatography
RT	retention time
SAX	strong anion exchange
SD	standard deviation
SEC	size exclusion chromatography
Sec	selenocysteine
SELENOP	selenoprotein P
SeM	selenomethionine
SEN	sensitivity
Ser	serine
sf	sector field
SN	*substantia nigra*
SNARE	soluble NSF attachment protein receptor
SNpc	*substantia nigra pars compacta*
SOD	superoxide dismutase
SPE	specificity
sPLS-DA	sparse Partial Least Square-Discriminant Analysis
TCA	tricarboxylic acid
Tf	transferrin
Thr	threonine
TMAH	tetramethylammonium hydroxide
ToF	time of flight

TXNRD   thioredoxin reductase

Tyr   tyrosine

UHR   ultrahigh resolution

UPLC   Ultra Performance Liquid Chromatography

UV   ultraviolet

Val   valine

List of Figures

separated and the ion beam is directed into a collision cell for fragmentation. Finally the ion beam reaches the ToF spectrometer where ions are accelerated to the detector.

Figure 1-8: Development and progression of PD. A) Schematic representation of decreased functional dopaminergic neurons and increased impairment associated with PD in pre-symptomatic and symptomatic phase. B) Braak stages 1-6 with affected brain region. Stages 1-3 are without clinical manifestation, the pre-symptomatic phase. With beginning of stage 4 clinical manifestation starts and develops with increasing stage. At stage 6 the maximum region in brain is affected and all clinical symptoms arise. Therefore, stages 4-6 are called symptomatic phase.

Figure 2-1: Overview of the thesis. The work is divided into three main investigations parts. The first part outlines the influence of different metals to PD. The second part illustrates the influence of some defined metabolites and additionally illustrates a metabolic profiling approach. The last part integrates the results of the first and second part to increase the insight into disease mechanisms and affected pathways.

Figure 3-1: Observed SEC-ICP-MS-chromatogram (, with graphical off-set) of Mn in CSF with fractions aligned (—, aligned chromatogram, with graphical off-set) by use of PeakFit^{TM} software. Species detected are „HMM" (—), „Citrate" (- - -), „Amino acids" (— · —), and „Inorganic species" (— · · —).

Figure 3-2: Box-plot of the most significant element-ratios observed by comparing CTR and PD. Especially ratios with small Cu-fractions, especially Cu-AA, in denominator are involved in these increased ratios in PD.

Figure 3-3: Observed SAX-ICP-MS-chromatogram (, with graphical off-set) of Se in CSF with fractions aligned (—, aligned chromatogram, with graphical off-set) by use of PeakFit^{TM} software. Species detected are SELENOP, U1, U2, SeIV, SeVI, and Se-HSA.

Figure 3-4: Results of Se-speciation in CSF of PD and CTR. A) Bar chart comparing the evaluated areas under the signal from PD and CTR for the separated Se-species; B) Bar chart comparing the evaluated areas under the signal from male and female samples for the separated Se-species; C) Scatterplot illustrating the correlation of age

vs. area under the signal of SELENOP for all samples; Scatterplot illustrating the correlation of age vs. area under the signal of SELENOP for D) CTR-samples and E) PD-samples.
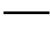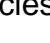
Figure 3-5: Observed CE-ICP-MS-chromatogram (, with graphical off-set) of Fe-redox speciation in CSF with fractions aligned (— , aligned chromatogram, with graphical off-set) by use of PeakFit[TM] software. Species detected are Fe(III) (—) and Fe(II) (—).

Figure 3-6: Results of the Fe(II)/(III) speciation in CSF of Parkinson patients and CTR. Illustrated are the differences of the Fe species in their A) concentrations with respective p-value and B) percentages distribution.

Figure 3-7: Rising Fe-concentrations with age in PD and CTR for A) Fe(II) and B) Fe(III). The slope is for both species higher in PD patients than in CTR.

Figure 3-8: Typically observed chromatogram of amino acid separation with the method AAA-direct[TM] in CSF with 1:3-dilution and amperometric detection. For proper concentration determination further dilution steps were measured.

Figure 3-9: Alterations in amino acid concentration in CSF of CTR and PD A) Significant difference of Ser and insignificant shift of Ile which display higher significance by comparing B) the difference in CTR and PD of patients with ages 40 – 60 years.

Figure 3-10: Results of analysis for age-dependence of amino acids in CSF. A) age-dependence of Gln with increasing concentrations with age in PD-patients. Significant amino acid differences within CTR group by comparing ages C) < 40 with > 60 and D) < 40 with 40 – 60 years.

Figure 3-11: Results of analysis for the influence of the sex in amino acid-concentration in CSF. Significant Differences were observed in the concentration of Thr between female and male patients in all measured samples (total) and in PD samples.

Figure 3-12: Results of analysis for the influence of the sex in the metal analysis within amino acid-fractions in CSF. The significance levels for the differences between female (red) and male (blue) participants are illustrated.

Figure 3-13: Extracted ion chromatograms (EIC) from serine and alanine in a CSF-sample illustrating the distribution between D- and L-enantiomeric forms of amino acids.

Figure 3-14: Results of enantioseparation of amino acids. A) Significant difference in D-Ala amount between CTR and PD; B) insignificant increase of L-Met and L-Ile; C) dependence of L-Thr intensity from age shows opposing behavior in CTR compared to PD.

Figure 3-15: The implemented statistical analysis models: A) sPLS-DA validated with 7 fold cross-validation, B) represented the area under the Receiver Operating Characteristic (ROC) curve, C) the classification error rates by which the number of components was tuned (7 cross-validation), D) OPLS-DA validated with 7 fold cross-validation, E) compounds, which significantly distinguished PD from controls, and F) compared intensities of selected lipids. Expl. var., explorative variance.

Figure 3-16: Schematic representation of MDEA. A) Connection of two compounds (nodes) by a specific mass difference representing a biochemical reaction (edge) and B) respective m/z-signals within spectra.

Figure 3-17: Over-represented mass differences obtained by MDEA. Z-scores > 2 correspond to p-values < 0.05.

Figure 3-18: Over-represented mass differences which are associated with the TCA cycle. Color code: Metabolites found directly by MDEA involved in TCA cycle are colored orange; precursor-metabolites found by MDEA synthesizing TCA cycle compounds are colored red; break-down products of TCA cycle compounds found by MDEA are colored purple.

Figure 3-19: Results of the Acetylcholinesterase fluorescent activity kit. A) Standard calibration curve showed high linearity und good coefficient of determination. B)
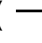
Comparison of the means ± SD of AChE activity in CTR and PD did not reveal a significant difference.

Figure 3-20: Results of the hSyn total ELISA-Enzyme immunoassay for quantitative determination of α-Synuclein in human CSF. A) Standard calibration curve showed a good coefficient of determination with quadratic equation. B) Comparison of the means ± SD of total α-Synuclein in CTR and PD did not reveal a significant difference.

Figure 3-21: Illustration of interrelation between metallomic and metabolomic data out of the same sample set with respective correlation value.

Figure 3-22: Statistical analysis of metallomic and metabolomic parameters. A) Block sPLS-DA analysis of metabolomic and metallomic parameters showing increased concentrations/ ratios for either PD or CTR; B) the correlations values for the PD patients and CTR for the metabolomic and metallomic block and C) classification performance of the model showing a stabilization of the error rates after the second component.

Figure 3-23: Loadings plot of the most important metallomic (green) related to the metabolomic biomarkers (red) in the first and second component. All depicted parameters are enhanced in PD. In the yellow box are the variables presented in Table 18, in the orange one the variables listed in Table 19

Figure S1: Observed SEC-ICP-MS-chromatogram (, with graphical off-set) of A) Fe, B) Cu, and C) Zn in CSF with fractions aligned (⸺ , aligned chromatogram, with graphical off-set) by use of PeakFit^{TM} software. Species detected are „HMM" (⸺), „Citrate" (– – –), „Amino acids" (— · —) and „Inorganic species" (— · · —).

List of Tables

Table 11: Significantly increased ratios derived from the amount values of species fractionation with respective p-values.

Table 12: Instrumental parameters for Se-speciation in CSF samples by use of SAX-ICP-MS.

Table 13: Program used for separation of the redox species Fe(II)/(III). Capillary was cleaned by the use of two washing steps including 7% HCl and 10% TMAH. An conductivity-pH-stacking enabled separation of Fe(II) and Fe(III).

Table 14: Retention times and concentrations of separated and measured amino acids in CSF for CTR- and PD-samples as well as respective p-values for comparison between both states.

Table 15: Instrumental parameters for elemental analysis of CSF amino acid fractions by use of ICP-sf-MS.

Table 16: Mean concentrations of measured metals Cu, Fe, Mg, Mn, Ni, Sr, and Zn in the amino acid fractions in CSF for CTR- and PD-samples. The highlighted values significantly ($p < 0.05$) differentiate between CTR and PD.

Table 17: Most important neutral masses to distinguish between PD and controls with respective molecular formula, possible compounds assignment and mean intensity ± standard deviation (SD). The p-values are the result of the general linear model (GLM) adjusted with DUNNET.

Table 18: The first block of related variables between metallomics and metabolomics. The variables are located within the 95th percentile of the most important variables. The p-values were calculated with the confounding variables age and gender and were adjusted with Benjamini-Hochberg.

Table 19: The second block of related variables between metallomics and metabolomics. The variables are located within the 50th and 95th percentile of the most important variables. The p-values were calculated with the confounding variables age and gender and were adjusted with Benjamini-Hochberg.

Table A1: SD of the measured metal concentrations of Cu, Fe, Mg, Mn, Ni, Sr, and Zn in the amino acid fractions in CSF for CTR- and PD-samples.

Table A2: Listed are all 243 core masses which significantly differentiate CTR and PD with respective mean intensity, SD, alteration in PD, SEN, SPE, positive predictive value (PPV), and negative predictive value (NPV).

Table A3: Instruments and Materials

Table A4: Chemicals

1. Introduction

1.1. Metallomics – Studying the metals

Metallomics was first defined by Williams in 2001 to describe all metal-containing species in an organism, the metallome (Williams, 2001). It considers the elemental distribution, the balanced concentration of free metal ions, and free element concentration in a cellular compartment, cell, or organism. Since metals and metalloids play a pivotal role in life, the research area of metallomics investigations expands. A special focus lies on metal/ metalloid location, distribution, speciation, and behavior in organisms (Hu *et al.*, 2013). Virtually all metals/ metalloids can act as a toxicant including also essential elements. Several metals/ metalloids are considered essential due to their involvement in life processes, e.g. selenium (Se) in glutathione peroxidase and copper (Cu) in cytochrome C oxidase. When not regulated adequately, they can be either in excess or lacking. Therefore, knowledge about metal/metalloid uptake, trafficking, function, and excretion in biological systems is of paramount importance (Mounicou *et al.*, 2009). Metals/ metalloids can act as active center in proteins and enzymes, so called metalloproteins. This has to be distinguished from metal-binding proteins which complex the metal/ metalloid, but do not evolve a specific function upon binding. Metals/ metalloids can also complex metabolic compounds produced by biochemical reactions (Michalke *et al.*, 2007).

Metallomics developed to a transdisciplinary research area since it finds application in the research areas of biochemical studies, clinical biology, pharmacology, nutrition, plant and animal physiology and geochemistry. Various methods to determine the metallome are discussed in this chapter. Special attention is paid to species separation and metal detection in biofluids as well as to hyphenated techniques for speciation analysis.

1.1.1. Separation of metal-species

In metallomics investigations a crucial part is the complete separation of different metal-species. In regard to the topic and the species-characteristics different separation types are available. Figure 1.1 illustrates these possible types of separation namely liquid chromatography (LC), high performance liquid chromatography (HPLC), gas chromatography (GC), and capillary electrophoresis (CE). GC separation is only suitable for volatile compounds. By means of derivatization also aqueous or solid samples can be transferred into volatile species. Derivatization reagents can be ethyl borate or Grignard compounds (Michalke and Nischwitz, 2010). The disadvantage of this separation technique is the possible loss of original speciation due to the derivatization step (Meermann and Sperling, 2012). Therefore, application of GC is limited to only covalently bound species with a defined scope (Wojcieszek *et al.*, 2017). Similarly to HPLC, CE has different separation types for different approaches like capillary zone electrophoresis (CZE), capillary gel electrophoresis (CGE), micellar electrophoretic capillary chromatography (MECC), and micellar electrokinetic chromatography (MEKC). CE is a highly effective separation technique with short analysis time, low sample consumption, and only minimal or no need for sample pretreatment (Timerbaev *et al.*, 2012). This method is highly suitable for element speciation because of nearly native buffer solutions and the capillaries having no stationary phase. This protects species from changes (Timerbaev, 2013). The analysis by CE needs only a small sample volume (< 100 nL), but due to the small volume the limit of detection (LOD) for element detection is worse than by HPLC separation. The often small concentrations of elements can be lower than the LODs accessible by CE separation in biofluids like cerebrospinal fluid (CSF) (Michalke and Nischwitz, 2010). Accordingly, in most cases a separation by LC or HPLC is most suitable. As shown in Fig. 1-1, different column-types are available to use appropriate techniques for a specific topic. Hereafter, the most important LC column types will be discussed.

2
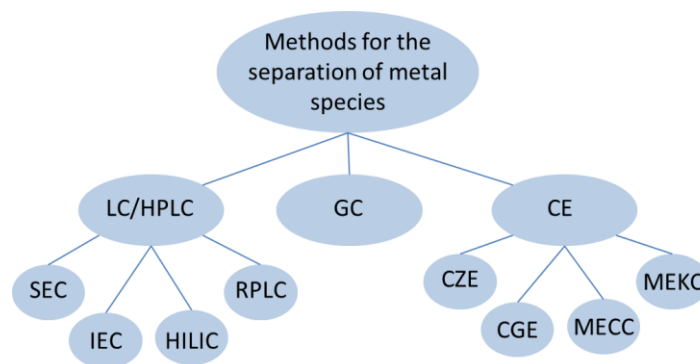
Figure 1-1: Separation methods of metal species are illustrated. The main applications for separations are liquid chromatography (LC), gas chromatography (GC), and capillary electrophoresis (CE). SEC-size exclusion chromatography, IEC-ion exchange chromatography, HILIC-hydrophilic interaction chromatography, RPLC-reversed phase liquid chromatography, CZE-capillary zone electrophoresis, CGE-capillary gel electrophoresis, MECC-micellar electrophoretic capillary chromatography, MECK-micellar electrokinetic chromatography.

Size exclusion chromatography

The size exclusion chromatography (SEC) or gel permeation is based on the molecular sieve effect and separates samples according to their size and shape (Szpunar, 2000b; Wojcieszek *et al.*, 2017). The SEC-columns are packed with porous organic polymers (gels) which form a network of pores with the same size. Molecules of a certain size can diffuse into these pores (Szpunar-Łobińska *et al.*, 1995). Therefore, retention time (RT) is related to the molecular size. The advantages of this method are the opportunity to separate element species with low stability like metalloproteins and low molecular mass (LMM)-compounds of transition metals. SEC-separation does not result in loss of element species or on-column changes and hence is suitable for the separation of complex biological matrices (Szpunar, 2000b; Michalke, 2003). By combining two columns with differing separation-ranges, the size separation can be extended. The SEC-columns are simple in their application and compatible with many mobile phase compositions (Koplik *et al.*, 2002), but SEC also has limitations. The method has only a small number of theoretical plates and therefore only a limited separation efficiency.

This means, especially for complex samples, each eluted fraction can still contain more than one compound of the same or similar molecular mass/size.

Ion exchange chromatography

Ion exchange chromatography (IEC) can be divided into anion exchange chromatography (AEC) and cation exchange chromatography (CEC). This separation technique is based on electrostatic interactions of positively or negatively charged metal-species with the stationary phase. In AEC the stationary phase contains cationic functional groups and in CEC the stationary phase contains anionic functional groups (Szpunar, 2000a). The method has high separation efficiency and is suitable for the separation of covalently bound metal-species like chromium-, selenium-, and arsenic-compounds. Metal-ions only loosely bound can be replaced by other metals from the buffer (Michalke, 2003). Further disadvantages are the high salt content and the need for changing pH-value which can cause changes of the original species (Wojcieszek *et al.*, 2017).

Reversed Phase Liquid chromatography

Reversed Phase Liquid chromatography (RPLC) handles analyte separation with a non-polar stationary phase and a fairly polar mobile phase (Szpunar, 2000b). The method is highly flexible and reproducible, but for the separation of element species problems may arise. Due to the use of organic solvents and acids, species transfer reactions are possible. This can produce changes in loosely bound element species. Therefore, RPLC separation is only suitable for covalently bound element species (Michalke, 2003). More problems come up when coupling the separation method with inductively coupled plasma mass spectrometry (ICP-MS) for on-line detection of element species. Caused by the high concentrations of organic solvents several drawbacks will be present. On the one hand, the organic solvents have a cooling effect on the ICP plasma and also change the ionization characteristics which lead to a decreased sensitivity of the detector. On the other hand, the organic composition of the solvent causes a high carbon intake which increases the amount of polyatomic interferences (Michalke, 2003).

Hydrophilic interaction liquid chromatography (HILIC) combines several separation techniques in one. The column consists of a polar stationary phase (like normal phase LC) and uses a mobile phase similar to RPLC. Like IEC this type of chromatography also allows the analysis of charged molecules. HILIC is most suitable for the separation and analysis of uncharged highly hydrophilic and amphiphilic compounds (Buszewski and Noga, 2012). Due to the use of RPLC-like solvents similar problems arise in detection of element species and on-line coupling to ICP-MS.

1.1.2 Detection of metal-species

Various techniques are available to identify and measure metals. Most suitable techniques are spectroscopic systems for trace element and ultra-trace element determination (Brown and Milton, 2005). Current techniques comprise atomic absorption spectrometry (AAS), optical emission spectroscopy (OES), and mass spectrometry (MS). All of these techniques have their special field of application with advantages and disadvantages, compared in Table 1.

Table 1: Comparison of spectroscopic methods for (ultra-trace) element detection. AAS-atomic absorption spectrometry, OES-optical emission spectroscopy, MS-mass spectrometry, LOD-limit of detection.

method	AAS	OES	MS
Elements per measurement	1	up to 60	up to 60
Amount of possible measurable elements	~ 70	~ 70	all
Interferences	low	rel. high	high
LOD	middle	low	very low
Sample need for detection of various elements	high	low	low

Dynamic range	low	high	high

In the following chapter only MS will be explained in more detail. All MS-systems compose of four main components: ion source, ion optics, separation or ion analyzer, and detector. Nowadays, the most common ion source is inductively coupled plasma (ICP). The setup of the torch is shown in Fig. 1-2 A. It is made up of three concentric quartz tubes which are inside a radiofrequency (RF) coil. The plasma gas argon (Ar) perfuses the tubes and the plasma is ignited through a tesla spark. The ignition induces ionization of the Ar and the introduced sample aerosol from nebulizer/ spray chamber. By an ohmic resistor temperatures up to 10,000 K are reached. Inside plasma the sample is dried, vaporized, atomized, and ionized as shown in Fig. 1-2 B.
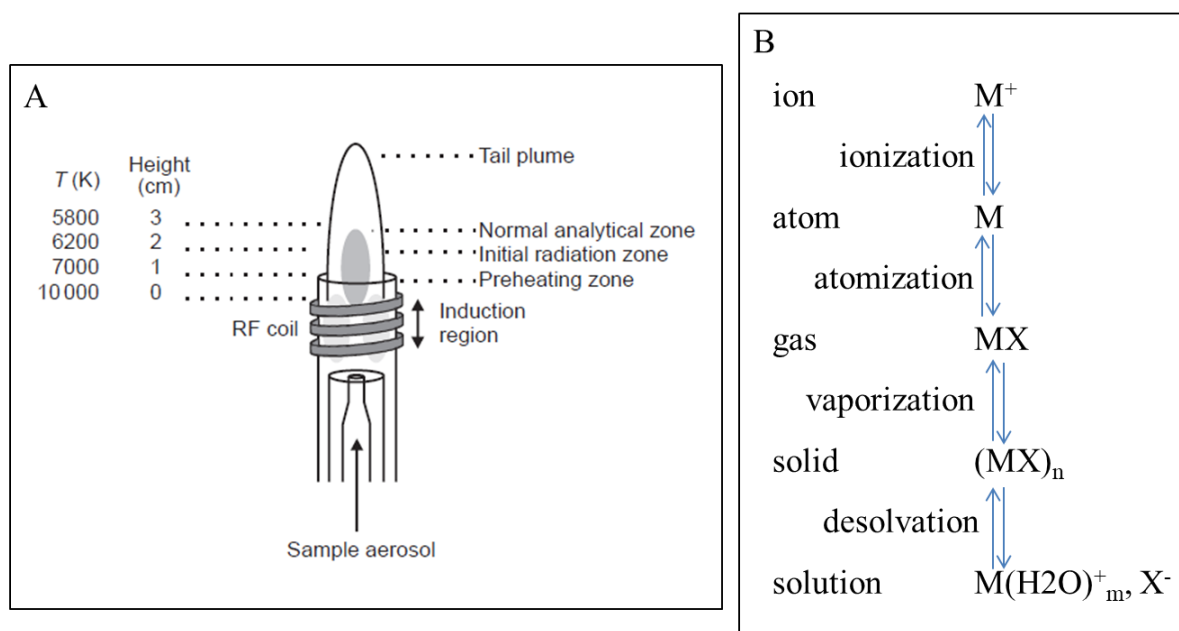
Figure 1-2: Principles of ICP-MS. A) Setup of ICP-torch with zones, respective position and temperature (adapted from (Hou *et al.*, 2016)); B) Process of metal ionization in plasma.

ICP-MS has several advantages like relative independence of sample matrix, very good LODs and multiple elements can be measured within one run. But there is also one major disadvantage in ICP-MS, the presence of polyatomic interferences. These

interferences are atoms or ions with the same mass-to-charge (m/z)-ratio the analyte has. Sources of interferences might be the sample matrix, chemicals used for sample preparation, plasma and atmospheric gases (May and Wiedmeyer, 1998). Possible polyatomic interferences of the trace-elements of interest within this thesis are listed in Table 2. Most of these elements exist in different isotopic states, but only the ones with highest abundance are listed here.

Table 2: Typical polyatomic interferences of the most abundant element-isotopes of Cu, Fe, Mn, Se, and Zn in ICP-MS (May and Wiedmeyer, 1998).

metal	abundance	interferences
^{63}Cu	69.17%	$^{40}Ar^{23}Na^+$, $^{23}Na^{40}Ca^+$, $^{46}Ca^{16}O^1H^+$, $^{36}Ar^{12}C^{14}N^1H^+$
^{56}Fe	91.75%	$^{40}Ar^{16}O^+$, $^{40}Ca^{16}O^+$, $^{37}Cl^{18}O^1H^+$, $^{40}Ar^{15}N^1H^+$
^{55}Mn	100.0%	$^{40}Ar^{14}N^1H^+$, $^{39}K^{16}O^+$, $^{37}Cl^{18}O^+$, $^{40}Ar^{15}N^+$, $^{23}Na^{32}S^+$
^{80}Se	49.82%	$^{40}Ar_2^+$, $^{32}S^{16}O_3^+$
^{64}Zn	48.60%	$^{32}S^{16}O_2^+$, $^{31}P^{16}O_2^1H^+$, $^{48}Ca^{16}O^+$, $^{32}S_2^+$

To overcome the drawback of polyatomic interferences several technologies have been developed. Here, the used technologies are shortly described. The first one removes interferences by introducing a reaction gas (e.g. O_2, NH_3, CH_4) into a specific cell to trigger a chemical reaction, the so called dynamic reaction cell (DRC). The chemical reaction can change either the analyte or the interference and the software adapts the measurement accordingly. A similar approach is the collision cell, sometimes additionally equipped with kinetic energy discrimination (KED) to remove products with low velocity. This technique uses non-reactive gases (e.g. He) to collide with interferences and removes them in a mass separator, mainly quadrupoles (Q). Conventional ICP-QMS systems feature a reaction or collision cell and an analyzing quadrupole acting as mass filter. More recent devices are equipped with three quadrupoles (QQQ). These systems have an analyzing quadrupole before and after the

reaction/ collision cell to enhance efficiency in eliminating interferences. The schematic setup of the used system is shown in Fig. 1-3. The installed universal cell can act as both DRC and collision cell with KED.
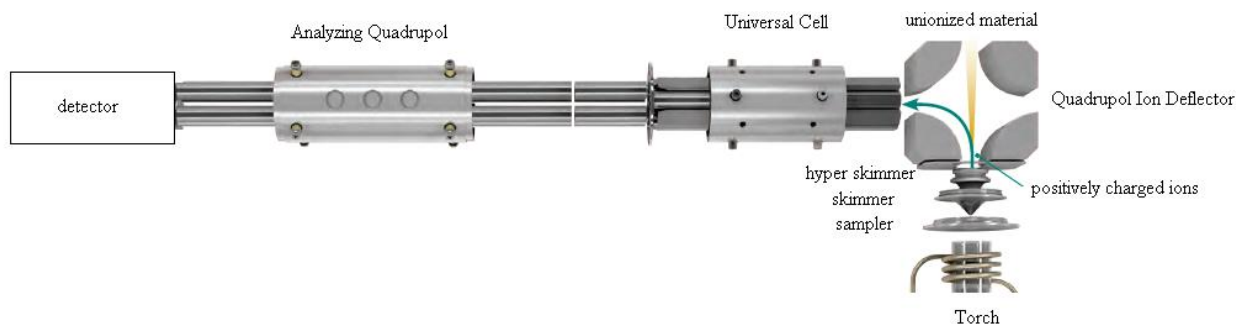
Figure 1-3: Schematic representation of NexIon 300D (adapted from Perkin Elmer brochure (Perkin, 2015). The first quadrupole removes unionized material and the charged ions are guided into the universal cell. Within this cell interferences can be removed either by collision or through a specific reaction with a reaction gas (DRC). Afterwards the ion beam is guided into the analyzing quadrupole and finally to the detector.

Another technology is a sector field (sf) system which enables high resolution. By the use of a double focusing ICP-sf-MS no additional gas is needed. The basis is a combination of a sf-mass analyzer and an electrostatic analyzer. The setup of the Element2 ICP-sf-MS system is illustrated in Fig. 1-4. The principle is based on a reverse Nier-Johnson geometry. More specifically, the ions are focused first by a magnetic sector field and afterwards by an electrostatic sector field. The higher resolution of ICP-sf-MS enables the separation of most polyatomic interferences. Therefore, by the use of a sector field device no further cell for collision or reaction is needed. The disadvantages of ICP-sf-MS are the high cost price as well as relatively long time for switching between two masses.

8
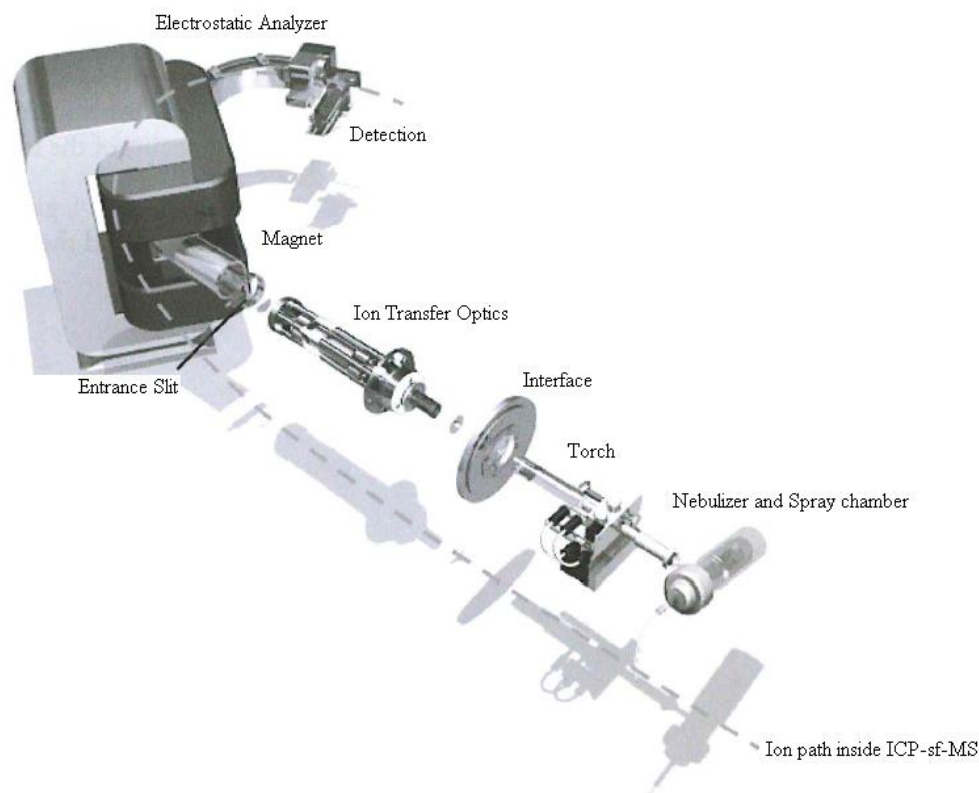
Figure 1-4: Schematic setup of Element2 ICP-sf-MS (adapted from Thermo Fisher Scientific brochure (Thermo)). The ion beam follows the inverse Nier-Johnson geometry. Directly after the ion source the ion beam is guided through the magnet for mass dispersion, followed by the electrostatic analyzer for energy dispersion and finally to the detector.

1.1.2 Hyphenated techniques

The hyphenation of techniques like coupling of HPLC with ICP-MS increases the size of information (Kubáň *et al.*, 2005). A separation based on chromatographic techniques provides RT and the subsequent spectroscopic detection yields the intensity and respective elements. All mentioned separation techniques from chapter 1.1.1 can be coupled to the discussed systems from chapter 1.1.2 for element analysis. Hyphenation of techniques can be done on-line, where the effluent of the separation device is directly led to the nebulizer and spray chamber of the element detection system. Sometimes hyphenation can be done technically simple, but some techniques need more complex interface constructions (Michalke, 2005). The second option is to collect fractions of

chromatographic separation which afterwards off-line can be analyzed by a second system, e.g. ICP-MS.

When coupling to different systems several requirements have to be met. As already described in chapter 1.1.1 various eluents necessary for separation are not suitable for ICP-MS detection since high intake of organic solvents (e.g. MeOH, EtOH) has a cooling effect on ICP-plasma and, additionally, increase carbon intake leading to sources of interferences. Therefore, separation conditions and eluents have to be adapted accordingly for hyphenation.

For the speciation of metal compounds hyphenation is of essential interest. A species is "a specific form of an element defined as to isotopic composition, electronic or oxidation state, and/or complex or molecular structure" (Apostoli *et al.*, 2006). The distribution of these species in a defined system (e.g. CSF) is called speciation. The species (one or more) can be identified and measured by speciation analysis. For example, possible Fe redox-species are Fe(II) and Fe(III), their distribution in human body fluid is the redox-speciation of Fe and the detection of both species is called speciation analysis.

The advantage of the hyphenated techniques is the excess profit of knowledge. The speciation analysis reveals not only the influence of a specific trace element in its total concentration but speciation analysis also shows the connection to specific compounds, proteins and enzymes which are involved in a certain disease. With this additional information disease processes can be connected to pathways and the whole metabolism which are affected through disease. Therefore, by means of speciation analysis comprehensive disease research can be achieved.

1.2. *Metabolomics-studying the metabolism*

The term "metabolome" was introduced by Oliver et al. in 1998 (Oliver *et al.*, 1998). The metabolome describes the sum of metabolites within an organism and the changes due to external impact or disease. Metabolites are small molecules (< 2 kDa) of various classes of substances, intermediate or end products of all cellular metabolic reactions

(Wörmann *et al.*, 2012, Müller *et al.*, 2014). Estimations assume that the human metabolome composes of about 42,000 metabolites (Wishart *et al.*, 2007). This contains endogenous metabolites, means products of metabolic reactions, and exogenous metabolites, referring to ingested xenobiotic chemicals (Dudzik *et al.*, 2018). All organisms have a metabolic state which is optimized for proper function and living (=homeostasis). Any change, either environmentally or mutational, can influence the homeostasis and cause a defined metabolic response. The scope of metabolomics is to analyze this defined metabolic response in order to evaluate mechanisms and altered pathways e.g. in diseases.

There are two strategies for metabolomic investigations, the targeted and non-targeted analysis. As the names already display, with targeted analysis specific compounds are quantified and non-targeted analysis aims to evaluate as much compounds as possible. Accordingly, targeted analysis is hypothesis driven and non-targeted analysis needs no prior hypothesis, but can generate new hypothesis. Additionally, the non-targeted analysis often only allows obtaining semi-quantitative results and not all metabolites have to be identified (Wishart, 2007). In fact, non-targeted analysis sometimes is used for the spectral profile comparison of healthy and diseased states. In contrast to non-targeted analysis, targeted analysis can give more precise insights into pathway alterations and therefore is often used as follow-up analysis of non-targeted approaches.

Since enzymatic reactions and biodegradation are ongoing processes in biofluids, a proper sample handling is essential. The major points, which need to be considered, are the inactivation of ongoing metabolic processes, securing metabolite stability during pre-processing steps, and finally sample stability during storage which includes preventing samples from frequent freeze-thaw-cycles. Therefore, it is recommended to aliquot and store biological samples quick and contamination-free at -80°C.

There exist mainly two platforms for the characterization of metabolites. The first one is nuclear magnetic resonance (NMR) and the second one is mass spectrometry (MS). Both techniques are widely used and have specific advantages and disadvantages which define their specific field of application. In NMR identification is done by the

chemical environment of protons. Thereby, signal intensity can be related to quantitative results. Additionally, NMR yields a high reproducibility and highly resolved spectra within a short timescale. Moreover, it can be used for structural information. Sample pre-processing is quite easy in NMR and it's a non-invasive method. The disadvantage of NMR is the comparably low sensitivity, metabolites of only low concentration in a sample can´t be detected. The sensitivity can be increased by increasing the magnetic field. In complex matrices also overlap of signals can appear which can be simply solved by two-dimensional approaches. In contrast to NMR, MS identifies metabolites with high precision by their molecular mass, more specifically by their mass-to-charge ratio (m/z). Ionizable metabolites are the precondition to measure by MS. To fulfill this criterion, applications like electrospray-ionization (ESI) have been developed (explained in chapter 1.2.1). Since high amounts of salt, protein and high metabolite concentration have negative influence on ionization, a proper sample pre-processing is necessary. Like for ICP-MS, it is possible to couple MS with various separation techniques (GC, LC, CE) to reduce matrix effects and complexity of samples. Moreover, hyphenation gives further information about physical and chemical properties of compounds and can be used as another identification-tool. The advantage of MS-detection is high sensitivity; also very low concentrated metabolites can be analyzed.

None of the techniques can cover all metabolites, as already shown in several publications (Wishart *et al.*, 2008). Therefore, to get a complete and comprehensive metabolite overview it is necessary to use several techniques and methods to cover as much metabolites as possible.

1.2.1 Methods for metabolomic investigation

As already mentioned, metabolomic investigations can be either targeted or non-targeted. Depending on the application, different MS-based techniques are available for metabolite measurement and identification. The used approaches are discussed in more detail in this section.

Electrospray Ionization

Electrospray ionization (ESI) is one of several ionization sources. Especially in chemical and biochemical analysis ESI is one of the most used techniques, due to its high ionization efficiency. Moreover, even large non-covalently bound complexes can be ionized since there is no mass limitation and ions are very stable (Wilm, 2011).

The principle of ESI is illustrated in Fig. 1-5. A high voltage (2-5 kV) is applied to the tip of the spray needle resulting into an electrical field. A Taylor cone emerges at the tip of the needle producing aerosol particles. The nebulizer gas N_2 aids the aerosol formation and, additionally, leads to solvent evaporation. At some point droplet size decreased to the so called Rayleigh-limit and a Coulomb fission produces desolvated ions which are directed to MS measurement (Cech and Enke, 2001). Dependent on the applied voltage, production of positively charged ions or negatively charged ions can be realized.
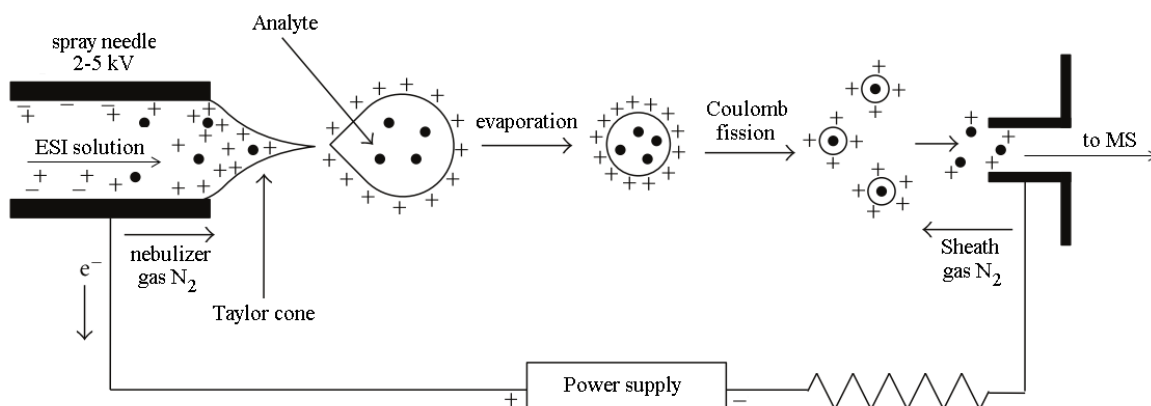
Figure 1-5: Principle of electrospray ionization (ESI) process (adapted from (Banerjee and Mazumdar, 2012)). An electric field is build up through a high voltage at the needle. The emerging Taylor cone produces aerosol particles. The solvent evaporates and the Coulomb fission produces desolvated ions which are guided to MS.

13

Fourier transform-ion cyclotron resonance-mass spectrometry

Fourier transform-ion cyclotron-mass spectrometry (FT-ICR-MS) is a MS-based technique that offers ultra-high resolution and mass accuracy (Nikolaev *et al.*, 2011). This technique allows for the concurrent detection of thousands of metabolites in a complex sample matrix (Forcisi *et al.*, 2015) as well as the assignment of putative molecular formulas (Breitling *et al.*, 2006a; Breitling *et al.*, 2006b) to each experimentally detected feature. The analysis by FT-ICR-MS is semi-quantitative and considers the intensity of each detected feature as a measure of their concentration. Therefore, this technique is suitable for profile screening in a discovery oriented way (Moritz *et al.*, 2013).

The used solariX[TM] FT-ICR-MS system is schematically illustrated in Fig. 1-6 A. The instrument is equipped with an ESI-source for ion generation. The generated ion beam is guided through funnel systems and an octapole to focus the beam. The following quadrupole acts as selective ion mass selector and a multipole accumulates and pre-selects ions before transferring them into ICR-cell for mass analysis. The ICR-cell is the centerpiece of this kind of instruments. The working principle of the ICR-cell in excitation and detection mode is demonstrated in Fig. 1-6 B. The ICR-cell is surrounded by a superconducting cryo-magnet (12 T) which forms a spatial uniform magnetic field. The ions are transferred into this magnetic field and are forced to move in orbits in the ICR-cell following their ion cyclotron motion. The radius of the orbit is only depending on mass, charge, and applied magnetic field. Since these initial orbits are too small for detection, ions get excited to increase their moving radius with a spiral like movement as illustrated in Fig. 1-6 B. An RF potential is mass-selectively applied to the ions through two excitation plates which are placed orthogonal to the two detection plates. The ions are brought in phase and move to higher orbit and, finally, can be detected. In detection mode the radius of ions stays stable at the higher orbit. A detector is measuring the induced image currents that evolve through the circulating ions that exceed detector plates resulting in a time-domain spectrum. The application of Fourier transformation leads to the frequency-domain spectrum and after mass correction to the final mass spectrum.
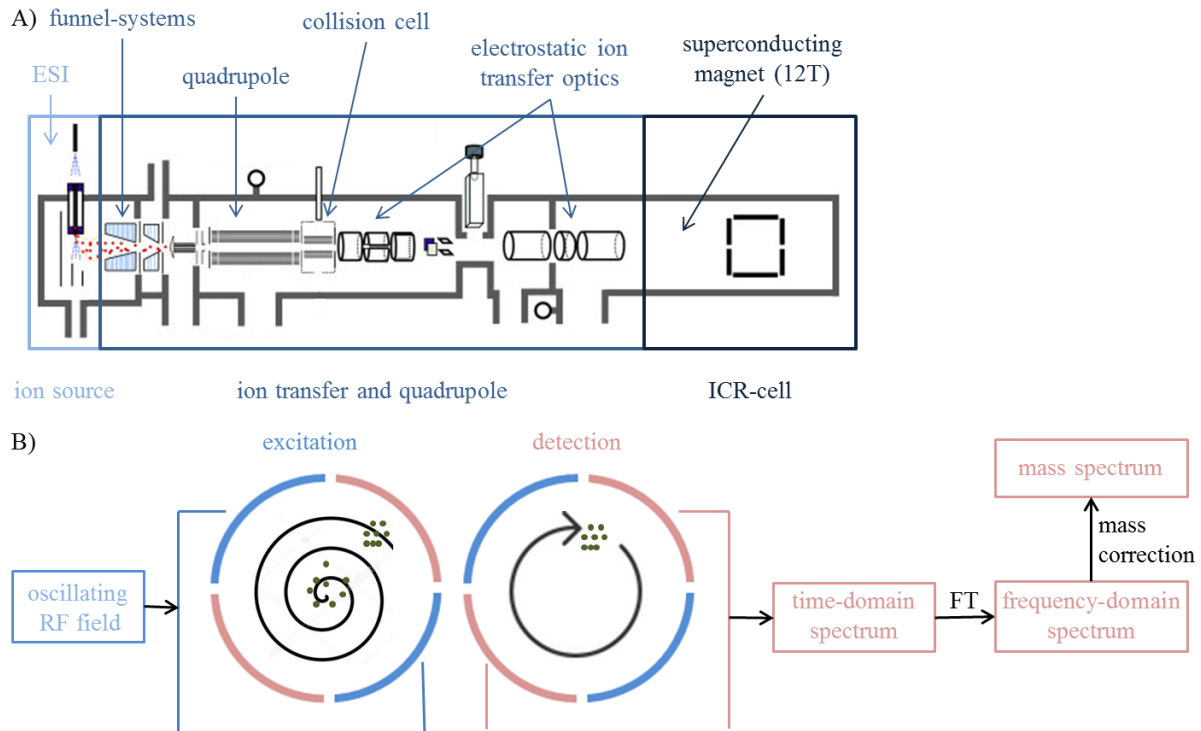
Figure 1-6: Principles of FT-ICR-MS measurement. A) schematic setup of solariX^{TM} FT-ICR-MS (adapted from (Park *et al.*, 2013)). Sample is ionized by ESI and guided through funnel-systems to a quadrupole and collision cell before getting transferred to ICR cell for detection. B) Working principle of ICR cell in excitation and detection mode. In excitation mode ions move to higher orbits in dependence on their mass, charge, and the magnetic field. In detection mode the radius of the orbit stays stable and the detector measures the induced image current.

Ultrahigh resolution-time of flight-mass spectrometry

Ultrahigh resolution-time of flight-mass spectrometry (UHR-ToF-MS) is another type of MS-based metabolomic analysis. ToF is a commonly used technique since it features high speed of detection, detection of very small masses (>80 kDa), and is comparably inexpensive in contrast to FT-ICR-MS. The used maXis^{TM} UHR-ToF-MS is schematically illustrated in Fig. 1-7. The system is a hybrid Qq-ToF dual stage reflector system with orthogonal ion acceleration. The capital Q stands for the mass resolving quadrupole and the lowercase q stands for the collision cell.
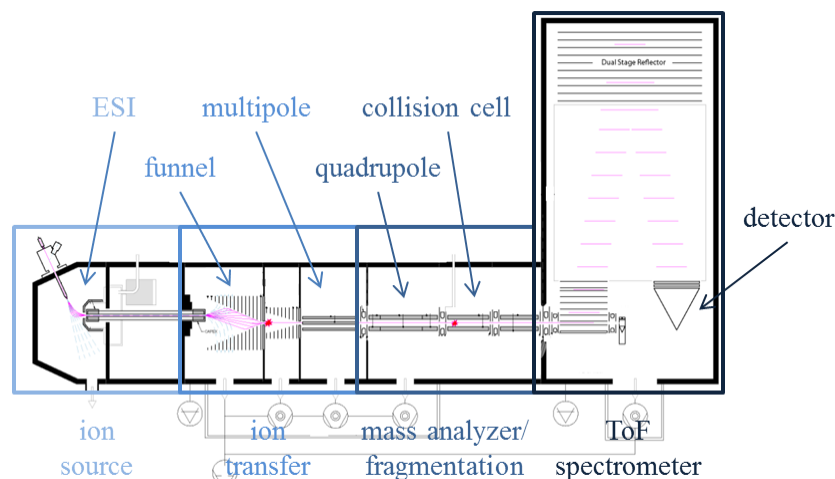
Figure 1-7: Schematic setup of maXis^{TM} UHR-TOF-MS (adapted from Bruker Daltonic brochure (Bruker, 2008)). Within the ion source ions are generated which are guided to the quadrupole. There a specific mass range is separated and the ion beam is directed into a collision cell for fragmentation. Finally the ion beam reaches the ToF spectrometer where ions are accelerated to the detector.

The system is mainly constructed out of 4 parts. The ion source generates ions (in positive or negative mode) by ESI. The ion transfer part separates the analyte ions from drying gas and solvent and transfers ions to the quadrupole. Within the multipole, ions are transported and focused for quadrupole. The following part is the mass analyzing quadrupole which delineates a specific ion mass or mass range. Afterwards, in the collision cell, fragmentation is proceeded by the help of collision gases like N_2 or Ar. Finally, the ion beam reaches the ToF spectrometer where ions are accelerated to the detector. The separation is based on ions passing a field-free drift region of defined length and getting separated according to their m/z-ratio. Thereby lighter ions pass the drift region faster than equally charged larger ions. The relation between the time used for passing the drift tube (t), the length of drift tube (s) the used voltage (U) and the electron charge (e) to m/z-ratio is shown in equation (1).

$$t = \frac{s}{\sqrt{2eU}} * \sqrt{\frac{m}{z}}$$

(1)

A reflector deflects ions back into the flight tube into the direction of the detector. Moreover, the reflector normalizes energy differences and improves resolution.

1.2.2 Metabolomic investigations in Parkinson´s disease

Metabolomic investigations in medical applications have two major goals, first the identification of affected metabolites and pathways for hypothesis generation and second the discovery of biomarkers for early diagnosis and therapeutic monitoring (Botas *et al.*, 2015). A major problem, especially in metabolomic investigations in neurodegenerative diseases like PD, is the non-availability of human brain tissue. Additionally, diagnosis relies on clinical presentation which occurs only after 50% of dopaminergic neurons are lost. Therefore, early biomarkers are lacking, but due to the dynamic metabolic system a set of molecules could be indicative for disease. Cerebrospinal fluid (CSF) is in close contact with the brain and more easily accessible than brain tissue. Therefore, most commonly CSF is used in metabolomic investigations regarding neurodegeneration, but also other biofluids are used to get an insight into PD.

Wishart et al. invented the Human Metabolome Database (HMDB) which reports all known metabolites within CSF, concentration ranges and abnormal concentrations in different diseases (Wishart *et al.*, 2007). They detected 70 metabolites in CSF by the use of NMR, GC-MS and LC-MS methods. A literature survey revealed about 300 metabolites, belonging to 33 different compound classes, to be present and detected in CSF (Wishart *et al.*, 2008). A follow up study in 2012 by the same group yielded in an increased amount of 476 metabolites detectable in CSF-samples (Mandal *et al.*, 2012). More specifically, metabolomic CSF-studies of PD-patients showed different outcomes. Burté et al. found mainly altered metabolites of the fatty acid oxidation pathway (Burté *et al.*, 2017). Other non-targeted studies report decreased levels of 3-hydroxyisovaleric acid, tryptophan, and creatinine (Trupp *et al.*, 2014; Wu *et al.*, 2016), benzoate (LeWitt *et al.*, 2017), caffeine and its metabolites (Hatano *et al.*, 2016) and malondialdehyde (MDA) (de Farias *et al.*, 2016) in various biofluids. Several reviews report the numerous studies in different biofluids (Botas *et al.*, 2015; Gonzalez-Riano *et al.*, 2016; Andersen *et al.*, 2017; Havelund *et al.*, 2017; Powers *et al.*, 2017).

1.3. Parkinson´s disease

Parkinson´s disease (PD) is a neurodegenerative disease already known since more than 200 years. The first description of PD was the "Essay on the shaking palsy" authored by James Parkinson in 1817 (Parkinson, 2002). Although PD is known since that time, no distinct diagnostic tests are available to identify this severe and progressive disease. PD is the second most common neurodegenerative disease affecting about 1% in the population over age 65 (Chinta and Andersen, 2008). The diagnosis is mainly based on its clinical manifestation as well as on the response to levodopa (Jankovic, 2008), but diagnosis is difficult in early stages due to the long preclinical phase (Parnetti *et al.*, 2013). PD is characterized by the four cardinal features tremor at rest, rigidity, bradykinesia, and postural instability. These symptoms appear only after reduction of dopamine levels to greater than 60% of normal levels (Bernheimer *et al.*, 1973). Additionally, a broad range of non-motor symptoms like sleep abnormalities, depression, and cognitive disorders are associated with PD and may arise before manifestation of the main clinical features (Hoehn and Yahr, 2001; Jankovic, 2008). On autopsy a pathological confirmation of PD is possible by finding Lewy bodies within the brain (Hughes *et al.*, 1992; Wakabayashi *et al.*, 2007). The presence of Lewy bodies and the loss of dopaminergic neurons in *Substantia nigra pars compacta* (*SNpc*) are the pathological hallmark of PD. There are several factors possibly involved in PD-development and progression. A multifactorial etiology is widely accepted (Gorell *et al.*, 1999; Forte *et al.*, 2004; Gorell *et al.*, 2004; Forte *et al.*, 2005; Gaeta and Hider, 2005; Jomova *et al.*, 2010). In about 5-10% of all PD cases familial factors are involved, mainly due to mutations of PARK genes (Wirdefeldt *et al.*, 2011). The remaining 90-95% of PD patients display sporadic disease onset. Factors which may be involved in sporadic disease onset are genetic mutations, exposure to pesticides (Bhatt *et al.*, 1999; Dick *et al.*, 2007), herbicides and other chemicals involved in farming (Tuchsen and Jensen, 2000; Hancock *et al.*, 2008), environmental or occupational exposure to metals (Willis *et al.*, 2010; Racette *et al.*, 2012; Brouwer *et al.*, 2015), misfolded and aggregated a-synuclein (Fink, 2006; Park *et al.*, 2011; Carboni and Lingor, 2015), oxidative stress (del Hoyo *et al.*, 2010), inflammation (Taylor *et al.*, 2013), mitochondrial dysfunction (Subramaniam and Chesselet, 2013; Anandhan *et al.*,

18

2017), and pathogenic mechanisms (Jankovic, 2008). The involvement of smoking, alcohol, physical activity, body mass index and diet is reviewed in (Wirdefeldt *et al.*, 2011). Especially oxidative stress seems to play a major role in PD-pathogenesis since the brain is more susceptible to oxidative stress damage than other organs. This high risk for oxidative stress is caused by low amounts of antioxidants like glutathione (GSH), high levels of polyunsaturated fatty acids (PUFAs), and an increased amount of iron in specific brain regions (Chinta and Andersen, 2008). Post-mortem studies indicate the role of oxidative damage (Sofic *et al.*, 1988).

1.3.1 Braak stages

Braak et al. analyzed PD at different stages and found PD-progress in six neuropathological stages (Braak *et al.*, 2003; Braak *et al.*, 2004). The processes underlying PD need years to reach its full extant in central nervous system (CNS) and only the late phase, the symptomatic phase, of PD can be assessed clinically. The Fig. 1-8 A and 1-8 B represent the progress of PD and the six Braak stages with respectively affected brain region. In the pre-symptomatic phase Lewy neurites (LN) develop in the dorsal nucleus of the vagal nerve and in the adjoining intermediate reticular zone (stage 1). The area where LN can be found is increasing with stages. In stage 2 LN are within coeruleus-subcoeruleus complex and with beginning of stage 3 LN appear in substantia nigra pars compacta (SNpc). Additionally, Lewy bodies (LB) start to occur. At this time point the SN is macroscopically intact and there is no visible sign of neuronal loss, but at some point the symptomatic phase starts with clinically manifestation of PD (stage 4). In stage 4 also the cerebral cortex is drawn into the disease process. Stages 5 and 6 are characterized by the manifestation of the full range of PD-associated clinical motor and non-motor symptoms, the PD-progress reaches the greatest extent and LB can be found in the entire neocortex.
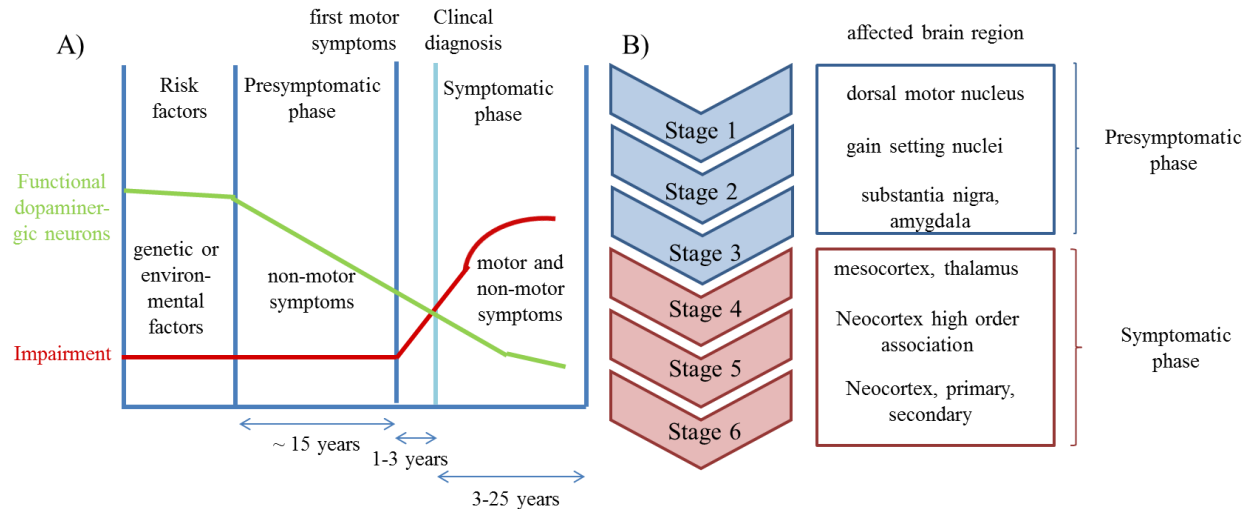
Figure 1-8: Development and progression of PD. A) Schematic representation of decreased functional dopaminergic neurons and increased impairment associated with PD in pre-symptomatic and symptomatic phase (adapted from (Eggert and Berg, 2015)). B) Braak stages 1-6 with affected brain region. Stages 1-3 are without clinical manifestation, the pre-symptomatic phase. With beginning of stage 4 clinical manifestation starts and develops with increasing stage. At stage 6 the maximum region in brain is affected and all clinical symptoms arise. Therefore, stages 4-6 are called symptomatic phase (adapted from (Braak *et al.*, 2004)).

1.3.2 Essential trace metals

The human body needs 11 essential trace elements, which act as cofactor or catalyst in lots of enzymes and proteins, represented in Table 3. Although only accounting for 0.02% of total body mass, they have a vast influence on body functions (Prashanth *et al.*, 2015). Essential trace elements are Co, Cr, Cu, Fe, I, Mn, Mo, Ni, Se, Si, and Zn (Mertz, 1981), but in excess they can be highly toxic. Therefore, in a healthy state metals are kept at relatively low level. Metals play a key role in intracellular oxidation balance as they can act pro-oxidant or anti-oxidant. These elements are tightly regulated in body and the uptake into brain via blood brain barrier (BBB) or blood cerebrospinal fluid barrier (BCB) follows strict specifications. Various transporters, proteins, and enzymes control the uptake, transport and export into/ from the brain to prevent from overload. Alterations in this regulated homeostasis are suggested to cause

neurodegeneration (Bowman *et al.*, 2011). Moreover, synergistic combinations of metals increase the risk for neurodegenration (Gorell *et al.*, 2004). Thereby, metal dyshomeostasis is associated with aggregation and fibrillation of specific proteins, free radical production and alterations in metal transport (Kozlowski *et al.*, 2012) leading to damage, cell death, and, finally, to neurodegeneration.

Table 3: The essential trace elements Cu, Fe, Mn, and Zn. The daily requirement of each element, their involvement in physiological important functions and proteins/enzymes in which they are incorporated and act as active center are listed.

	Cu	Fe	Mn	Zn
Daily requirement (Prashanth *et al.*, 2015)	2-5 mg	1-2 mg	2-5 mg	15-20 mg
Involved in functions	• Hemoglobin synthesis • Cellular respiration • Neurotrans-mitter synthesis	• Binding/ transport/ release of O_2 • Synthesis/ metabolism of neurotrans-mitter	• Ox. Phosphoryl. • Fatty acid/ cholesterol metabolism • Maintenance of nerve function	• Carbohydrate/ lipid/ protein metabolism • Nucleic acid/ protein synthesis
Incorp-orated in proteins/ enzymes	• ceruloplasmin, SOD, tyrosinase, uricase, cytochrome c oxidase	• Ferritin, transferrin, cytochrome C reductase, catalases, peroxidases	• SOD, arginase, pyruvate carboxylase, glutamine synthase	• SOD, MT, transferases, hydrases, lyases, RNA polymerase

Especially the redox active metals Cu, Fe, Mn and the non-redox active metal Zn are of interest. Redox-activity can cause high amounts of reactive oxygen species (ROS) within the body. Particularly the Fenton reaction (for Fe) or Fenton-like reactions (other redox active metals like Mn and Cu) are involved in ROS production. Ferrous iron together with hydrogen peroxide forms ferric iron and the highly reactive hydroxyl radical: $Fe^{2+} + H_2O_2 \rightarrow Fe^{3+} + OH^{\bullet} + OH^{-}$. The resulting Fe^{3+} can accelerate ROS production by conversion into Fe^{2+}: $Fe^{3+} + O_2^{\bullet-} \rightarrow Fe^{2+} + O_2$ (Batista-Nascimento *et al.*, 2012). The ROS production is a potential trigger of neurodegeneration causing mitochondrial dysfunction, DNA breakage, and neuronal injury.

Although Zn is not redox active, it seems to be involved in neurodegeneration. Upon electrical stimulation Zn is released by synaptic vesicles in mammalian cerebral cortex and induces the response of various neurotransmitters (Cuajungco and Lees, 1997; Frederickson *et al.*, 2005). Zn is also involved in reducing ROS by free radical scavenging when associated with metallothionein (MT). On the one hand, Zn serves as inhibitor of nitric oxide synthase (Persechini *et al.*, 1995) and on the other hand it can reduce oxidative stress by binding to thiol groups (Maret, 1995). However, pharmacological doses of Zn induce neuronal death (Yokoyama *et al.*, 1986; Kim *et al.*, 1999; Mortadza *et al.*, 2017). High Zn levels lead to mitochondrial dysfunction (Pivovarova *et al.*, 2014). Zn toxicity to mitochondria is increased in presence of Ca-ions (Ji and Weiss, 2018). Equally, excess Cu causes higher brain Cu levels, reduced glutathione and SOD-activity, and raised lipid peroxidation (Ozcelik and Uzun, 2009). Additionally, a short overload or long-term low exposure to Mn turned out to be toxic and persons are at higher risk of developing PD (Finkelstein and Jerrett, 2007; Lucchini *et al.*, 2007; Lucchini *et al.*, 2009).

Furthermore, trace elements are involved in fibrillation and aggregation of α-synuclein forming LB, whose presence is a major hallmark of PD (Fink, 2006). Iron as well as Cu, Mn, and Zn seem to influence the aggregation of α-synuclein. Increased levels of Fe lead to increased aggregation of α-synuclein (Li *et al.*, 2010a). The complex between ferrous Fe and α-synuclein has a 1:1-stoichiometry and can be oxidized to a complex with ferric Fe. With this oxidation, hydrogen peroxide is produced as a byproduct (Peng

et al., 2010). Also Mn is able to facilitate the aggregation of α-synuclein (Uversky *et al.*, 2001). Moreover, Mn enhances the expression of α-synuclein as shown in *in vitro* cell models (Cai *et al.*, 2010; Li *et al.*, 2010b). Zn and Cu accelerate the aggregation of α-synuclein, either alone or in combination (Paik *et al.*, 1999; Valiente-Gabioud *et al.*, 2012; Zawisza *et al.*, 2012). Several chemicals like pesticides can even increase the aggregation of α-synuclein in presence of metal-ions (Uversky *et al.*, 2002).

On the whole, transition metals play a crucial role in the etiology of PD. Impaired metal concentrations can increase neurological burden by increasing oxidative stress, accelerating protein aggregation, and mitochondrial dysfunction, but metals are also involved in antioxidant processes since they are cofactors in important antioxidant proteins like SOD and MT. Literature presents the impairment associated with metal accumulation. However, it is still unclear whether this accumulation is the primary event or the secondary effect of neurodegenerative processes in PD.

2. Aims and Objectives

Neurodegeneration is an increasing problem in society due to increasing age of population and due to increasing environmental pollutions. Diseases like Alzheimer´s disease (AD), PD, and amyotrophic lateral sclerosis (ALS) are age-dependent diseases. Consequently, with increasing age of society the number of affected population is increasing. This also enhances the costs of care and the necessity of trained staff. As a result of missing cure, the absolute amount of patients is heavily increasing.

To get a comprehensive overview about differences in PD patients compared to controls, the CSF of diseased and neurologically healthy persons was investigated. The investigation was divided into three parts. The first part addresses the metallomics, means the investigation of relevant metals in CSF. The second part deals with metabolomics, in other words the metabolites in CSF were evaluated. Within the third part a data integration combines the results of the metallomics investigations with the metabolomics investigations to even increase the knowledge about changes ongoing in PD patients. Finally, the comparison between both groups of patients was meant to show differences in metallomics and metabolomics in order to identify an explanatory approach for the development and progression of Parkinson´s disease.

As shown in picture 2-1 each part is divided into different analytical tasks and is explained in the respective chapter. Within the metallomics part, the influence of different metals was examined from different points of view. The first task was a determination of the concentration of Cu, Fe, Mn, and Zn in CSF (chapter 3.2). These four metals are most discussed in the literature in regard to PD. Subsequently, a species characterization by SEC-ICP-MS of the mentioned metals was done (chapter 3.3). Additionally, speciation approaches were performed in order to separate species of selenium compounds (chapter 3.4) and different oxidation states of Fe (chapter 3.5). Selenium as well as iron are key metals in neurodegenerative processes since they are involved in oxidative stress reactions. Fractions of separated amino acids (part of metabolomics part) were collected. These fractions were also analyzed for their metal

concentration. For this task, the range of metals was enlarged to Cu, Fe, Mg, Mn, Ni, Sr, and Zn (chapter 3.6).

Metallomics

- Concentration of Cu, Fe, Mn and Zn   {chapter 3.2}
- Species characterization of Cu, Fe, Mn and Zn   {chapter 3.3}
- Speciation of Se   {chapter 3.4}
- Determination of oxidative states   {chapter 3.5}
- Metal determination in amino acid fractions   {chapter 3.6}

Metabolomics

- Determination of amino acids   {chapter 3.6}
- Determination of D-/L-amino acids   {chapter 3.6}
- Metabolic profiling   {chapter 3.7}
- Determination of specific PD-markers   {chapter 3.8}

Data integration of Metallomics & Metabolomics
{chapter 3.9}

Figure 2-1: Overview of the thesis. The work is divided into three main investigations parts. The first part outlines the alteration of different metals to PD. The second part illustrates the perturbation of some defined metabolites and additionally illustrates a metabolic profiling approach. The last part integrates the results of the first and second part to increase the insight into changes between the compared groups.

The second part of this work has shed light on the metabolic composition of CSF and the specific differences between PD and controls. Since the metallomic investigation showed specific changes in amino-acid-fractions, amino acids were separated and analyzed (chapter 3.6). Additionally, an enantioseparation of amino acids was

performed to even enhance the knowledge about this compound class in relation to PD (chapter 3.6). The major task within the metabolomics part was an untargeted metabolic profiling to unravel affected metabolites and to generate a new hypothesis (chapter 3.7). Finally, specific markers for oxidative stress and neuroinflammation were investigated (chapter 3.8).

A really important topic within this work is the combination of these two parts. The data integration of metallomics and metabolomics was performed in order to understand the mutual interactions between metals and metabolites (chapter 3.9).

All obtained results are shown within the next chapters and are discussed in relation to literature.

3. Results and Discussion

3.1 Patients

The investigations were done in a case-control design to compare both patient groups against each other and find possible differences indicating affected mechanisms and pathways in disease. We had a total of 134 CSF samples taken at Cologne University Hospital by standardized lumbar puncture. The samples were taken for routine analysis in the hospital and originally were not intended for research purposes. CSF samples are only allowed to take after medical indication. Since not planned for speciation, samples were not aliquoted and frozen to -80°C directly after sampling, but stood up to six hours at room temperature. Therefore, possibly sample degradation and species changes could have happened in the meantime. Several studies indicate a fast metabolic conversion and degradation of species and metabolites in only short timeframes after sample-isolation (Wishart *et al.*, 2008; Michalke *et al.*, 2009; Diederich and Michalke, 2011).

The 134 samples were divided into 33 PD-samples and 101 neurologically healthy controls. Since it is not allowed to perform a lumbar puncture in persons without any complaints, control samples originate from persons with neurological symptoms but without any neurological diagnosis. Typical diagnoses are headache and migraine. The cases are diagnosed with Parkinson´s disease, but have different manifestations of symptoms and various concomitant diseases. As different the manifestations as different is the medication of patients. Nineteen of PD-patients didn´t had a medication (mostly due to first diagnosis), 3 patients got a different medication (acetylsalicylic acid, second-generation antipsychotics, and tricyclic antidepressants) and the remaining patients got specific PD-drugs. The first category of PD-drugs is dopamine or dopamine agonists like L-dopa, Madopar[®], Clarium[®], and Sifrol[®]/Pramipexol. The second category contains drugs hampering the degradation of dopamine like Azilect[®] and amantadine and the third one removes the excess of acetylcholine so called anticholinergics like Artane[®]. Two of the PD-patients got electrodes for deep brain stimulation, a method

improving motor symptoms as well as non-motor symptoms as reviewed in (Moldovan *et al.*, 2015).

The average age of PD-patients is 65 years (range 40-82 years) and for the control (CTR)-patients 45 years (range 18-82 years). The mean duration of the disease is 1.4 years (range from first diagnosis -18 years). To overcome the inhomogeneity in age, all results have been tested for influence of age in both groups separately and together. Some investigations, only done for a subset of samples, have been selected to increase comparability in age.

Due to the differences in PD-manifestation, treatment, and duration of disease no further association of values with these features was possible to define. Moreover, long standing at room temperature most probably caused degradation and metabolic conversion of samples which could not be defined more closely.

3.2   *Determination of Cu, Fe, Mn and Zn in CSF*[1]

A lot of indications in neurodegeneration research are leading to the involvement of different metals into development and progress of diseases. Redox active metals are involved in the generation of oxidative stress, a major injury process in all neurodegenerative diseases. Especially in PD, metals are also involved in the misfolding and aggregation of the protein α-synuclein. Most notably, the metals Cu, Fe, Mn and Zn are in focus. The redox activity of Cu, Fe, and Mn can induce or increase the amount of oxidative stress within brain and adjacent fluids and tissues. Zn is not redox active, but also an essential metal for many biological functions within human body. Therefore, the determination of these four metals in CSF is of paramount importance. For the investigation of neurodegenerative diseases CSF is the most suitable compartment. It is in close contact to the brain and hence can reflect changes in the chemical composition.

---

[1] The following chapter has been partially prepublished in (Willkommen *et al.*, 2018*b*)

For the metal determination approach we used the full set of samples for analysis, means a total of 134 CSF samples. Out of these samples, 33 originated from PD-patients (age ± SD: 65.1 ± 12.9 years; sex: 10 female, 23 male; disease duration ± SD: 1.39 ± 3.7 years) and 101 samples were taken from neurologically healthy controls (age ± SD: 44.8 ± 17.3 years, sex: 63 female, 38 male).

The concentrations of Cu, Fe, Mn, and Zn were measured by means of ICP-sf-MS at the instrument Element2 (Thermo Fisher Scientific, Germany). Samples were diluted 1:10 or 1:20 in Milli-Q-water for appropriate analysis. A multi-elemental standard was used for a 4-point calibration (0 ng/L, 250 ng/L, 500 ng/L and 1000 ng/L of each metal). For all measurements rhodium (Rh) was constantly introduced as internal standard with a final concentration of 1 µg/L. Technical parameters are summarized in Table 4.

Table 4: Instrumental parameters for elemental analysis of CSF samples by use of ICP-sf-MS.

parameter	specification
Analytes detected	^{55}Mn, ^{56}Fe, ^{63}Cu, ^{66}Zn, ^{103}Rh
Detection mode	Medium resolution
Conditions	1170 W RF power
	16 L Ar/min plasma gas flow
	0.99 L Ar/min nebulizer gas flow
	0.65 L Ar/min auxiliary gas flow

The respective concentrations in each sample were calculated by the instruments software, based on the calibration done. Before and after each sample block, consisting of 6 samples, a blank and a multi-elemental standard were measured to control

variations of the instrument. Afterwards, element concentrations were recalculated by a laboratory data management system (Elana 3.3; HM Informatik AG, Ilmenau, Germany) to obtain final concentration values. The used software aligns concentrations to blank and control standard concentrations as well as to dilution factor.

Results and Discussion

The elemental status of CSF gains knowledge about neurodegenerative diseases. Several trace elements are important co-factors in various enzymes, but in excess can be deleterious to the human brain. Consequently, the concentration of metals in CSF of PD patients in comparison to CTR samples was measured already several times. These investigations report inconsistent outcomes. Therefore, a concentration determination within our sample set was carried out in order to assess the levels of Cu, Fe, Mn, and Zn in CSF. The results of our evaluation are listed in Table 5 as mean values with respective standard deviation (SD) for CTR and PD. A general linear model (GLM) was applied to lg(x+1) transformed concentrations. The transformation was done in order to reach the normality of the errors and to reduce the skewed distributions. In the GLM the least square means were calculated to identify alterations between CTR and PD. A significance level $p<.05$ was considered to be statistically significant (* $p<.05$, ** $p<.01$, *** $p<.001$). The evaluation was done in SAS, version 9.3 (SAS Institute Inc., Cary, NC, USA)

Table 5: Mean concentrations of the elements Cu, Fe, Mn and Zn in CSF of PD compared to CTR with respective p-values for differentiation. None of the elements is significantly different between both states, although changes are present especially for Fe.

element	concentration CTR ± SD in µg/L	concentration PD ± SD in µg/L	p-value
Cu	38.57 ± 33.11	43.18 ± 25.74	0.991
Fe	18.84 ± 10.10	24.93 ± 14.63	0.434
Mn	0.50 ± 0.31	0.45 ± 0.25	1.000
Zn	15.80 ± 7.59	18.98 ± 7.01	0.891

As shown with respective p-values all four trace metals are insignificantly different in PD compared to CTR. The highest differentiation power is provided by Fe which is slightly increased in PD. As already mentioned, in literature inconsistent outcomes for CSF investigation are reported. A decrease of the concentration of Fe either significant (Bocca *et al.*, 2006; Alimonti *et al.*, 2007) or insignificant (Gazzaniga *et al.*, 1992; Jimenez-Jimenez *et al.*, 1998; Forte *et al.*, 2004; Maass *et al.*, 2018) was reported, but also an increase, again, either significant (Qureshi *et al.*, 2006) or insignificant (Hozumi *et al.*, 2011). Besides the difference in tendency of concentration, also the range of concentration differs heavily. Some values are within the same range as obtained within our investigation (Forte *et al.*, 2004; Bocca *et al.*, 2006; Alimonti *et al.*, 2007), but the other obtained values are increased by a factor of 10 compared to our values (Gazzaniga *et al.*, 1992; Jimenez-Jimenez *et al.*, 1998; Qureshi *et al.*, 2006; Hozumi *et al.*, 2011). The same is true for published concentration range of Cu, Mn and Zn in CSF of PD patients and CTR. The values reported by (Forte *et al.*, 2004; Bocca *et al.*, 2006; Alimonti *et al.*, 2007) are in the same range as obtained within our investigation. In the cases of Cu and Zn the concentrations are increased by a factor of 10 of (Jimenez-

Jimenez *et al.*, 1998; Qureshi *et al.*, 2006), in case of Mn the levels of (Gazzaniga *et al.*, 1992; Hozumi *et al.*, 2011) are increased by a factor of 10. In parallel to Fe, for Cu, Mn, and Zn the tendency of increased or decreased values is inconsistent among studies. For Cu four studies with insignificantly decreased values (Jimenez-Jimenez *et al.*, 1998; Bocca *et al.*, 2006; Qureshi *et al.*, 2006; Alimonti *et al.*, 2007) and three studies with increased values (Gazzaniga *et al.*, 1992; Forte *et al.*, 2004; Hozumi *et al.*, 2011) are published. For Mn three studies with increased (Jimenez-Jimenez *et al.*, 1998; Forte *et al.*, 2004; Hozumi *et al.*, 2011) and three studies with decreased values (Gazzaniga *et al.*, 1992; Bocca *et al.*, 2006; Alimonti *et al.*, 2007) could be found. The majority of published levels of Zn in CSF showed a decreasing trend for PD (Jimenez-Jimenez *et al.*, 1998; Forte *et al.*, 2004; Bocca *et al.*, 2006; Qureshi *et al.*, 2006; Alimonti *et al.*, 2007), whereas only one study found significantly increasing concentrations (Hozumi *et al.*, 2011).

All of these studies show different elemental fingerprints for the measured trace elements, for none of them a consistent trend of either increasing or decreasing concentration could be observed. Consequently, a single element can´t be used as a marker for PD. Different reasons are already mentioned within literature. On the one hand, there are clinical parameters, such as inappropriate patient and CTR groups or blood contamination in the samples (Mariani *et al.*, 2013; Jimenez-Jimenez *et al.*, 2014). On the other hand, individual variations due to medication, origin, diet or additional diseases can influence the metal concentration in CSF. A differentiation based on an elemental fingerprint gained a good classification of PD and CTR by the combined use of six trace elements (Se, Fe, As, Ni, Mg and Sr) (Maass *et al.*, 2018). Since differentiation based on a single element failed, an approach with combining several elements to differentiate PD from non-PD could help clinics to separate the PD-patients from different diseases.

Although our investigations showed only insignificant shifts in total metal concentrations, the trend of increasing Fe-concentrations in PD was more distinct. Fe is an essential cofactor for a lot of enzymes mandatory for normal brain function, but in excess can be deleterious. The balance of Fe is controlled by the iron-regulatory proteins IRP1 and

IRP2 (Rouault, 2006). Fe accumulates in brain while aging and neurodegeneration (Lan and Jiang, 1997; Zhang *et al.*, 2010; Ramos *et al.*, 2014). The accumulation of Fe can finally lead to neuronal death via various ways. On the one hand side, Fe produces ROS via Fenton and Haber-Weiss reaction (Sun *et al.*, 2016). On the other hand side, mitochondrial dysfunction can lead to lower synthesis of Fe-S clusters (Lill *et al.*, 2006), followed by divalent metal transporter 1 (DMT1) activation and Fe accumulation. The accumulation again causes oxidative stress and oxidative stress leads to lipid peroxidation, protein misfolding and aggregation and finally to cell death (Zucca *et al.*, 2017). Therefore, the slightly increased Fe-concentrations observed in the CSF of PD patients might be the sign of neurodegenerative processes ongoing in the brain. It remains unclear whether the accumulation of Fe is a reason or the response to neurodegenerative processes.

Conclusion

We investigated the metallomic composition of CSF by determining the concentration levels of Cu, Fe, Mn, and Zn. The concentrations were insignificantly differentiating between CTR and PD. The inconsistent values reported in literature are leading to the conclusion that single levels of metals in CSF are not suitable for biomarker use. However, the combination of several metals might be sufficient for differentiation. Nevertheless, trends of increasing Cu and Fe concentrations are leading to misbalances in metal-homeostasis which needs to be further addressed.

3.3   *Species characterization*[2]

3.3.1 Characterization by means of SEC-ICP-MS

The differentiation of PD and CTR based on the determination of total elemental concentrations was not possible. The influencing factors on the total concentration are too diverse among patients. Therefore, a more detailed analysis of metals with specific binding partners seems to be more informative. Metals like Fe, Cu, Mn, and Zn are part

---

[2] The following chapter has been partially prepublished in (Willkommen *et al.*, 2018*b*)

of various essential proteins and enzymes (e.g. Fe in ferritin or transferrin), but can also be complexed by organic compounds like citrate (Cit) within human body. The knowledge about the different binding partners can give further information about the mechanisms and pathways which are involved in disease onset and progression. Therefore, to characterize different species is of great interest in studying human diseases. Our approach used SEC for the separation of different size-fractions in the CSF-samples. Since CSF is still a complex sample matrix the drawbacks, already mentioned in chapter 1.1.1, exist. This means low separation capacity does not allow a complete speciation, but only a species characterization according to their molecular mass.

Study participants and Method

For the species characterization approach we used again the full set of samples for analysis, means a total of 134 CSF samples. Out of these samples, 33 originated from PD-patients (age ± SD: 65.1 ± 12.9 years; sex: 10 female, 23 male; disease duration ± SD: 1.39 ± 3.7 years) and 101 samples were taken from neurologically healthy controls (age ± SD: 44.8 ± 17.3 years, sex: 63 female, 38 male).

The species characterization of Fe, Mn, Cu and Zn was realized by the hyphenation of a separation technique, High Performance Liquid Chromatography (HPLC)-system (Knauer 1100 Smartline inert Series), with an element-selective detection, an ICP-MS-system (NexIon 300D, Perkin Elmer). The HPLC-system was equipped with two columns to ensure the separation of high and low molecular mass (HMM/LMM) compounds. A glass body column (600x10 mm ID) packed with Toyopearl TSK HW 55S (TosoHaas, Stuttgart, Germany) and a separation range from 1-700 kDa was used for the separation of HMM. A second PEEK column (250 x 8 mm ID) was packed with Toyopearl TSK HW 40S (TosoHaas, Stuttgart, Germany) for the separation of LMM (below 2 kDa). The eluent was chosen according to Neth et al. (Neth *et al.*, 2015b). The effluent of the columns passed a UV-detector (254 nm, 220 nm) and was introduced through a Meinhard nebulizer and a cyclon spray-chamber to ICP-MS for element-selective detection. Instrumental Parameters of measurement are listed in Table 6.

Table 6: Instrumental parameters for elemental analysis of CSF samples by use of SEC-ICP-MS. DRC-dynamic reaction cell.

Parameter	Specification
Analytes detected	^{55}Mn, ^{57}Fe, ^{63}Cu, and ^{66}Zn
Detection mode	DRC mode with NH_3 as reaction gas
Conditions	1300 W RF power 17 L Ar/min plasma gas flow 0.92 L Ar/min nebulizer gas flow 0.52 mL NH_3/min cell gas flow 1000 ms dwell time

Column mass calibration

Prior to sample measurement, a column mass calibration was carried out for both SEC columns. The retention times (RT) of the listed standards (Table 7) were recorded either by use of the UV-detector or ICP-MS. The calibration of column is necessary for assignment of possible unknown species eluting while CSF analysis. The obtained RT can be used to determine the approximate molecular weight.

Table 7: Standards with known molecular weight used for column mass calibration are listed. The respective retention time which was obtained for the used column combination was added.

compound	Molecular weight (MW) in kDa	Log MW	RT in min
Ferritin	440	5.64	28.5
γ-globulin	190	5.18	38.1
arginase	107	5.07	31.2
transferrin	78	4.89	39.4
HSA	66	4.82	39.0
β-lactoglobulin	37	4.56	42.6
Oxidized glutathione (GSSG)	0.612	2.79	52.1
Reduced glutathione (GSH)	0.307	2.49	46.6
citrate	0.192	2.28	51.8
Glutamic acid	0.147	2.17	68.0
Inorganic Fe	0.056	1.74	95.0

The obtained RTs were correlated to respective molecular masses to receive mass calibration curves for both used columns. For HMM-compounds the calibration equation $\log(MW)=-0.0009RT^3+0.0977RT^2-3.5058RT+46.998$ ($R^2=0.9942$) and for LMM-species $\log(MW) = -0.014RT+3.0772$ ($R^2=0.9546$) was calculated.

Results and Discussion

With the use of the applied method, we were able to separate four different size fractions as illustrated in Fig. 3-1 exemplarily for Mn (typical SEC-ICP-MS-chromatograms of Fe, Cu and Zn are illustrated in Appendix Fig. A1). The fractions are named by characteristic compounds of the fraction or by characteristic size information. We could separate "high molecular mass" (HMM), "Citrate" (Cit), "Amino acids" (AA), and "Inorganic species" (IOS). Each fraction contains most probably more than one compound, but without further separation. The four separation areas were defined by the implemented column mass calibration. As already shown, several compounds of different molecular weight were measured and the respective retention times recorded to obtain a size calibration equation.
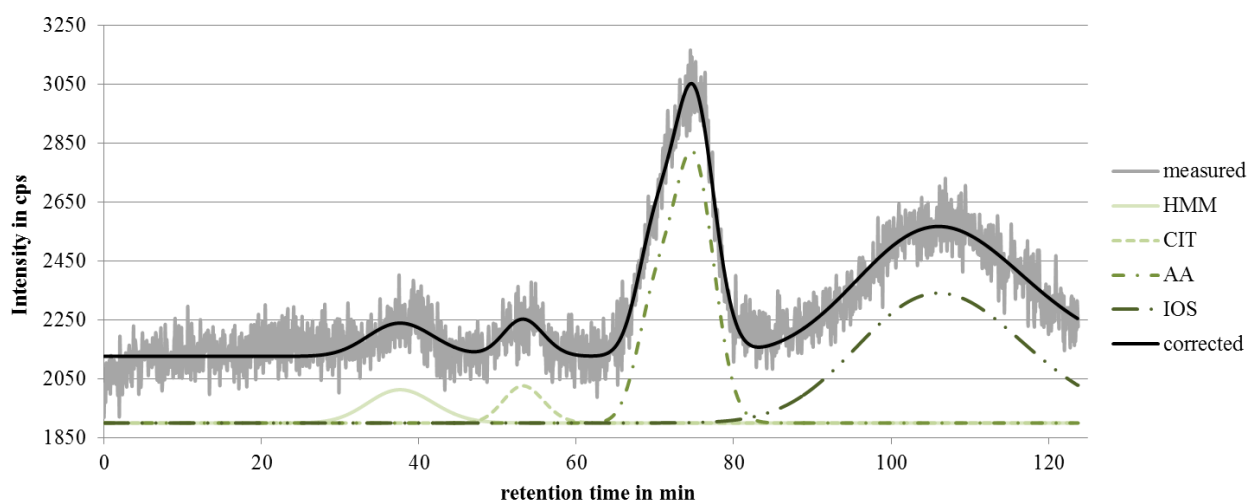
Figure 3-1: Observed SEC-ICP-MS-chromatogram (, with graphical off-set) of Mn in CSF with fractions aligned (— , aligned chromatogram, with graphical off-set) by use of PeakFit[TM] software. Species detected are „HMM" (—), „Citrate" (- - -), „Amino acids" (- · -), and „Inorganic species" (— · · —).

The evaluation of chromatograms was done by use of the software PeakFit[TM]. This program was applied to identify the species fractions and to calculate peak-areas. The mean concentrations of the various elements and species fractions are listed in Table 8 for CTR and PD. Like for the total concentrations, a GLM was applied to the lg(x+1)

transformed concentrations to differentiate CTR and PD. Again, a significance level p<.05 was considered to be statistically significant (* p<.05, ** p<.01, *** p<.001).

Table 8: Mean concentrations ± SD of Fe, Cu, Mn, and Zn derived from the separated size-fractions. None of the values significantly differentiate between CTR and PD. Inter-individual variations are too big. HMM-high molecular mass; AA-amino acid, IOS-inorganic species.

		$c_{(Fe)}$ in µg/L	$c_{(Cu)}$ in µg/L	$c_{(Mn)}$ in µg/L	$c_{(Zn)}$ in µg/L
HMM	CTR	0.15±0.41	33.99±60.46	0.03±0.06	1.88±2.79
	PD	0.20±0.48	33.86±24.64	0.03±0.04	1.86±1.71
Citrate	CTR	0.31±0.60	11.49±9.78	0.05±0.05	3.90±4.44
	PD	0.51±0.67	11.85±8.97	0.04±0.03	4.25±2.49
AA	CTR	0.85±1.41	6.11±9.61	0.12±0.09	2.80±2.31
	PD	1.16±1.12	3.93±3.73	0.10±0.07	3.05±1.86
IOS	CTR	20.73±13.98	< LOD	0.36±0.28	9.54±6.19
	PD	28.13±21.46	< LOD	0.31±0.23	11.71±5.47

As shown in Table 8, the distribution of the elements to the four different size fractions is approximately the same for Fe, Mn, and Zn but opposite for Cu. Cu is mainly associated with HMM, to a lesser extent to Citrate and AA, and is not present in its inorganic form. In contrast to Cu, the metals Fe, Mn, and Zn mainly exist in their inorganic form and smaller amounts are associated with HMM, Citrate, and AA. These findings are consistent with literature. Cu was also found to be mainly bound to HMM in CSF (Nischwitz *et al.*, 2008). A proportion of about 35% of the total Cu content is bound to ceruloplasmin in CSF according to Capo et al. (Capo *et al.*, 2008). Ceruloplasmin is a

Cu-storage protein able to bind up to 6 Cu-ions and with antioxidant capacity by scavenging radicals (Hung *et al.*, 2010a; Barbariga *et al.*, 2015). Ceruloplasmin has been investigated in CSF of PD-patients. The concentration for PD-patients was found to be 1915±223 µg/L and for CTR to be 1566±157 µg/L (Loeffler *et al.*, 1994). Fe, Mn, and Zn are mainly bound to HMM in serum and have a defined transport into CSF. The transport of LMM-compounds is less controlled and therefore higher amount of metals associated with these species can possibly reach CSF (Michalke and Nischwitz, 2010). Different ways of transportation for the mentioned metals are reviewed by Yokel (Yokel, 2006). Mn-citrate transport across neural barriers is controlled only slightly (Crossgrove and Zheng, 2004; Yokel and Crossgrove, 2004). Different studies indicate Mn-citrate to be the predominant species in CSF (Crossgrove and Zheng, 2004; Yokel and Crossgrove, 2004; Nischwitz *et al.*, 2008), but our investigations indicate inorganic Mn rather than Mn-citrate to be the predominant species. NMR-investigations showed a degradation or transformation of citrate up to 50% in CSF samples standing at room temperature for 72 h (Levine *et al.*, 2000). Since our samples stood up to 6 h while clinical investigation before being stored at -20 °C, partial degradation and transformation of Mn-citrate to inorganic Mn could not completely excluded. This could explain our finding.

Since species characterization was able to give further insights to other neurodegenerative diseases like AD (Richarz and Bratter, 2002), Manganism (Neth *et al.*, 2015a) and ALS (Vinceti *et al.*, 2013), our approach was planned to give further information about metals associated with different proteins, amino acids, and other small molecules. The partial least square means of each metal fraction was calculated after log(x+1)-transformation. Differences between CTR and PD were calculated after Scheffe adjustment. The statistical output of the comparison between CTR and PD gained no significant differentiation, however trends were anyway found. The three highest ranked differences (CTR compared to PD) are:

1.) Decrease of Cu-AA fraction (p=0.06)

2.) Increase of Fe-IOS fraction (p=0.16)

3.) Increase of Zn-IOS fraction (p=0.18)

Additionally, we calculated the normalized species percentages distribution of each sample (normalized to total element concentration = 100%). Since the inter-individual variation observed in total element concentration can hide intra-individual species shifts, this approach can reflect these changes of species pattern more precisely. In Table 9 the percentages distribution of the elements is listed.

Table 9: Mean percentages ± SD of Fe, Cu, Mn, and Zn derived from the separated size-fractions. None of the values significantly differentiate between CTR and PD. Inter-individual variations are too big. HMM-high molecular mass, AA-amino acid, IOS-inorganic species.

		% Fe	% Cu	% Mn	% Zn
HMM	CTR	0.63±1.48	60.48±17.13	5.52±7.98	9.22±11.24
	PD	0.50±0.69	67.41±9.56	5.77±6.12	9.65±6.96
Citrate	CTR	1.51±2.40	24.95±10.58	8.38±6.87	20.33±10.67
	PD	1.57±1.47	23.86±7.55	9.15±5.93	20.14±4.45
AA	CTR	4.23±4.86	14.57±18.09	22.28±9.00	15.87±9.11
	PD	3.56±2.01	8.73±6.95	22.59±6.80	14.63±7.39
IOS	CTR	93.64±7.76	0.00±0.00	63.82±13.56	55.71±15.23
	PD	94.37±3.49	0.00±0.00	62.49±12.24	55.58±9.69

Statistical analysis again showed no significant differences, but trends. For the percentages values the three highest ranked differences (CTR compared to PD) are:

1.) Increase of Cu-HMM fraction (p=0.12)

2.) Increase of Cu-LMM fraction (p=0.31)

3.) Decrease of Cu-AA fraction (p=0.35)

Trends were mainly found for Cu species, especially a shift from Cu-AA toward Cu-HMM species. This indicates a strong involvement of Cu species to the etiology of PD. Cu is a tightly regulated trace element; any disruption of its homeostasis can lead to severe diseases of the central nervous system. Disease like Menkes and Wilson´s disease are proven to be associated with Cu-deficiency or excess (Davies *et al.*, 2016). As already mentioned earlier, Cu is primarily bound to HMM in CSF (Nischwitz *et al.*, 2008). About 35% of total Cu is bound to ceruloplasmin, a Cu-storage protein with antioxidant capacity (Capo *et al.*, 2008; Hung *et al.*, 2010b; Barbariga *et al.*, 2015). Moreover, Cu is associated with metallothionein (MT) and superoxide dismutase (SOD). MT as well as SOD are antioxidant compounds present in CSF. An increase of the Cu-HMM fraction in CSF might be associated with increased oxidation processes in brain due to neurodegeneration. As a reason of increased oxidation processes the concentration of anti-oxidative compounds is enhanced. An enlarged concentration of ceruloplasmin was found in vascular dementia as response to inflammation (Arnal *et al.*, 2010). Therefore, enhanced Cu-HMM might not only be a reason of increased oxidative stress but also of inflammatory processes.

3.3.2 Ratios of species-fractions

Since species characterization did not show significant differentiation between CTR and PD, literature also points to the importance of the balance between different elements and species. This means a change in element- or species-ratios seems also to be involved in PD, because any misbalance can increase the risk of oxidative stress (Fernsebner *et al.*, 2014; Michalke *et al.*, 2017). Therefore, ratios between different species-fractions and between species-fractions and total element concentrations have been calculated. The ratios were compared for differing behavior in CTR and PD. In Table 10 the significant ratios derived from the percentages values of species characterization are listed. Additionally, Fig. 3-2 shows the three ratios with highest significance to be increased in PD-samples.

Table 10: Significantly increased ratios (PD vs. CTR) derived from the percentages values of species fractionation with respective p-values. AA-amino acid, c-concentration, Cit-citrate, IOS-inorganic species, LMM-low molecular mass.

ratio	Alteration (CTR to PD)	p-value
total $c_{(Fe)}$ vs. $AA_{(Cu)}$	↑	<0.001
total $c_{(Zn)}$ vs. $LMM_{(Cu)}$	↑	0.002
$IOS_{(Mn)}$ vs. $AA_{(Cu)}$	↑	0.005
$LMM_{(Mn)}$ vs. $AA_{(Cu)}$	↑	0.009
total $c_{(Fe)}$ vs. $LMM_{(Cu)}$	↑	0.014
$AA_{(Mn)}$ vs. $LMM_{(Cu)}$	↑	0.018
$LMM_{(Mn)}$ vs. $LMM_{(Cu)}$	↑	0.021
$Cit_{(Zn)}$ vs. $AA_{(Cu)}$	↑	0.033
$IOS_{(Zn)}$ vs. $AA_{(Cu)}$	↑	0.036
$LMM/IOS_{(Zn)}$ vs. $AA_{(Cu)}$	↑	0.046
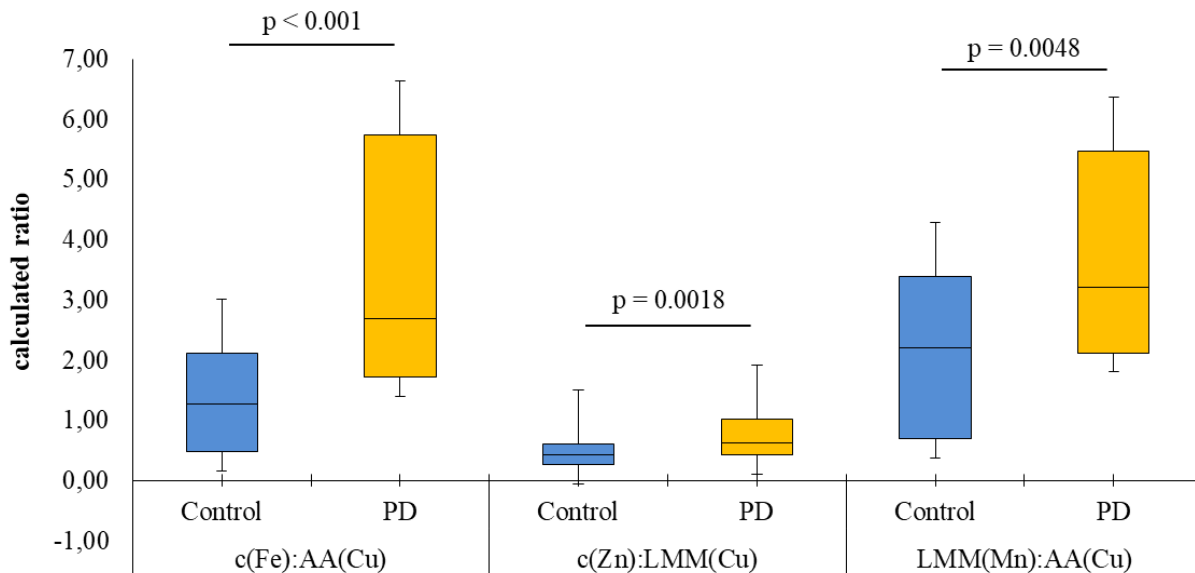
Figure 3-2: Box-plot of the most significant element-ratios observed by comparing CTR and PD. Especially ratios with small Cu-fractions, especially Cu-AA, in denominator are involved in these increased ratios in PD.

It is obvious from Table 10 and Fig. 3-2, that all of the significant ratios are increased in PD. Thereby, in the denominator was always a LMM-species, more specifically the AA-species, of Cu. The most significant ratio could be observed between Fe and Cu. A misbalance between these two elements was already shown in literature. Ahmed and Santosh (Ahmed and Santosh, 2010) investigated inter-element ratios in serum of 42 CTR- and 45 PD-samples showing affected ratios between Cu/Fe, Cu/Zn, Fe/Zn, Mn/Zn, Fe/Mn, and Cu/Mn. A recent study evaluated element interactions in 110 CSF-samples of CTR- and PD-patients (Sanyal *et al.*, 2016). They found altered ratios for Cu/Fe and Fe/Mn. The Fe- and Cu-homeostasis is closely connected in brain. A rat-experiment with either Fe-overload or Fe-deficiency showed the direct impact on Cu-regulation (Monnot *et al.*, 2011). An Fe-overload caused an significantly decreased Cu-concentration (56%) in CSF, while Fe-deficiency triggered an increase in Cu-concentration (52%). Additionally, Cu-transport into CSF is significantly enlarged in Fe-deficiency (Collins, 2006; Monnot *et al.*, 2011). A detailed review of the influence of Fe

and Cu on the homeostasis of the respective other element is given by (Skjorringe *et al.*, 2012).

Since most ratios involve Cu-AA fraction, amino acids seem to play a prominent role in PD-etiology. In line with this change in AA-metabolism, shifts were also discovered in a rat model with induced manganism (Neth *et al.*, 2015b). In general, misbalanced Cu-species have an important impact in development and progression of PD (Rowinska-Zyrek *et al.*, 2015). Since Cu is a redox-active metal (in human body oxidation states +1/+2), it can cause oxidative cell damage via Fenton-like reactions (Sayre *et al.*, 1999; Dringen *et al.*, 2013; Rowinska-Zyrek *et al.*, 2015). Cu, in both oxidation states, is also capable to form complexes with α-Synuclein, an important protein in PD-pathology, further accelerating ROS-formation (Rowinska-Zyrek *et al.*, 2015). As central atom, Cu is part of the anti-oxidative enzyme Cu-Zn-SOD, reducing the amount of ROS (Yang *et al.*, 1998). Therefore, Cu is an important factor for proper brain function, misbalances in Cu-metabolism can lead to reduced anti-oxidative function (Cu-Zn-SOD) (Yang *et al.*, 1998) and/or enhanced ROS-production (Sayre *et al.*, 1999; Bolognin *et al.*, 2009; Rowinska-Zyrek *et al.*, 2015) and finally to modifications in neurotransmission (Kozlowski *et al.*, 2012).

When calculating the ratios from the metal concentrations of each species, again 10 highly significant interactions can be evaluated, as listed in Table 11. Again, most of the ratios contain the Cu-AA fraction. This underlines the importance of amino acids, especially when bound to Cu in the pathophysiology of PD.

Table 11: Significantly increased ratios (PD vs. CTR) derived from the amount values of species fractionation with respective p-values. AA-amino acid, c-concentration, IOS-inorganic species.

ratio	Alteration (CTR to PD)	p-value
$IOS_{(Fe)}$ vs. $AA_{(Cu)}$	↑	0.005
total $c_{(Fe)}$ vs. $AA_{(Cu)}$	↑	0.006
$IOS_{(Fe)}$ vs. total $c_{(Mn)}$	↑	0.011
$IOS_{(Fe)}$ vs. $IOS_{(Mn)}$	↑	0.012
total $c_{(Fe)}$ vs. $IOS_{(Mn)}$	↑	0.013
$IOS_{(Zn)}$ vs. $AA_{(Cu)}$	↑	0.029
$AA_{(Fe)}$ vs. $AA_{(Cu)}$	↑	0.031
total $c_{(Fe)}$ vs. $AA_{(Mn)}$	↑	0.036
$IOS_{(Fe)}$ vs. $AA_{(Mn)}$	↑	0.040
$AA_{(Fe)}$ vs. $IOS_{(Mn)}$	↑	0.044

Apart from Cu, several ratios between Fe and Mn are affected in PD. Both trace metals share similar chemical properties; they are redox-active and partly use same transporters to cross neural barriers. Therefore, Fe and Mn have a closely connected metabolism which can lead to misbalances in the ratios of them if one or the other is enhanced in the human body. The Fe- and Mn-speciation was evaluated in vivo in rats after a non-toxic injection of $MnCl_2 \cdot 4H_2O$ (Diederich *et al.*, 2012). One hour after the

injection native Mn-carriers were strongly increased in serum. Additionally, LMM-species of Mn, especially Mn-Cit was formed within this timeframe. After 4 days the serum was cleared from the Mn overload. Interestingly, iron speciation was completely unaffected through Mn-injection. In contrast to these results, within a study, the Fe-homeostasis while Mn-exposure was investigated (Zheng *et al.*, 1999; Li *et al.*, 2006; Wang *et al.*, 2008) and the results indicate a disruption in Fe-homeostasis through Mn-exposure. They found an increased efflux of Fe from CSF to blood in Mn-exposure scenarios. Therefore, Mn-exposure facilitates Fe transport from CSF to blood, especially via DMT1. Moreover, Mn-exposed ferroalloy smelting workers were investigated in comparison to ferroalloy office workers and control subjects (Cowan *et al.*, 2009). Significantly increased Mn-concentrations were found in saliva, plasma, erythrocytes, urine, and hair of the Mn-exposed workers. Additionally, significantly reduced plasma and erythrocyte levels of Fe were proven. The decrease of Fe-concentration is the effect of the Mn-exposure. Hence, the Mn overload causes a disruption in Fe-homeostasis. The affected ratios found within our investigations may be also a sign of influenced Fe-/Mn-homeostasis through neurodegeneration.

Conclusion

The species fractionation of Cu, Fe, Mn, and Zn by means of SEC-ICP-MS illustrated the distribution of the elements to the different size fractions. None of these fractions significantly differentiated between CTR and PD, but we were able to find trends. Especially, the Cu-fractions showed a more significant variation between the states, indicating Cu-species to be promising study targets. Since it is widely accepted that metal homeostasis is disrupted through neurodegeneration, we tried to further investigate this metal balance in CSF. We have calculated ratios between different species to assess their balance. This approach showed several significant changes comparing CTR values with PD values. Again, Cu underlined its important position within this species characterization. Especially the Cu AA-fraction showed a high involvement in dysregulated ratios and needs to be analyzed in future experiments.

3.4 Se-speciation

Another essential trace element in human body and health is selenium (Se). Se is important for normal function of the central nervous system (CNS) since it is involved in motor performance, coordination, memory, and cognition. Within human body 25 Se-proteins have been found with various biological functions. Whereas, not for all proteins a specific function was already unraveled. Se-proteins always have selenocysteine (Sec) at their active site. A major function of Se-enzymes is their antioxidant power, especially glutathione peroxidases (GPX 1-4, 6). Therefore, GPX is of interest in relation to neurodegeneration. Additionally, Selenoprotein P (SELENOP) is important when speaking about neurological diseases like PD. SELENOP is the major Se-transporter throughout the whole body. Because of the overwhelming importance of different Se-species, speciation approaches addressing Se and its various binding forms are of paramount importance. Up to now, studies mainly focus on the concentration of Se in different body fluids or refer only one Se-species. Our approach, moreover, separated several Se-species within one measurement by hyphenated techniques to get more detailed information about involvement of species.

Study participants and Method

For this approach, only a reduced amount of samples have been analyzed due to partially low sample volume left. A comparable set of 13 PD-samples (age: 70.8 ± 8.7 years; 6 female, 7 male) and 13 control-samples (64.4 ± 11.2 years; 5 female, 8 male) were measured.

A HPLC-system (ICS 5000, Thermo Fisher), equipped with a strong anion exchange (SAX, AS-11, Thermo Fisher Scientific) column for separation, was hyphenated to ICP-MS (NexIon 300D) for the concurrent detection of Se-species. The method was adapted from Vinceti et al. (Vinceti *et al.*, 2017). In brief, the mobile phase consists of eluent A (3.33 mM Tris-HAc buffer, 5% MeOH, pH 8) and eluent B (10 mM Tris-HAc buffer, 500 mM NH_4Ac, 5% MeOH, pH 8). Gradient was as follows: 0-3 min 100% eluent A (0% eluent B); 3-10 min 100-70% eluent A (0-30% eluent B); 10-23 min 70-45% eluent A (30-55% eluent B); 23-26 min 45-43% eluent A (55-57% eluent B); 26-28 min 43-0%

eluent A (57-100% eluent B); 28-52 min 0% eluent A (100% eluent B); 52-54 min 0-100 % eluent A (100-0% eluent B); 54-60 min 100% eluent A (0% eluent B). The injection volume was 20 µL and the eluent flow 0.8 mL/min. The column effluent passed a UV-detector (220 nm) and was introduced through a Meinhard nebulizer and a cyclon spray-chamber to ICP-MS. The instrumental parameters of ICP-MS are listed in Table 12.

Table 12: Instrumental parameters for Se-speciation in CSF samples by use of SAX-ICP-MS. DRC-dynamic reaction cell.

parameter	specification
Analytes detected	^{77}Se, ^{78}Se, and ^{80}Se
Detection mode	DRC mode with CH_4 as reaction gas
Conditions	1300 W RF power
	17 L Ar/min plasma gas flow
	0.96 L Ar/min nebulizer gas flow
	0.58 mL CH_4/min cell gas flow
	200 ms dwell time

Results and Discussion

The speciation approach was able to separate SELENOP, SeM, GPX, SeIV, SeVI, Se-HSA and two unknown Se-containing compounds (U1, U2). Figure 3-3 illustrates a typical chromatogram obtained for a CSF-measurement. Not all Se-compounds are present in all samples.
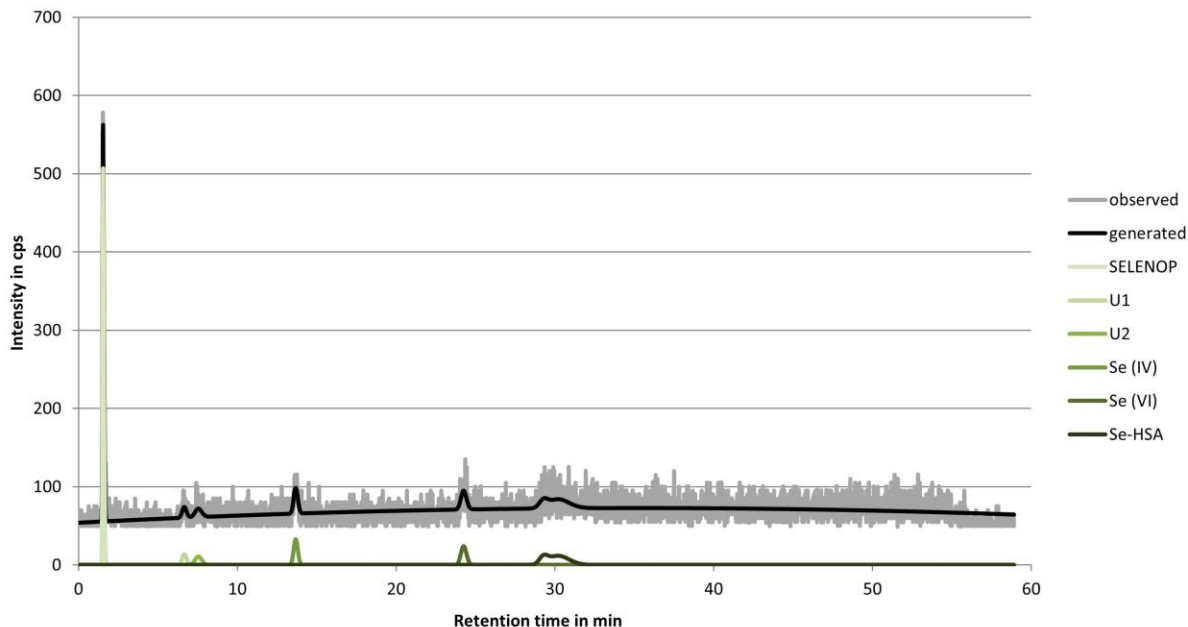
Figure 3-3: Observed SAX-ICP-MS-chromatogram (, with graphical off-set) of Se in CSF with fractions aligned (——, aligned chromatogram, with graphical off-set) by use of PeakFit[TM] software. Species detected are SELENOP, U1, U2, SeIV, SeVI, and Se-HSA.

For the speciation no Se-concentration has been determined, but the area under each signal was calculated by the use of PeakFit[TM] software. These areas could then be compared as shown in Fig. 3-4 A for PD vs. CTR as well as in Fig. 3-4 B for female vs. male. The statistical analysis revealed no significant difference in any of the compared species-signals. A t-test was performed in order to highlight differences between PD and CTR. A decrease in SELENOP (p = 0.55) and an increase in the unknown compound U2 (p = 0.51) showed up in PD. In comparison of males and females, a insignificant higher value for SeM (p = 0.19) and SeVI (p = 0.16) was observed. Additionally, age-dependence of Se-species was analyzed by means of Pearson correlation. A correlation of calculated area vs. age for all data points resulted for all species in a random distribution means no correlation with age. The fractionation into the groups (PD and CTR) showed for some species possible correlations. Fig. 3-4 E shows the correlation of age vs. SELENOP in PD, which has a moderate negative correlation (r = - 0.45). In PD also the species U2 (r = 0.45) and Se-HSA (r = 0.37)

showed a moderate correlation. In CTR only SeIV (r = 0.36) showed a moderate correlation.
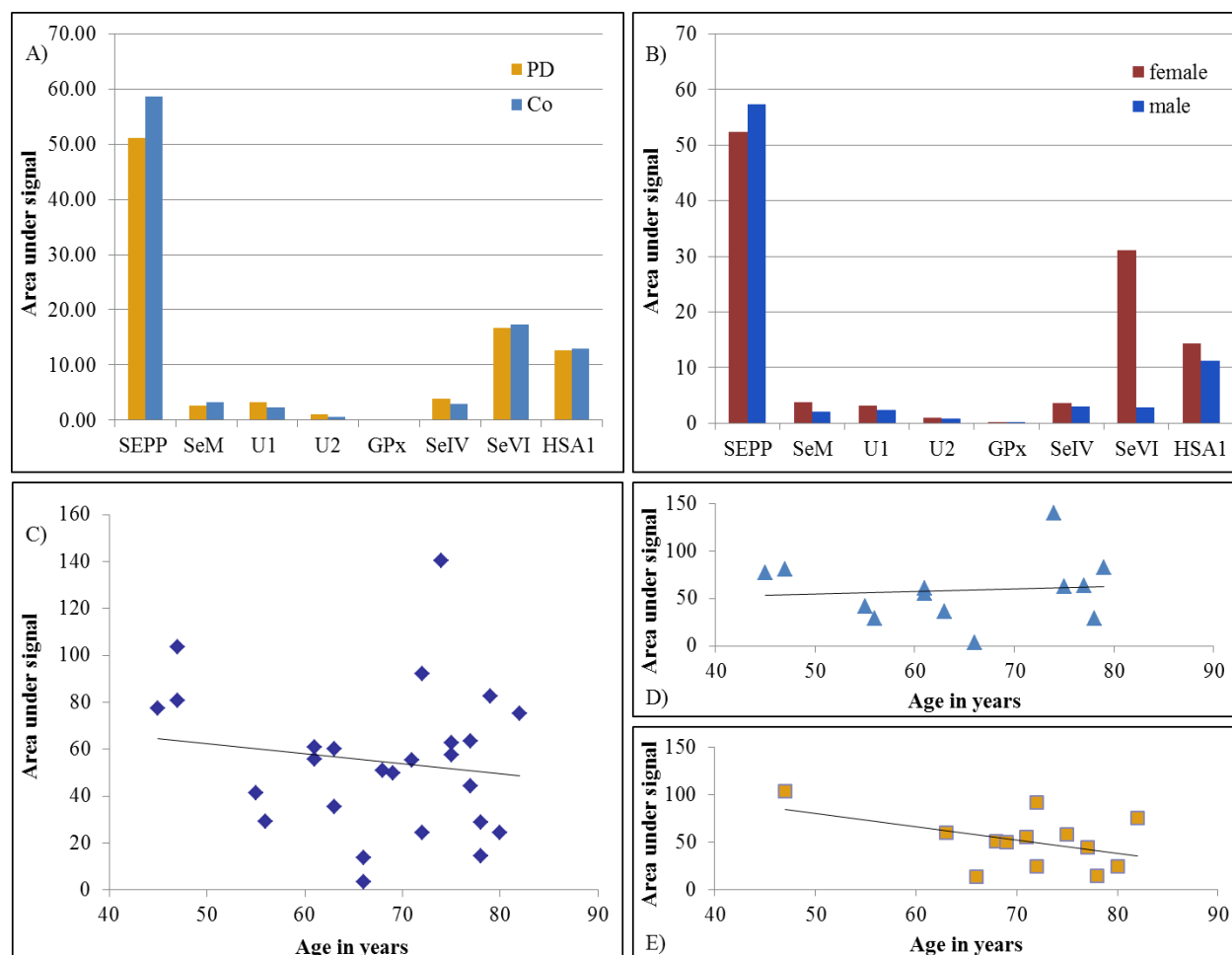
Figure 3-4: Results of Se-speciation in CSF of PD and CTR. A) Bar chart comparing the evaluated areas under the signal from PD and CTR for the separated Se-species; B) Bar chart comparing the evaluated areas under the signal from male and female samples for the separated Se-species; C) Scatterplot illustrating the correlation of age vs. area under the signal of SELENOP for all samples; Scatterplot illustrating the correlation of age vs. area under the signal of SELENOP for D) CTR-samples and E) PD-samples.

A speciation in CSF of PD patients hasn´t been done before. Therefore, a comparison with already published data is restricted to total Se concentration or analysis of specific Se-containing compounds. Total Se concentration has been measured already several

50

times in CSF as well as in other body fluids. The results within the same body fluid are consistent. In CSF increasing amounts of Se have been found in PD (Aguilar *et al.*, 1998; Qureshi *et al.*, 2006; Maass *et al.*, 2018) and the same is true for plasma (Zhao *et al.*, 2013). In contrast, serum Se levels decrease in diseased subjects (Nikam *et al.*, 2009; Ahmed and Santosh, 2010). The increased amount of Se in CSF seems to be a consequence of oxidative stress involved in neurodegeneration. Antioxidant compounds like GPX and thioredoxin reductases (TXNRD) were suggested to be increased to remove higher amounts of ROS within brain (Ellwanger *et al.*, 2016).

Since not all functions of selenoproteins are known and proven, SELENOP is also suggested to play a role in antioxidant activity but most likely it seems to be the major Se-transporter in the body, having 10 Sec residues. A mouse model with combined deletion of selenocysteine lyase and SELENOP (Scly$^{-/-}$ and SELENOP$^{-/-}$) caused severe neurological dysfunction and significantly decreased GPX activity in brain compared to wild-type mice. Additionally, TXNRD activity was also reduced markedly (Byrns *et al.*, 2014). Another study also investigated the influence of deleted SELENOP gene (SELENOP$^{-/-}$) but together with low and high Se-diet. A low Se-diet (0.1 mg Se/kg) in the SELENOP$^{-/-}$ mice caused a reduction to 43% of brain Se and the mice developed a reduced motor coordination. Afterwards, a high Se-diet (2 mg Se/kg) increased brain Se levels again to the control level (Hill *et al.*, 2003). A reduction of SELENOP, as observed within our investigation, therefore leads to reduced antioxidant capacity and accumulation of oxidative stress. This imbalance between oxidant damage and antioxidant capacity is hypothesized to be a crucial step in the development of neurodegeneration (Ansari *et al.*, 2004).

Conclusion

Although Se-speciation turned out to be very important in neurodegenerative research (Solovyev *et al.*, 2013; Mandrioli *et al.*, 2017), our investigations didn´t show any significant change in the Se-species. The applied method separated several Se-species and we observed shifts by comparing CTR and PD or female and male participants. The results lead to the assumption that specific Se-species are important in other neurodegenerative disease but not in PD or a shift of species happened during storage

or sample taking. Therefore, further experiments are necessary to prove or disprove the results.

3.5   *Determination of the oxidative states of iron*

Fe is an essential trace element in human body, but in excess can lead to severe neurological diseases (Lan and Jiang, 1997; Zucca *et al.*, 2017). The toxicity of Fe as well as the bioavailability and the metabolic conversion is depending on the species, more specifically on the oxidation state. Ferrous iron (Fe(II)) turned out to be much more toxic to cells by generating free radicals through Fenton reaction (Sun *et al.*, 2016). Fe(II) reacts with hydrogen peroxide to form ferric iron (Fe(III)) and the highly reactive hydroxyl radical: $Fe^{2+} + H_2O_2 \rightarrow Fe^{3+} + OH^{\bullet} + OH^-$. The resulting Fe(III) can accelerate ROS production by conversion into Fe(II): $Fe(III) + H_2O_2 \rightarrow Fe(II) + O_2^{\bullet-} + 2H^+$. Moreover, the resulting superoxide anion radical can further react with Fe(III) to form the critical species Fe(II): $Fe^{3+} + O_2^{\bullet-} \rightarrow Fe^{2+} + O_2$ (Batista-Nascimento *et al.*, 2012). The emerging amount of ROS can lead to the cascade of neurodegeneration by causing lipid peroxidation (Nikam *et al.*, 2009), inflammatory immune response (de Farias *et al.*, 2016), and mitochondrial dysfunction (Subramaniam and Chesselet, 2013). The investigations within the sample set already showed increased concentration of Fe in CSF of PD patients. The knowledge of changes in the Fe(II)/(III)-speciation might provide further insights into Fe-induced ROS production in PD.

Study participants and Method

For the determination of the redox species Fe(II)/(III) we used a sub-set of 28 samples. The samples are divided into 14 PD samples (age: 63.9 ± 11.4 years; sex: 6 female, 8 male) and 14 CTR samples (age: 57.5 ± 15.2 years; sex: 5 female, 9 male).

The used method for this approach is presented in (Michalke *et al.*, 2019). In short, we used capillary electrophoresis (CE) for the separation of the redox-couple and subsequent element-selective detection by use of ICP-MS. The separation is based on a conductivity-pH-stacking within capillary and an acidic background electrolyte. The used program is summarized in Table 13.

Table 13: Program used for separation of the redox species Fe(II)/Fe(III). Capillary was cleaned by the use of two washing steps including 7% HCl and 10% TMAH. An conductivity-pH-stacking enabled separation of Fe(II) and Fe(III).

compound	Pressure in mbar	kV in µA	time in min
7% HCl	EXT	0	10
10% TMAH	EXT	0	10
0.2% HCl	EXT	0	1
Sample	200	0	0.1
10% TMAH	200	0	0.15
20 mM HCl	250	+ 25	4.5

The capillary effluent was directed to ICP-MS for determination of Fe. Additionally, 20 mM NH_4Ac (pH 7.0) was used as auxiliary electrolyte at the ICP-MS interface. For ICP-MS measurement DRC mode with NH_3 as reaction gas (0.6 mL NH_3/min) was used to analyze the isotopes ^{56}Fe and ^{57}Fe. Further parameters of ICP-MS detection are: plasma gas flow 17 L Ar/min, nebulizer gas flow 0.96 L Ar/min, auxiliary gas flow 1.2 L Ar/min, and dwell time 30 ms.

Results and Discussion

By use of the applied method we were able to separate the species Fe(II) and Fe(III). A typical electropherogram of the separation is illustrated in Fig. 3-5. The Fe-species are clearly separated, but Fe(III) shows a broader peak than Fe(II) does. With further optimization of the used method an even clearer separation and peak shape was achieved (Michalke *et al.*, 2019).
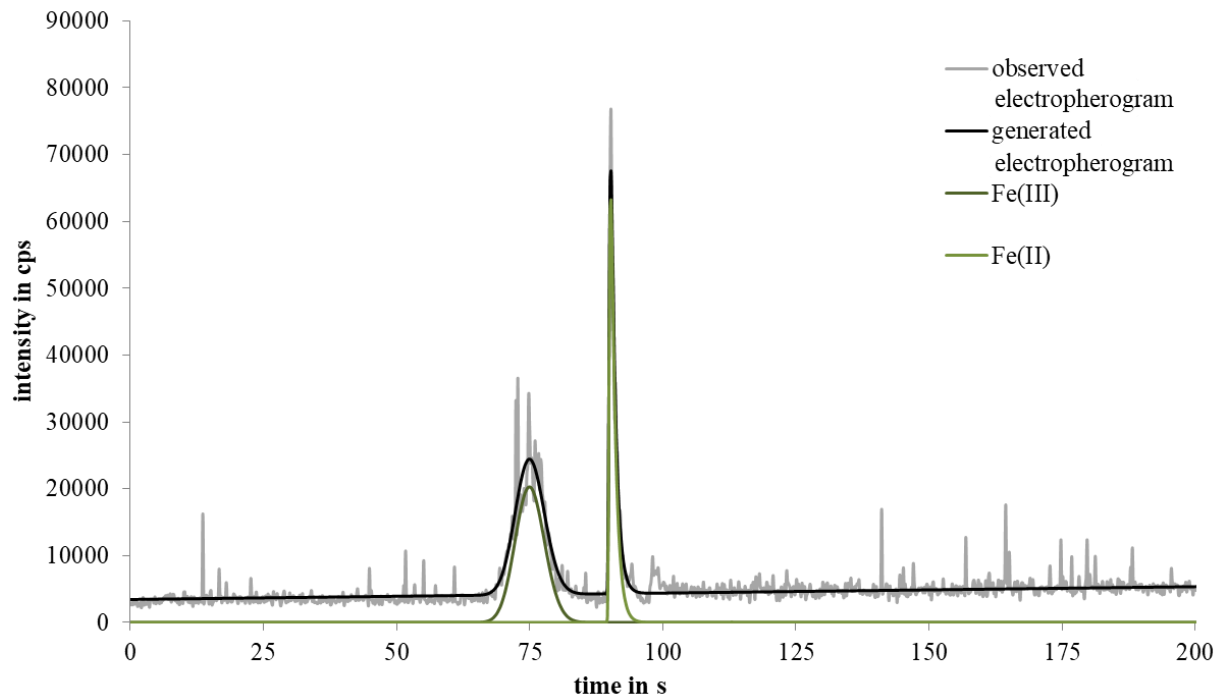
Figure 3-5: Observed CE-ICP-MS-electropherogram (⩘, with graphical off-set) of Fe-redox speciation in CSF with fractions aligned (—— , aligned electropherogram, with graphical off-set) by use of PeakFit[TM] software. Species detected are Fe(III) (—) and Fe(II) (—).

The electropherograms were evaluated by use of PeakFit[TM] software and the amounts of the ratio Fe(II)/(III) were compared for differences in CTR and PD to investigate the trend in disease. The results of this comparison are illustrated in Fig. 3-6 A for the concentration values as well as in Fig. 3-6 B for normalized percentages values. The differences were analyzed by t-test performed in Microsoft Excel 2010. A significance level <.05 was considered to be statistically significant.
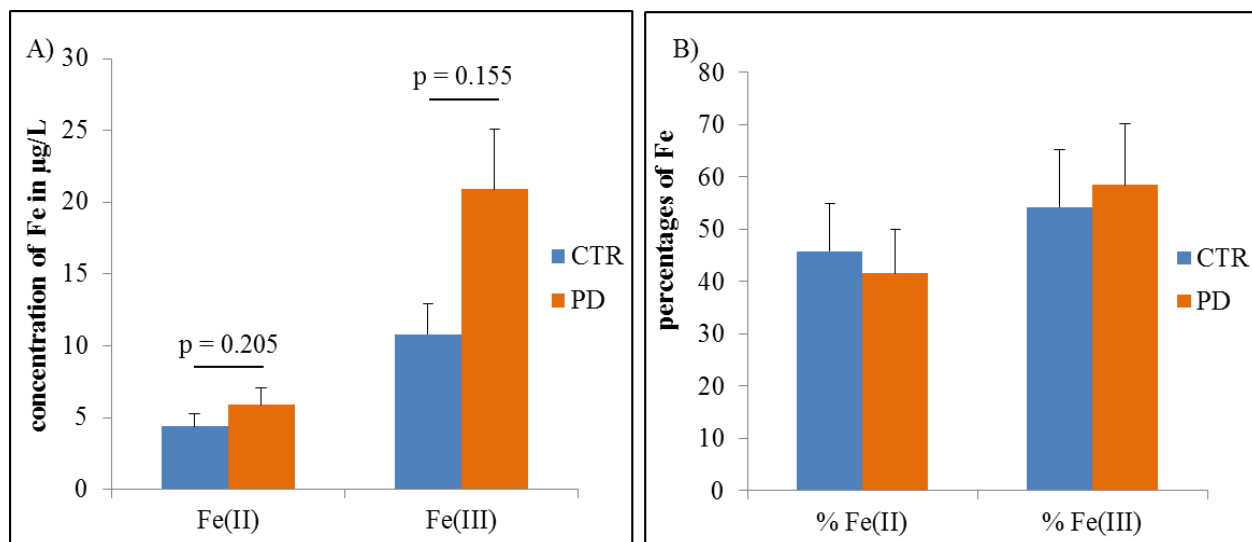
Figure 3-6: Results of the Fe(II)/(III) speciation in CSF of Parkinson patients and CTR. Illustrated are the differences of the Fe species in their A) concentrations with respective p-value and B) percentages distribution.

In concordance with the total amount of Fe in the CSF samples, the concentrations of Fe(II) and Fe(III) were increased in PD. The rise of Fe(III) is higher and also reaches higher significance level than for Fe(II). This is even more obvious when going to normalized percentages values. These normalized values show an increase of Fe(III) which is paralleled by decreased Fe(II) values. Fe is known to be involved in the production of ROS via Haber-Weiss and Fenton reaction. Especially the redox-active Fe(II) species are producing the highly reactive hydroxyl radical ($^\bullet$OH). Since in PD an increase of ROS and oxidative stress is assumed, increased values of Fe(II) were expected. Nevertheless, early Fe(II)/Fe(III) speciation studies using spectrophotometric methods showed significantly increased Fe(III) concentrations in SN of PD patients (Sofic *et al.*, 1988; Riederer *et al.*, 1989). Additionally, investigations in SN of PD patients showed only Fe(III) to be present in this tissue (Galazka-Friedman *et al.*, 1996; Chwiej *et al.*, 2007). In contrast to these findings, recent studies are pointing to a shift of Fe-species towards Fe(II) what is in concordance with the assumption of enhanced oxidative stress in neurodegeneration (Michalke *et al.*, 2017). Increased concentrations of Fe(II) in AD brain where found by (Quintana *et al.*, 2006; Salvador, 2010). Moreover,

a shift in Fe-redox-species towards Fe(II) was also found in a rat model with manganism (Fernsebner *et al.*, 2014).

Species stability is an important point of concern in Fe(II)/Fe(III) speciation which needs to be addressed. Any contact to O_2, an interruption of the frozen storage condition, or freeze-thaw-cycles can alter the native equilibrium of Fe(II)/(III) ratio (Fernsebner *et al.*, 2014; Solovyev *et al.*, 2017). Investigations showed a conversion of Fe(II) towards Fe(III) already 5 min after sample preparation (Michalke *et al.*, 2019). The amount at this time point was 66% of originally Fe(II) concentration. Since our sample set was not intended for scientific use and stood up to six hours at room temperature, a shift of Fe-species is very likely. Additionally, samples were not stored under an inert atmosphere (Ar) instead of air to prevent from oxidation. Further investigations needs to be done in order to quantify the trend of Fe(II)/Fe(III) species in CSF of PD patients.

Moreover, we considered age as an influencing factor to Fe(II)/Fe(III) speciation. A Pearson correlation was done to investigate the influence of age on the species concentrations. Moderate positive correlation coefficients were found for Fe(II) (CTR: r = 0.52; PD: r = 0.64) and for CTR of Fe(III) (CTR: r = 0.54). The correlation of concentration and age in PD patients for Fe(III) shows a nearly random distribution (PD: r = 0.28). The linear regression of concentrations of Fe(II) and Fe(III) against age is illustrated in Figs. 3-7 A and 3-7 B.
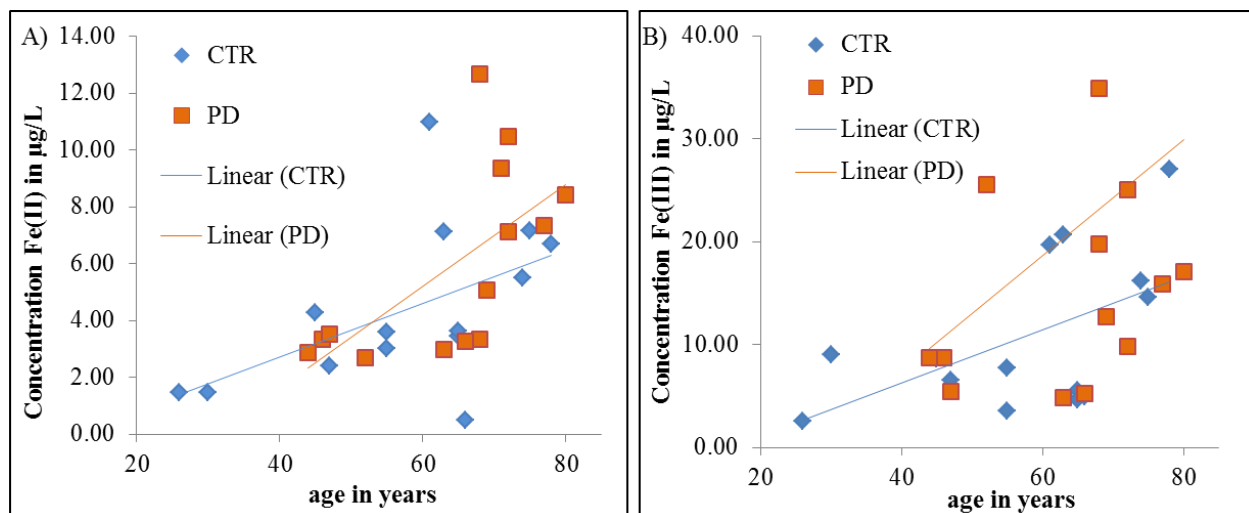
Figure 3-7: Rising Fe-concentrations with age in PD and CTR for A) Fe(II) and B) Fe(III). The slope is for both species higher in PD patients than in CTR.

A slight linear increase of Fe and Fe-storage proteins neuromelanin and ferritin with age was also found in SN (Zecca *et al.*, 2004a). Moreover, increased Fe-concentrations were revealed in the basal ganglia of aged individuals (Hebbrecht *et al.*, 1999; Ramos *et al.*, 2014). An accumulation of iron with age especially in brain is widely accepted (Zecca *et al.*, 2004b; Ward *et al.*, 2014). Reasons for the accumulation of Fe with age are increased BBB permeability, changes in the Fe homeostasis what is paralleled by a shift of Fe distribution within brain (Farrall and Wardlaw, 2009; Xu *et al.*, 2012). The increase of Fe with age in brain and CSF seems to be closely related to an increase in oxidative stress via Fenton and Haber-Weiss reaction to form ROS. The increase is present in CTR as well as in PD, but the slope of the increased concentrations is higher in PD. This finding leads to the assumption that in PD the risk of producing ROS and the damage resulting out of this is higher than in CTR.

Moreover, we evaluated the influence of the respective gender on the measured values or on the redox species. This statistical analysis did not reveal any significance.

Conclusion

What this all amounts to is, that the redox speciation of Fe in CSF of neurodegenerative patients is of high importance. Although our investigations couldn´t show a significant differentiation between CTR and PD, we found alterations in the amount of Fe(II) and Fe(III). To ensure species stability, directly deep freezing of samples and storage under Ar atmosphere is recommended. We were able to prove the accumulation of Fe in elderly participants for Fe (II) as well as for Fe(III). The slope of increased concentrations was greater in PD patients, indicating higher burden due to oxidative stress.

3.6   Determination of amino acids

3.6.1 Amino acid analysis

Amino acids are important building blocks in human life. They are the basic elements in proteins; some are known neurotransmitters or play a role in the hormonal balance. Therefore, the analysis of amino acids has been the target of various studies. Especially, the amino acid amount in brain (D'Aniello *et al.*, 2005), CSF (Molina *et al.*, 1997), blood (Lin *et al.*, 2017) and serum (Corso *et al.*, 2017) has been of concern. Although several studies investigated the amount of amino acids in CSF and compared the amount in PD-patients and respective controls, the results are inconclusive. Distinctions in amino acid amount and shifts in comparison of PD and CTR may arise due to varying sample size, PD-medication and therapy, used method, sample storage, and handling. Moreover, age and sex can significantly alter CSF-amino acid-levels (Ferraro and Hare, 1985). Since species characterization or, more specifically, the ratios indicated a possible involvement of amino acids, especially when associated with Cu, a further analysis to investigate amino acids seemed promising. Therefore, the results of amino acid separation were tested for differences comparing PD-patients and CTRs, but also for age-dependence and differences between male and female participants to get a comprehensive overview.

Study participants and Method

Again, only a reduced amount of samples has been measured due to decreasing sample amount. A total of 20 PD-samples (age: 64.85 ± 11.75 years; sex: 8f, 12m) and 34 CTR-samples (age: 51.29 ± 18.0 years; sex: 18f, 16m) has been measured.

For the analysis of amino acids the method AAA-Direct[TM] was used (Thermo Scientific, 2018). An ICS 5000 (Thermo Scientific, Bremen, Germany) HPLC system was connected to the columns AminoPac PA10 Guard (2x50 mm, Thermo Scientific, Bremen, Germany) and AminoPac PA10 Analytical (2x250 mm; Thermo Scientific, Bremen, Germany). The injection volume was 10 µL and the column temperature 30 °C. The mobile phase consists of eluent A, Milli-Q water (18.2mΩ cm; Milli-Q Purification System), eluent B, 250 mM NaOH, and eluent C, 1.0 M NaAc. Gradient was as follows: 0-2 min 84% eluent A, 16% eluent B, 0% eluent C; 2-12.1 min 84-68% eluent A, 16-32% eluent B, 0% eluent C; 12.1-16 min 68% eluent A, 32% eluent B, 0% eluent C; 16-24 min 68-36% eluent A, 32-24% eluent B, 0-40% eluent C; 24-40 min 36% eluent A, 24% eluent B, 40% eluent C; 40-40.1 min 36-20% eluent A, 24-80% eluent B, 40-0% eluent C; 40.1-42.1 min 20% eluent A, 80% eluent B, 0% eluent C; 42.1-42.2 min 20-84% eluent A, 80-16% eluent B, 0% eluent C; 42.2-65 min 84% eluent A, 16% eluent B, 0% eluent C. The flow rate was 0.25 mL/min. The column effluent was directed to the integrated pulsed amperometric detection (IPAD) equipped with a gold electrode. Fractions were collected manually from the amino acids Arg, Glu, Gln, Ala, Gly, Ser, Ile, Leu, SeM, His, Phe, Tyr.

Results and Discussion

With the applied method we were able to separate and analyze the amino acids arginine (Arg), lysine (Lys), glutamic acid (Glu), glutamine (Gln), alanine (Ala), threonine (Thr), glycine (Gly), valine (Val), serine (Ser), proline (Pro), isoleucine (Ile), leucine (Leu), methionine (Met), norleucine (Nle), seleno-methionine (SeMet), histidine (His), phenylalanine (Phe), cysteine (Cys), seleno-cysteine (Sec), and tyrosine (Tyr). All samples were measured in four different dilution steps (1:3, 1:50, 1:100, and 1:3000) to ensure proper concentration determination for all amino acids. A typical chromatogram

of amino acid separation and amperometric detection of a 1:3-diluted sample is illustrated in Fig. 3-8.
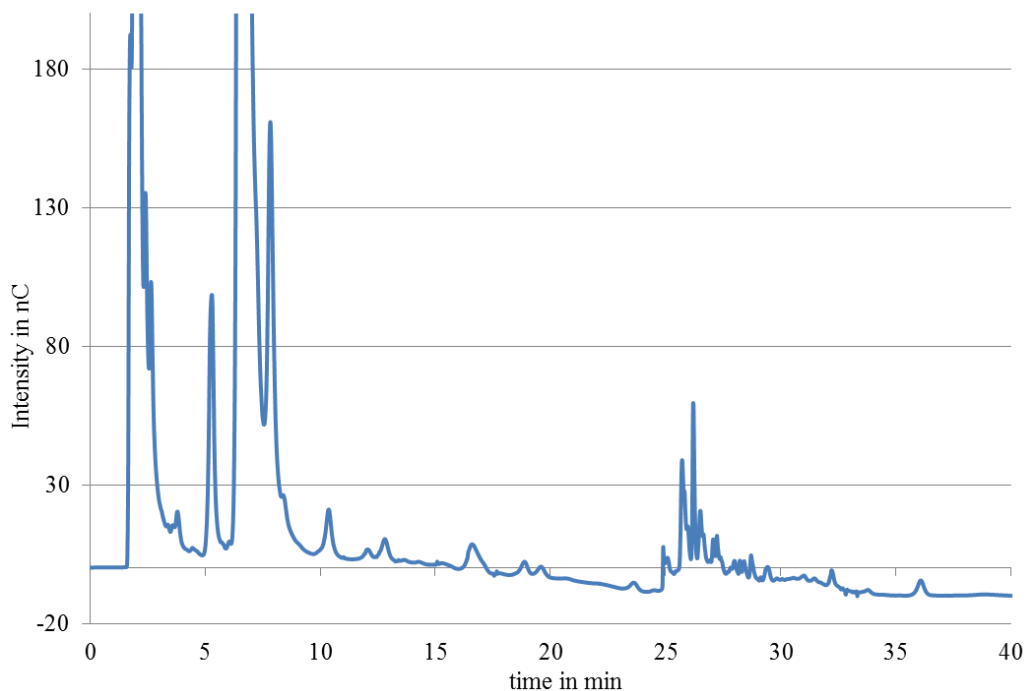
Figure 3-8: Typically observed chromatogram of amino acid separation with the method AAA-direct[TM] in CSF with 1:3-dilution and amperometric detection. For proper concentration determination further dilution steps were measured.

By use of the applied method it was possible to separate and quantify 20 amino acids in CSF. The retention times and the measured mean concentrations of each amino acid in CTR- and PD-samples are listed in Table 14. Moreover, respective p-values to statistically differentiate between CTR and PD are revealed.

Table 14: Retention times and concentrations of separated and measured amino acids in CSF for CTR- and PD-samples as well as respective p-values for comparison between both states.

Amino acid	RT in min	Concentration ± SD in µmol/L in CTR	Concentration ± SD in µmol/L in PD	p-value
Arg	1.9	13807.9 ± 12409.1	16995.1 ± 18317.0	0.505
Lys	3.8	27.14 ± 17.71	26.41 ± 11.21	0.858
Gln	5.3	416.09 ± 139.29	456.45 ± 101.15	0.235
Asn	6.0	1.34 ± 0.60	1.48 ± 0.75	0.467
Ala	6.6	18135.9 ± 7627.2	20730.0 ± 6957.0	0.218
Thr	7.2	3.50 ± 2.10	4.42 ± 3.07	0.268
Gly	7.8	1188.20 ± 1118. 33	1246.78 ± 654.61	0.813
Val	8.4	4.45 ± 2.49	5.29 ± 3.10	0.318
Ser	10.4	10.48 ± 2.86	12.04 ± 1.86	0.022
Leu	12.1	9.54 ± 4.16	10.95 ± 3.53	0.201
Ile	12.8	15.17 ± 5.49	18.22 ± 5.51	0.061
Met	13.7	2.73 ± 2.20	3.28 ± 3.15	0.505
Nle	14.3	0.77 ± 0.35	0.82 ± 0.50	0.680
SeMet	17.1	1.41 ± 0.85	1.43 ± 0.76	0.955
His	25.7	11.09 ± 3.13	10.96 ± 2.38	0.867
Phe	26.5	10.99 ± 2.26	11.87 ± 2.57	0.263
Glu	28.7	20.71 ± 6.74	23.49 ± 13.21	0.621
Cys	29.8	0.60 ± 0.18	0.67 ± 0.33	0.588
Sec	30.6	19.19 ± 5.26	18.68 ± 4.25	0.735

	Tyr	32.2	9.27 ± 3.15	10.03 ± 3.14	0.407

Not all of the amino acids are present in all of the samples. Especially, concentrations of SeMet, Glu, and Cys were in most samples lower than the limit of detection (LoD). The highest concentrations were obtained for Ala, Arg, Gly, and Gln in the CSF-samples, what is partially in concordance with D´Aniello et *al.* who found Glu, Gln, and Ala to be most abundant in CSF (D'Aniello *et al.*, 2005).

The comparison of amino acids of CTR- and PD-samples showed a significant difference only for Ser ($p = 0.022$). Moreover, Ile depicted a marked increase in PD, although insignificant ($p = 0.061$) as illustrated in Fig.3-9 A. The significance of both alterations (Ser and Ile) is even increasing by comparing PD and CTR in the age-group of 40-60, demonstrated in Fig. 3-9 B. Within this age-group Ser is significantly increased ($p = 0.0049$) and also Ile is increased significantly ($p = 0.036$). In the age-group >60 Ser and Ile are increased but insignificantly, indicating a possible involvement of both amino acids in starting processes of neurodegeneration.

Trupp et *al.* found various amino acids to be increased in plasma of PD patients. Next to increased values of Ser, they found elevated levels of Met, Thr, Ala, pyroglutamate, and ketoleucine (Trupp *et al.*, 2014). Additionally, significantly increased amount of Ser was found again in plasma of PD patients by LeWitt et al. (LeWitt *et al.*, 2017). A significantly increased Ser-concentration in CSF was also found by Molina *et al.* in AD-patients compared to controls (Molina *et al.*, 1998). Ser is an important neuromodulator of NMDA and involved in a cascade which induces neurodegeneration (Katsuki *et al.*, 2004) as discussed in the D-/L-amino acid chapter (see chapter 3.6.3). Additionally, Ser is involved in the synthesis of GSH (Meiser *et al.*, 2016), an antioxidant compound which is reduced in PD (Bogdanov *et al.*, 2008). An increase in Ser-concentration may be associated with increased synthesis of GSH. In PD enhanced oxidative stress is hypothesized, this may be paralleled by increased necessity of GSH-synthesis. Therefore, increased levels of Ser seem to be involved in the neurodegenerative processes ongoing in PD.

Moreover, we found increased concentrations of Ile in CSF. These elevated levels were especially in the age-group 40-60 significantly different in CTR and PD. Several studies found the concentration of Ile to be altered in PD, but the results are inconclusive. Lower concentrations of Ile in PD were reported in CSF (Mally *et al.*, 1997; Molina *et al.*, 1997; Wuolikainen *et al.*, 2016) and plasma (Wuolikainen *et al.*, 2016). In contrast to these lower levels, higher concentrations of Ile in CSF of PD-patients were found by (Van Sande *et al.*, 1971; Lakke and Teelken, 1976; Lakke *et al.*, 1987; Wu *et al.*, 2016). The differing observations can be caused by differences in sample size, therapy, method of detection and quantification, sample storage and sample pretreatment. Although no specific function of Ile is known in CNS, in muscles Ile is known to contribute to increased glucose consumption and utilization (Doi *et al.*, 2003) as well as to the up-regulation of glucose transporters (Nishitani *et al.*, 2005). Therefore, increased concentrations of Ile may be associated with increased utilization of glucose. This enhanced utilization of glucose seems to be linked to a higher energy demand through disease. The body needs more energy to maintain normal metabolic processes.

These changes of Ser and Ile together with the insignificant shifts of other amino acids indicate a defect in specific metabolic amino acid pathways which may contribute to the pathophysiology of PD. Moreover, the increased concentration of Ile seems to be associated with enhanced energy requirement in the diseased patients.
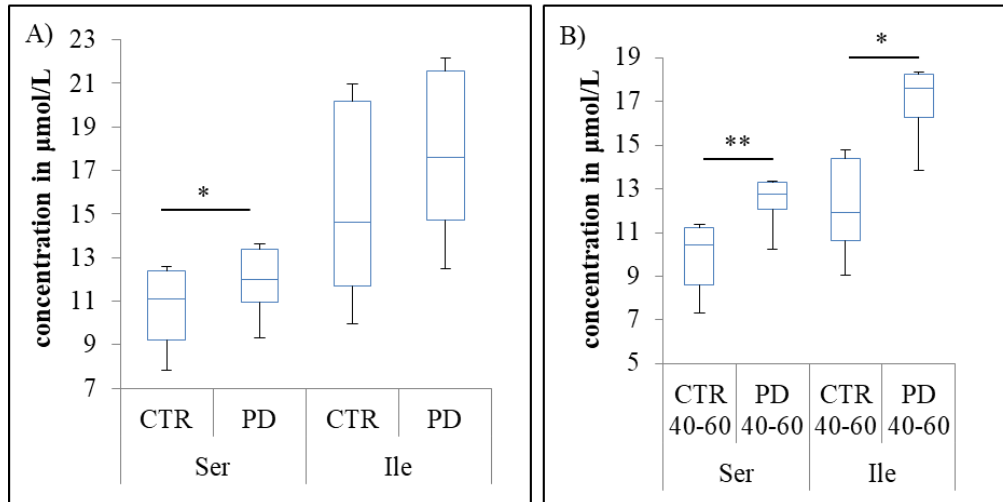
Figure 3-9: Alterations in amino acid concentration in CSF of CTR and PD A) Significant difference of Ser and insignificant shift of Ile which display higher significance by comparing B) the difference in CTR and PD of patients with ages 40 – 60 years.

The results were further analyzed for dependence of age. Therefore, the concentrations of each amino acid were analyzed by means of Pearson correlation in three different groups. First, all values (PD and CTR together) were correlated against age and in a second and third approach the values of PD and CTR alone are correlated against age. This application showed a moderate positive age-dependence for Gln in the PD-samples ($r = 0.52$), as illustrated in Fig. 3-10 A. The concentration of Gln is increasing slightly with increasing age. Additionally, the amino acids showed significantly differences in their concentration by comparing the different age-groups especially in CTR with t-test. In Fig. 3-10 B a significantly increased Ala-concentration ($p = 0.020$) is illustrated in the age-group >60 compared to the age-group <40. In contrast to Ala, the concentrations of Asn ($p = 0.021$), Thr ($p = 0.004$), and Phe ($p = 0.006$) are significantly decreased in the age-group 40-60 compared to CTR-patients younger than 40, illustrated in Fig. 3-10 C.

The influence of age on the amount of amino acids was investigated in CSF by (Ferraro and Hare, 1985). They found increasing levels of Asp, Gly, Val, Ile, Leu, Phe, and 3-methylhistidine and decreasing levels of Ser, GABA, and conjugated β-alanine with

64

increasing age in CSF. The results showed a marked influence of age on the CSF-concentrations of several amino acids. Opposing to these changes, we found decreasing concentrations of Phe with age and increasing concentrations of Ala. Chen and Preston investigated the amino acid uptake at the BCB in aging ovine (Chen and Preston, 2012). They investigated the behavior of Leu, Phe, Ala, and Lys and found impaired amino acid transporters in old BCB leading to raised amino acid influx. Additionally, a deficient Thr concentration was associated with neurological dysfunctions (Titchenal *et al.*, 1980) which, however, are more prominent in elderly people (Broe *et al.*, 1976; Callixte *et al.*, 2015).
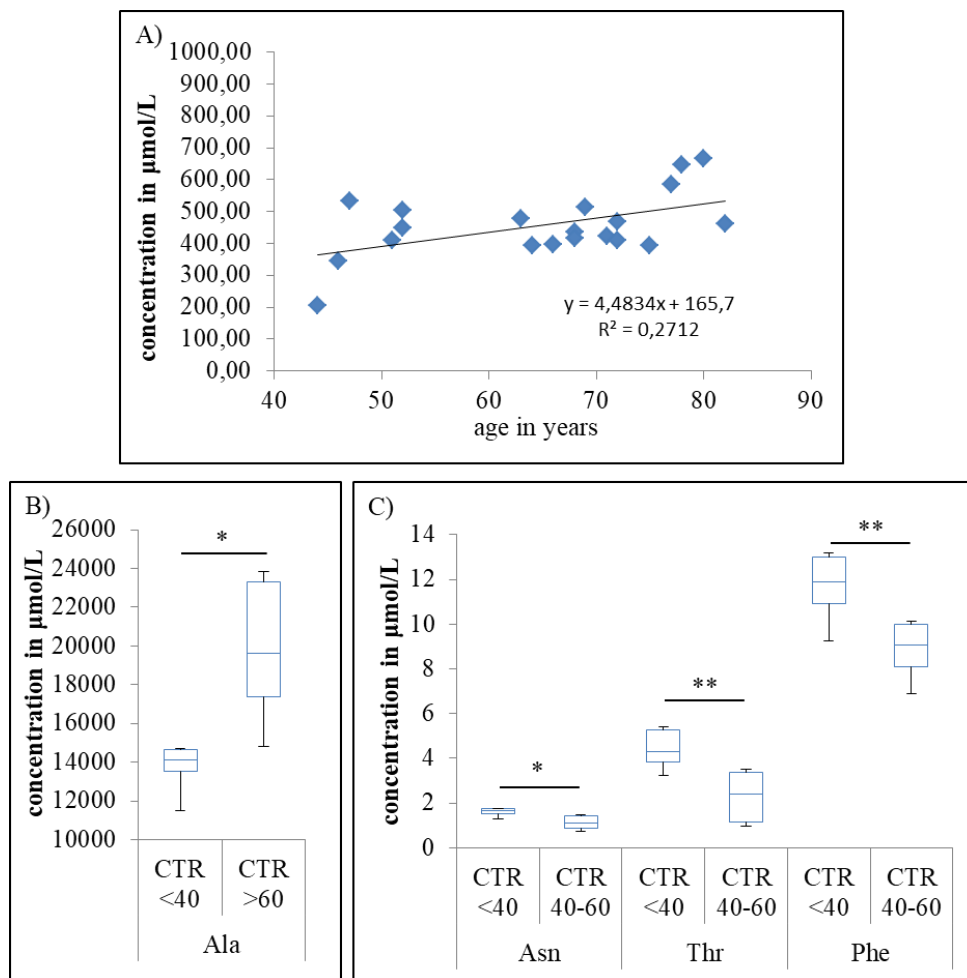
Figure 3-10: Results of analysis for age-dependence of amino acids in CSF. A) age-dependence of Gln with increasing concentrations with age in PD-patients. Significant

amino acid differences within CTR group by comparing ages C) < 40 with > 60 and D) < 40 with 40 – 60 years.

Apart from the dependence of age, also the influence of sex was analyzed within the amino acids. The results showed, for our sample-set, a significant difference in the Thr-concentration by comparing female and male participants. The differentiation was found for the total sample-set ($p = 0.019$) as well as for the PD-values ($p = 0.071$). Fig. 3-11 displays the significant reduced concentration of Thr in male participants.

Like for the age, also sex was found to influence the amount of amino acids in CSF. Especially Tyr, Arg and conjugated Asp were found to be higher in male subjects than in female ones. Our results pointed to a significantly reduced Thr concentration in male participants.
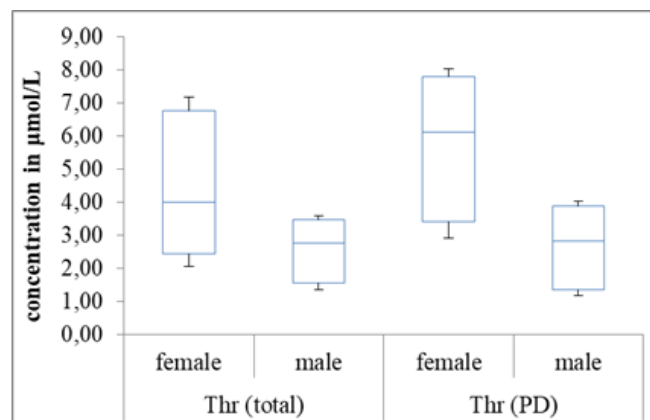
Figure 3-11: Results of analysis for the influence of the sex in amino acid-concentration in CSF. Significant differences were observed in the concentration of Thr between female and male patients in all measured samples (total) and in PD samples.

3.6.2 Metal-determination in amino acid fractions

Proteins are macromolecules built up of amino acids which are connected through peptide bonds. Metalloproteins are a special kind of proteins having one or more metal atoms as a cofactor and being not catalytically active. Proteins with a catalytically active metal atom as cofactor are called metalloenzymes. These metalloenzymes perform

crucial functions in human metabolism. The broad spectrum of different metalloenzymes is presented in (Valdez *et al.*, 2014). These enzymes are involved in most of the metabolic processes in the human body and are making a contribution to several different mechanisms like anti-oxidation, transport and storage of metals, and nucleotide synthesis (Sun and Chai, 2010). Our investigations in PD already showed a strong shift of the amino acid-fraction associated with Cu in SEC-ICP-MS. Moreover, we found significantly increased concentrations of Ser in CSF of PD patients and again shifted values for other amino acids. To combine these findings with the amount of metals associated with the amino acids, we collected fractions of 12 amino acids for further metal-analysis.

Methods

The collected fractions from amino acid analysis were further analyzed for their total elemental concentrations by ICP-sf-MS. For the determination of Cu, Fe, Mg, Mn, Ni, Sr, and Zn samples were diluted mainly 1:25 (also 1:100, 1:50 and 1:33 depending on sample volume). For these samples an 8-point calibration was carried out (10 ng/L, 50 ng/L, 100 ng/L, 250 ng/L, 500 ng/L, 1 µg/L, 5 µg/L, and 10 µg/L). For all measurements Rh as internal standard was constantly introduced with a final concentration of 1 µg/L. The instrumental parameters of ICP-sf-MS are listed in Table 15.

Table 15: Instrumental parameters for elemental analysis of CSF amino acid fractions by use of ICP-sf-MS.

parameter	specification
Analytes detected	^{24}Mg, ^{25}Mg, ^{55}Mn, ^{56}Fe, ^{60}Ni, ^{63}Cu, ^{66}Zn, ^{87}Sr, and ^{103}Rh
Detection mode	Medium resolution
Conditions	1170 W RF power
	16 L Ar/min plasma gas flow
	0.99 L Ar/min nebulizer gas flow
	0.64 L Ar/min auxiliary gas flow

Results and Discussion

The approach was intended to get further information about specific amino acids and metals which are associated with these amino acids. Fractions of twelve different amino acids were collected for further metal analysis. The method for amino acid separation was presented in chapter 3.6.1. The fractions were collected after passing the detector of amino acid analysis. The metal-analysis was done off-line without hyphenation of techniques. Therefore, no information of background-metal status is available, but we can hypothesize that this background is comparable between runs.

In Table 16 the mean concentrations of the measured metals in respective amino acid fractions (without background subtraction) are listed for CTR and PD (values of SD are presented in Table A1). The concentrations which significantly ($p < 0.05$) differentiate between CTR and PD are highlighted in red.

Table 16: Mean concentrations of measured metals Cu, Fe, Mg, Mn, Ni, Sr, and Zn in the amino acid fractions in CSF for CTR- and PD-samples. The highlighted values significantly ($p < 0.05$) differentiate between CTR and PD.

Amino acids	Metal	$c_{(Cu)}$ in µg/L	$c_{(Fe)}$ in µg/L	$c_{(Mg)}$ in µg/L	$c_{(Mn)}$ in µg/L	$c_{(Ni)}$ in µg/L	$c_{(Sr)}$ in µg/L	$c_{(Zn)}$ in µg/L
Arg	CTR	14.66	60.99	34.66	0.72	2.44	2.27	19.16
	PD	8.11	110.03	27.98	1.00	14.22	2.49	20.40
Gln	CTR	5.21	64.87	29.70	3.20	5.44	2.43	16.34
	PD	9.44	191.67	31.17	1.02	10.56	2.21	83.15
Ala	CTR	7.69	86.23	31.80	1.32	3.59	2.14	18.53
	PD	0.96	29.90	14.79	0.90	0.95	1.17	10.71
Gly	CTR	97.72	91.38	31.54	2.08	7.72	2.77	42.42
	PD	7.81	65.93	37.74	1.04	1.19	2.23	19.01
Ser	CTR	6.81	56.81	39.47	0.82	7.74	2.22	46.01
	PD	3.39	53.18	14.81	0.67	34.87	1.68	19.47
Ile	CTR	5.11	52.75	39.63	0.67	1.65	2.66	25.21
	PD	12.47	66.20	27.54	0.55	13.12	1.85	13.99
Leu	CTR	7.19	45.56	27.43	0.68	1.95	2.11	20.06

	PD	7.87	60.22	14.15	0.45	0.61	2.12	23.92
SeM	CTR	7.86	50.59	25.97	0.46	0.83	2.16	31.56
	PD	2.64	61.34	8.99	0.48	0.39	2.22	22.34
His	CTR	3.98	77.00	27.52	1.29	7.40	6.27	20.58
	PD	13.36	85.54	26.22	1.21	2.52	6.30	19.64
Phe	CTR	44.67	76.16	40.56	1.27	0.56	8.73	24.26
	PD	9.33	78.81	32.47	1.19	1.97	8.94	45.71
Glu	CTR	13.03	60.22	50.10	0.91	1.42	30.31	32.85
	PD	6.87	27.02	61.28	0.80	2.86	29.48	35.02
Tyr	CTR	14.91	64.07	60.05	1.15	16.49	89.04	40.15
	PD	5.96	90.23	45.97	1.11	2.23	86.40	39.19

The six highlighted fields in Table 16 show a significantly decreased concentration in PD, namely the concentrations of Fe detected in the Glu-fraction ($p = 0.0492$), Cu in the SeM-fraction ($p = 0.0392$), Mg in the Ser-fraction ($p = 0.0274$), and Cu ($p = 0.0236$), Mg ($p = 0.0128$), and Sr ($p = 0.0241$) in the Ala-fraction. Additionally, some values showed a strong shift although insignificant; the concentration of Cu in Tyr-fraction ($p = 0.0786$) and Mg in the Leu-fraction ($p = 0.0945$) were decreased in PD and the concentration of Zn in the Phe-fraction was increased ($p = 0.0823$). Metals are associated to amino acids via non-covalent or weak interactions like hydrogen bonds, hydrophobic interactions, π-π-stacking interactions, and cation-π-interactions (Shimazaki *et al.*, 2009; Shimazaki *et al.*, 2015). Thereby, the side chain of respective amino acid plays a crucial role like the aromatic, positively, or negatively charged side chains apart from the amine and carboxylate moieties of amino acids (Martin, 2001).

Of course, the metal-amino acid fractions can be further characterized by their stability. A high stability constant (or formation constant) indicates a stable complex, means that the metal is strongly bound to the amino acid. In contrast to this strong binding, a low stability constant indicates a weak bond (Byrne *et al.*, 2011). For the significantly differentiating metal concentrations in the alanine fraction Sr has the lowest formation constant (log β_{ML} = 0.73), followed by Mg (log β_{ML} = 1.96) and the strongest formation constant is known for Cu. The metal Cu can form complexes with either one ligand of alanine (log β_{ML} = 8.4) or with two ligands of alanine (log β_{ML2} ~ 15) where the complex consisting of two alanine-ligands and one Cu-atom is notably stronger (Sovago *et al.*, 1993). The determination of stability constants of amino acid complexes with various metals is still a research field with ongoing knowledge gain. The research is mainly focusing on essential trace elements in human metabolism (Casale *et al.*, 1995; Demirelli and Köseoĝlu, 2005; Altun and Bilcen, 2010; Miličević and Raos, 2012; Gorboletova and Metlin, 2015; Pyreu and Bedenko, 2017).

Apart from the differentiation between CTR and PD, we investigated the influence of age by Pearson correlation, but couldn´t find any significant change of metal-concentrations dependent on age. Additionally, the difference between female and male participants was investigated by means of Student´s t-test. Several significantly

increased metal-concentrations in male participants were observed. The results of this analysis are presented in Fig. 3-12.
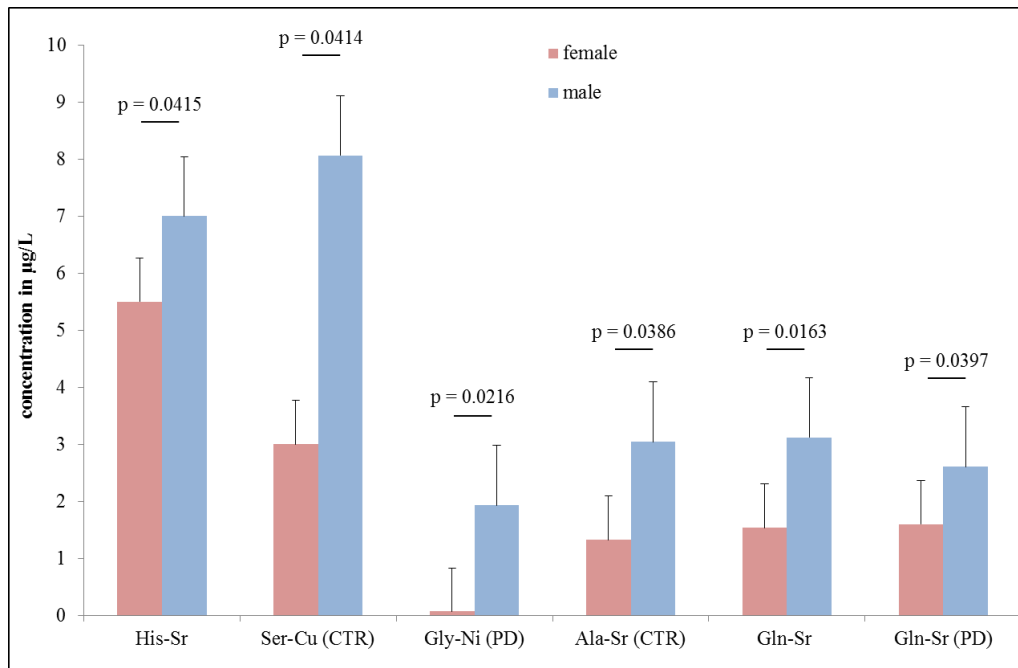
Figure 3-12: Results of analysis for the influence of the sex in the metal analysis within amino acid-fractions in CSF. The significance levels for the differences between female (red) and male (blue) participants are illustrated.

The evaluation was done for the comparison of female and males independent of CTR or PD and also for only CTR or PD participants. The overall comparison showed a significant rise of Sr-concentration in His- and Gln-fraction in males. Additionally, in the CTR-group an increase of Cu in the Ser-fraction and Sr in the Ala-fraction was observed in male participants. Focusing upon the PD-group also increased concentrations of Ni in the Gly-fraction and Sr in the Gln-fraction of male persons was found. What stands out in the evaluation is, that the differences between men and women mainly occurred with Sr. The element Sr is a non-essential trace element which is mainly introduced to the human body by food, like nuts, fruits, seafood, cereals, and milk (González-Weller *et al.*, 2013). Its function in the human body is practically unknown, especially anti-oxidant or pro-oxidant functions (Barneo-Caragol *et al.*, 2018). Sr has similar chemical and physical properties as Ca and both elements compete for the same transporters, but Sr

has a lower absorption and higher clearance. Therefore, Sr content is only 0.04% of the Ca content (Cannata-Andía *et al.*, 2010). A study investigating the elemental fingerprint in PD and matched CTR found Sr to belong to the classification model differentiating between healthy and diseased state, although Sr concentration did insignificantly differentiate the two states (Maass *et al.*, 2018). The results of the study were only correlated against the clinical parameters age, duration of disease, and levodopa equivalent dose but not with the sex of participants.

In summary, we found six element-amino acid combinations significantly differentiating between CTR and PD. Involved metals were Cu, Fe, Mg, and Sr which were reduced in PD. These findings fit with the results obtained by SEC-ICP-MS (chapter 3.3) where the Cu-amino acids fraction was shifted to lower concentrations in PD. Since Cu is an essential trace element incorporated to several proteins which are involved in the preservation of proper redox-balance any misbalance can finally lead to an elevation of oxidative stress and the cascade of neurodegeneration.

3.6.3 D-/L-amino acids

Several amino acids are known neurotransmitters in human brain (Alexander and Crutcher, 1990; Jiménez-Jiménez *et al.*, 1996). Amino acids in human biofluids are mainly present in their L-enantiomeric form, but several amino acids were also detected in their D-enantiomeric form in mammalian brain (Kera *et al.*, 1995; Hamase *et al.*, 2001) and CSF (Fisher *et al.*, 1998; Samakashvili *et al.*, 2011). Therefore, the concentration of D-amino acids is usually very low. D-amino acids can be present in free form or can be residues in proteins (Hamase *et al.*, 2002). Especially in aging, a transformation of L-form to D-form in proteins happens (Yekkala *et al.*, 2006) which can be indicative for different changes or diseases (Fisher *et al.*, 1998; Kalíková *et al.*, 2016). Since some amino acids already showed an altered concentration comparing CTR and PD in our investigations, a further analysis to detect the enantioselectivity of amino acids seemed to be an important topic. Especially serine showed a significant difference and is, therefore, a main object to study.

Study participants and Method

The investigations were done with only a subset of samples, since sample volume was nearly consumed. A subset of 14 CTR-samples (age: 57.5 ± 15.8 years; 5 female, 9 male) and 13 PD-samples (age: 62.9 ± 11.7 years; 6 female, 7 male) has been analyzed for enantiomeric amino acid composition.

For the separation and analysis of enantiomeric amino acids in CSF the method from (Müller *et al.*, 2014) was adapted accordingly. The CSF samples were measured after pre-column derivatization and separated within an Acquity UPLC system (Waters, Milford, USA) at a BEH C18 column (1.0 x 150 mm; Waters). Column temperature was set to 40 °C and temperature in the sampler was set to 25 °C. The injection volume was 10 µL in partial loop mode. The eluent consisted of eluent A, 20 mM NH_4Ac adjusted to pH 6.2 with acetic acid, and eluent B, 7% acetonitrile in MeOH. The flow rate was optimized to 0.1 mL/min and the gradient was as follows: 0 min 100% eluent A, 0% eluent B; 0-15 min 70% eluent A, 30% eluent B; 15-28 min 50% eluent A, 50% eluent B; 28-31 min 20% eluent A, 80% eluent B; 31-32 min 20% eluent A, 80% eluent B; 32-33 min 10% eluent A, 90% eluent B; 33-34 min 10% eluent A, 90% eluent B; 34-34.5 min 100% eluent A, 0% eluent B.

The derivatization mixture for pre-column derivatization was changed to a combination of o-phthalaldehyde (OPA) and IBDC to have appearance of D-enantiomer before L-enantiomer.

The column effluent was directed to a photodiode array (PDA) detector for wavelength analysis at λ = 210 nm and afterwards to a QqTOF-MS (maXis, Bruker Daltonics, Bremen, Germany) for mass-selective analysis.

The obtained results were calibrated by use of Genedata. The masses of the measured amino acids in positive ionization mode {M+H}[+] were used for RT check of standards and of quality control (QC) samples which were measured periodically within samples. A drift of RT would be obvious by checking QCs and can be corrected. With Genedata the quantitative evaluation of D-/L-amino acids were done. The obtained values are

normalized to total ion current and compared to find differences between CTR- and PD-samples. A two-sided Student´s T-test was used to find significant differences.

Results and Discussion

The used method which was developed and tested for plasma, urine, and mouse gut also worked in CSF and enantioselective separation of amino acids was done (Müller *et al.*, 2014). By the use of the chiral thiol isobutyryl-D-cysteine (IBDC) for derivatization of amino acids, the D-enantiomer appears at an earlier retention time than the L-enantiomer does. This is of great advantage since amino acids are known to be present in humans mainly in L-form. Therefore, overlapping signals can be avoided. The enantioseparation of amino acids in CSF showed L-Ser, D-Ser, L-His, L-Thr, L-Arg, L-Ala, L-Tyr, D-Tyr, L-Trp, L-Phe, L-Ile, and L-Leu in all samples, D-Ala and L-Met in most samples, and D-Met, D-Val, D-Leu in only a few samples. As it was expected, the L-enantiomeric form of amino acids is the dominant form. Some amino acids like Ser and Ala are also present in low amounts as D-form, illustrated in Fig. 3-13.
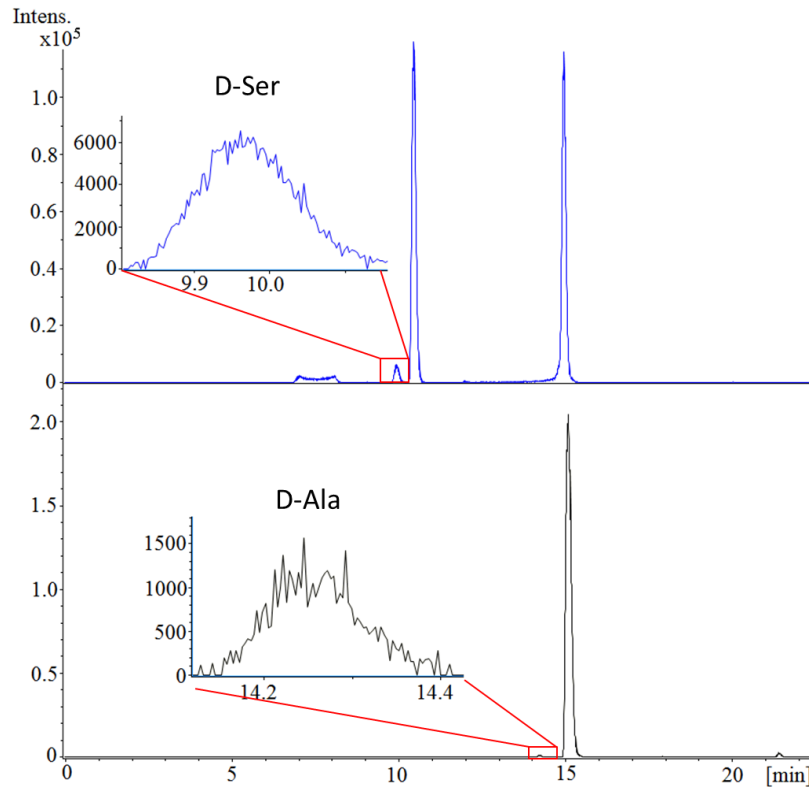
Figure 3-13: Extracted ion chromatograms (EIC) from serine and alanine in a CSF-sample illustrating the distribution between D- and L-enantiomeric forms of amino acids.

The analysis of all detected amino acids showed increased amount in the PD-samples. Especially D-Ala (p = 0.013) showed a significant difference between CTR-group and PD as illustrated in Fig. 3-14 A. Additionally L-Met (p = 0.063) and L-Ile (p = 0.081) showed a shift although insignificant (Fig. 3-14 B). Moreover, a Pearson correlation of values vs. age showed especially for L-Thr an opposing dependence as shown in Fig. 3-14 C. In case of CTR a strong positive correlation (r = 0.64) and in case of PD a moderate negative correlation (r = -0.59) showed up. L-Ser also had a positive correlation between value and age, but only for CTR-samples (r = 0.63).
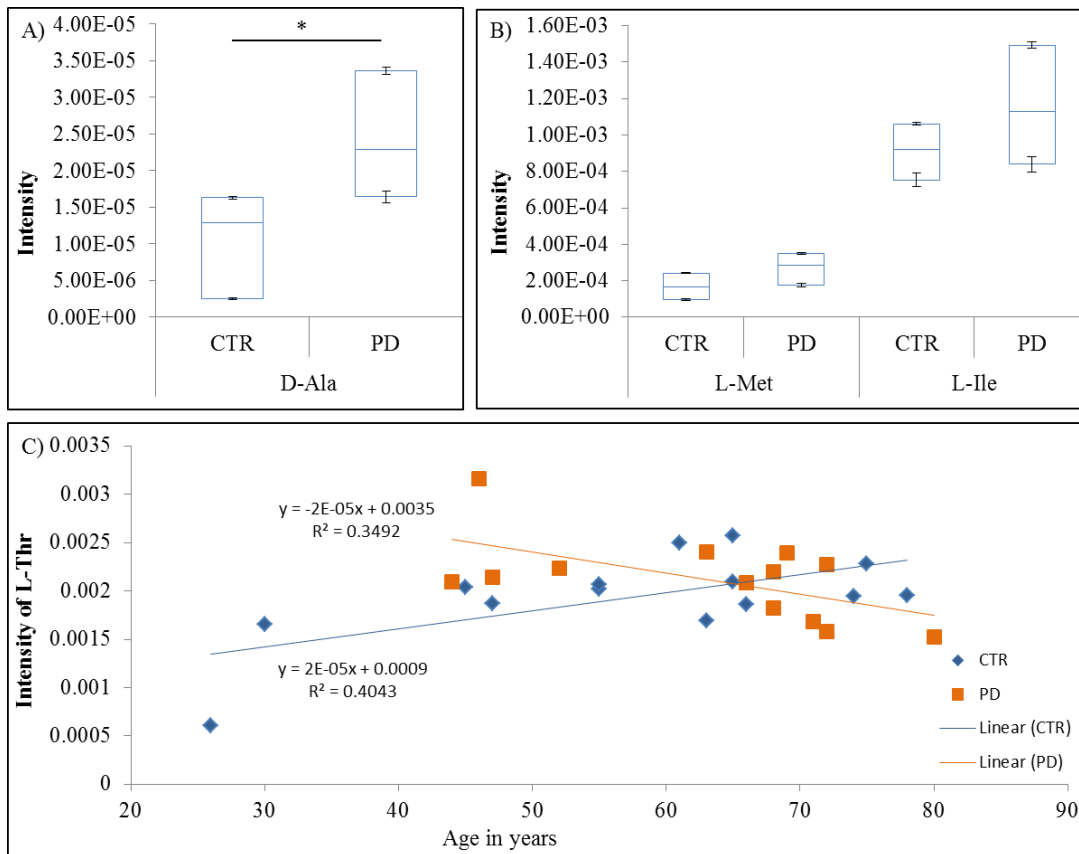
Figure 3-14: Results of enantioseparation of amino acids. A) Significant difference in D-Ala amount between CTR and PD; B) insignificant increase of L-Met and L-Ile; C) dependence of L-Thr intensity from age shows opposing behavior in CTR compared to PD.

D-Ala was found increased in CSF-samples of PD patients. It is the D-amino acid with the third highest abundance in brain after D-Ser and D-Asp (Hamase *et al.*, 2005). Since CSF is the repository of the brain, changes within brain can be also seen in CSF. Up to now there are no publications, where enantiomeric amino acids are analyzed in CSF of PD-patients. Therefore, a discussion related to known values and differences is impossible. In other neurodegenerative disease like AD, D- and L-amino acids are already analyzed. Fisher et al. found higher amounts of D-amino acid, especially free D-Ser and D-Asp, in CSF of AD patients. Additionally, they found significantly higher amounts of L-Glu and L-His in diseased patients. The differences can possibly reflect degenerative processes ongoing in AD (Fisher *et al.*, 1998). D-Ala is increased in AD-

brain, gray matter comparison showed significant differences (Fisher *et al.*, 1991). Whereas, no significant differences are obvious in white matter of AD-patients. Besides D-Ala, also D-Ser is detected in CSF samples and showed an increased value although insignificant (p = 0.33). Both amino acids are known neuromodulators of N-methyl-D-aspartate (NMDA) and are regulated by D-amino acid oxidase (DAAO) (Miyoshi *et al.*, 2011). DAAO is a flavin adenine dinucleotide (FAD)-containing enzyme which catalyzes the oxidative deamination of D-amino acids yielding H_2O_2 and imino acids. The enzyme has a high specificity towards the D-enantiomeric form of amino acids (Khoronenkova and Tishkov, 2008). The NMDA receptor is involved in normal and pathophysiological processes like memory formation, synaptic plasticity and development (Danysz and Parsons, 1998; Chervyakov *et al.*, 2011). Increased amount of D-Ala and D-Ser can possibly be involved in misbalances in degradation processes leading to higher concentrations of hydrogen peroxide and finally oxidative stress. Additionally, increased amount of both amino acids can also be involved in increased NMDA receptor activity leading to raised pathophysiological processes and potentially causing CNS dysfunction. For D-Ser a process inducing neuronal cell death is reviewed in (Martineau *et al.*, 2006). Shortly, the process involves the activation of glia by acute inflammation which induces the release of cell-death mediators (e.g. cytokines, ROS). Moreover, an increased serine racemase production leads to generation and efflux of D-Ser leading to over-activation of NMDA receptors and neuronal damage. This process is paralleled by mitochondrial ROS production, membrane lipid peroxidation and additional generation of inflammatory mediators promoting the inflammatory state. Finally, the induced cascade leads to neurodegenerative conditions also involved in onset and progression of PD (Sasabe and Suzuki, 2018).

Conclusion

Caused by the results of SEC-ICP-MS we evaluated the amount of amino acids in CSF of PD and CTR. The comprehensive analysis of amino acids in CSF was done by the method AAA-direct[TM]. The results showed especially increased Ser-concentrations in PD as well as a marked elevation of Ile. Serine is an important neuromodulator and known to be involved in a cascade inducing neurodegeneration. In a second approach

fractions of the separated amino acids were collected and further analyzed for their metal content. Within this investigation six significantly different metal contents have been found. In the changes involved metals were Cu, Fe, Mg, and Sr; involved amino acids were Ala, Ser, SeM, and Glu. Additionally, the samples were separated into D- and L- enantiomeric form of the amino acids. The predominant form of the amino acids was the L-enantiomer, but also D-enantiomeric forms have been found, e.g. Ser and Ala. D-Ala was significantly increased in PD. The overall changes in amino acid composition in PD might indicate defects in specific metabolic amino acid pathways. Moreover, amino acids are involved in numerous metabolic processes. Therefore, changes can reflect the pathophysiological changes occurring in PD.

3.7   Metabolomic investigations in CSF[3]

The human metabolism is defined by a large number of specific metabolic reactions. Exposure to external environmental factors or disease can greatly alter natural human metabolism. The investigation of these changes can help understanding the underlying mechanisms and to find medications which ameliorate the disease conditions. Various studies already investigated the CSF-metabolome of PD patients in comparison to controls. The results of these investigations point to a change in the amino acid metabolism (LeWitt *et al.*, 2013; Öhman and Forsgren, 2015; Wuolikainen *et al.*, 2016; Havelund *et al.*, 2017; Stoessel *et al.*, 2018), energy metabolism (Öhman and Forsgren, 2015; Trezzi *et al.*, 2017), and fatty acid metabolism (LeWitt *et al.*, 2017). By the use of targeted metabolomic investigations we already evaluated the differences of amino acids in the CSF of PD patients compared to CTR (see also chapter 3.6). A further non-targeted metabolomics approach was intended to increase the knowledge about differences in both states on the metabolite level.

---

[3] The following chapter has been partially prepublished in (Willkommen *et al.*, 2018*a*)

3.7.1 Metabolic profiling

Metabolic profiling is a specific type of metabolomic investigation. Within this method a characteristic fingerprint of a biological sample is generated. Afterwards, these fingerprints are compared between the healthy and diseased state to find significant differences in the groups. From the significantly different masses it is tried to identify compounds which can give a deeper insight into disease mechanisms and new hypothesis can be generated. Since no metabolomic technique can cover all metabolites (Wishart *et al.*, 2008), the use of multiple techniques and methods is mandatory to unravel as much metabolites as possible. The metabolomic investigations already done within CSF of PD are concentrating on GC-MS, LC-MS, and NMR analysis. To enhance knowledge and cover more possible affected metabolites, we decided to use a technique up to now not reported for metabolite determination in CSF of PD patients and CTR. Our investigation was performed with the non-targeted method FT-ICR-MS equipped with an ESI source to unravel the metabolomic space.

Study participants and Method

For the metabolic profiling approach we used a set of 126 CSF-samples for analysis. Out of these samples, 31 originated from PD-patients (age ± SD: 65.5 ± 12.2 years; sex: 9 female, 22 male; disease duration ± SD: 0.87 ± 2.2 years) and 95 samples were taken from neurologically healthy controls (age ± SD: 44.9 ± 17.3 years, sex: 59 female, 36 male).

CSF-samples needed appropriate preparation for measurement by FT-ICR-MS. A protein precipitation extraction (PPE) protocol, adapted from (Forcisi *et al.*, 2015), was performed. Prior to treatment, the frozen CSF-samples were thawed on ice and vortex-mixed for 30 seconds. Afterwards, an 80 µL aliquot of each sample was merged with 320 µL ice-cold MeOH. The samples were vortex-mixed for 30 seconds at room temperature and centrifuged at 18,900 x g for 10 min at 4 °C. The obtained supernatant was diluted 1/70 in MeOH before FT-ICR-MS analysis.

The used FT-ICR-MS (Solarix, Bruker, Bremen, Germany) was equipped with a 12 Tesla superconducting magnet (Magnex Scientific, Varian Inc., Oxford, UK) and an ESI

source (Apollo II, Bruker Daltonics, Bremen, Germany). The instrument was used for the acquisition of ultrahigh resolution mass spectra. Prior to the measurement of CSF-samples external calibration of mass spectra was performed by analysis of a 3 mg/L arginine solution in MeOH with calibration errors lower than 0.1 mg/L (analyzed arginine clusters: m/z 173.10440, 347.21607, 521.32775, 695.43943). All measurements were performed in negative ionization mode and ion accumulation time of 300 ms for higher sensitivity. The injection flow rate was 2 uL/min for electrospray. Operating temperature was 180 °C for rapid solvent evaporation inside the electrospray. The ESI nebulizer gas flow rate was 2 L/min and the dry gas flow rate 4 L/min. The spectra were recorded in a mass-to-charge-ratio (m/z) range of 123-1000. For the generation of each mass spectrum 300 scans were acquired. A time-domain transient of 4 MW size was produced for each acquisition, which yielded ultra-high resolution for all signals which are of metabolomic interest.

Processing of spectra and data analysis

The obtained spectra were calibrated by a calibration tool developed in-house in Matlab (Release 2016a, The MathWorks Inc., Natick, Massachusetts, US). The tool estimates the most probable calibration curve by calculating a density map. This map describes the mass accuracy along with the considered mass range. The extracted peaks were aligned within a 1 ppm tolerance window and stored in a data matrix (Lucio *et al.*, 2011). All masses with abundancy lower than 10% were not taken into account for further analysis. Additionally, intensities of absent masses were set to zero in the related samples. By the use of the in-house developed software *Netcalc*, we were able to remove spectral noise and isotope peaks. Moreover, the software assigns molecular formulas to the aligned peaks based on mass differences between the detected features (Tziotis *et al.*, 2011). Annotation was also done by the use of the web server MassTRIX with *Homo sapiens* as reference organism (Suhre and Schmitt-Kopplin, 2008; Wagele *et al.*, 2012) and the annotations were saved in the data matrix. We performed molecular formula propagation through mass difference networks to assign molecular formulas to each m/z. This method starts random walks from known m/z-peaks and connects mass differences with molecular formula labels (e.g. Δ m/z =

14.01565 → CH$_2$) to assign the unknown m/z-peaks. An optimization was done to revise conflicting relationships and to follow intrinsic m/z-error distribution of each spectrum. This so-called Netcalc algorithm acts as an unsupervised filter which diminishes the data size and finally uncovers the underlying biochemical network structure inside the dataset (Liu *et al.*, 2016). A further features finding algorithm, RelieF, was applied to the whole dataset. The RelieF algorithm is a supervised method to select relevant and irrelevant features within two known classes (CTR vs. PD). This was done in order to reduce the dataset. The new list of variables could enhance the efficiency of the further classification (PD vs. CTR) and to reduce possible overfitting and noise (Witten *et al.*, 2017). The use of the algorithm resulted in a reduced subset to 243 masses which were able to maximize the classification accuracy of the model. For all of the 243 masses sensitivity (SEN), specificity (SPE), positive predictive value (PPV) and negative predictive value (NPV) were listed in chapter 6.1.3. These parameters were calculated by the use of the reportROC package (RStudio Version 1.0.136 - © 2009-2016 Rstudio, Inc.). Additionally, a sparse Partial Least Squares-Discriminant Analysis (sPLS-DA) was calculated to increase the power of variable selection and in parallel to reduce dimension in the components. Moreover, sPLS-DA assigns the 243 metabolites for the differentiation between CTR and PD. A 7-fold cross-validation and a receiver operating characteristic (ROC) curve were used for the assessment of classification performance. The performance was calculated by Balanced Error Rate (BER) which is a suitable parameter for the comparison of unbalanced number of samples in each classification group (CTR and PD). The BER works out the average amount of wrongly classified samples in the classification groups (Rohart *et al.*, 2017) and was calculated by the MixOmics package (Rstudio Version 1.0.136 - © 2009-2016 Rstudio, Inc.). In addition, an Orthogonal Projections to Latent Structures-Discriminant Analysis (OPLS-DA) was built to describe the orthogonal variance. The values R^2 and Q^2 were calculated to classify the performance of fit and the prediction of OPLS-DA analysis. These analyses were done in SIMCA 13.0.3.0 (Umetrics, Umeå, Sweden).

For the metabolites, listed in Table 17, an analysis of covariance (ANCOVA) was performed in order to evaluate the influence of interactions of the factor (CTR vs. PD)

with age and gender of the participants. Subsequently calculated p-values (adjusted by Dunnett test) report the difference between CTR and PD controlled by gender. The calculations were done by general linear model (GLM) analysis in SAS 9.4 (SAS Institute Inc., Cary, NC, USA). The p-values are listed in Table 17.

Results and Discussion

By use of the non-targeted ESI-FT-ICR-MS approach, we analyzed the metabolic profiles of 31 PD-patients and 95 CTR samples. The obtained spectra were evaluated by extensive methods to calibrate and annotate elemental formulas to the m/z-values. Afterwards, a feature selection excluded data noise and information which was not related to the study design comparing PD and CTR. Thereby, features were reduced to 243 m/z-values (see also chapter 6.1.3) which were further analyzed for their separation power of PD and CTR. The supervised method sPLS-DA showed good separation of CTR and PD shown in Fig. 3-15 A. The ROC curve presented in Fig. 3-15 B was calculated from the first component (243 m/z-values) of sPLS-DA analysis showing a high performance of the classification model and therefore, is suitable for the differentiation of CTR and PD. The ROC curve was calculated based on predicted scores (Rohart *et al.*, 2017). Additionally, the performance plot of the sPLS-DA analysis, illustrated in Fig. 3-15 C, shows the Balanced Error Rate (BER) getting constant after the second component. Therefore, two components are sufficient to achieve good performance. Moreover, by use of the supervised OPLS-DA analysis the separation of CTR and PD is even clearer as indicated by high values for the goodness of fitting (R^2Y(cum) = 0.98) and of prediction (Q^2(cum) = 0.53) illustrated in Fig. 3-15 D. A cross validation Anova resulted in a highly significant p-value (p < 0.0001). Within both supervised methods, the separation between CTR and PD is not related to the age-difference of samples, since the youngest patients do not cluster together. From the 243 m/z-values, which we received from the both supervised methods, a total of 81 masses showed decreasing and 162 masses showed increasing signal intensities in PD compared to CTR. In Fig. 3-15 E the masses with decreased intensities are illustrated in blue, whereas increasing intensities are colored orange. The altered m/z-values which contribute to the separation of the model were assigned with the KEGG database. An

83

assignment was achieved for 32 of the m/z-values. In Table 17 the 15 most important metabolites from the biological point of view are listed. These metabolites belong to different metabolic pathways, especially fatty acids/ lipids (decanoic acid, 10-hydroxydecanoic acid, arachidonic acid, dihomo-γ-linolenic acid, diacylglycerol (DG), phosphatidylcholine (PC) and phosphatidylethanolamine (PE)) and sugar derivatives (D-glucose-6-sulfate, sedoheptulose, and α-mannosylglycerate). In Fig. 3-15 F the increased signal intensities of selected fatty acids are presented.
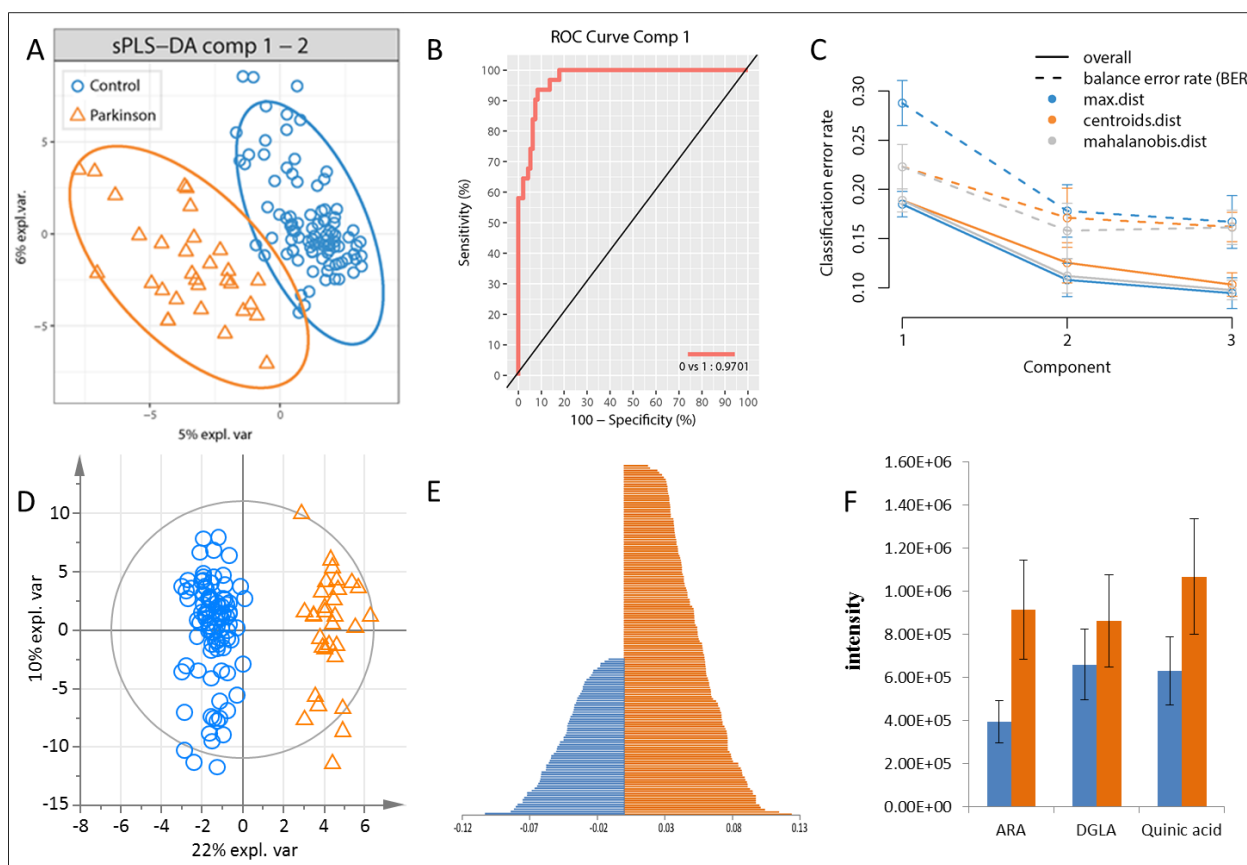
Figure 3-15: The implemented statistical analysis models: A) sPLS-DA validated with 7 fold cross-validation, B) represented the area under the Receiver Operating Characteristic (ROC) curve, C) the classification error rates by which the number of components was tuned (7 cross-validation), D) OPLS-DA validated with 7 fold cross-validation, E) compounds, which significantly distinguished PD from controls, and F) compared intensities of selected lipids. Expl. var., explorative variance.

Since age and gender were not matched within both investigated groups, we performed an ANCOVA analysis for the 15 most important metabolites to evaluate the influence of these factors. Age, as well as gender, can influence the metabolic homeostasis (Yoshii *et al.*, 1988; Molnar and Schutz, 1997; Lazzer *et al.*, 2010). The analysis showed no significant interaction between age and the differentiation of CTR and PD for the metabolites, but for arachidonic acid a significant interaction was found with gender ($p = 0.003$). The influence of gender on arachidonic acid concentration was also found by a meta-analysis of 51 publications to unravel the influence of hormones on the fatty acid composition in different body fluids (Lohner *et al.*, 2013). The p-values of the difference between CTR and PD controlled by gender are presented in Table 17 for the 15 selected metabolites.

Table 17: Most important neutral masses to distinguish between PD and controls with respective molecular formula, possible compounds assignment and mean intensity ± standard deviation (SD). The p-values are the result of the general linear model (GLM) adjusted with DUNNET.

Neutral mass	Theoretical molecular ion mass	molecular formula	Ion formula	Compound most probable in CSF	Mean Intensity ± SD (CTR)	Mean Intensity ± SD (PD)	alteration in PD	p-value
129.04261	128.03534	$C_5H_7NO_3$	$C_5H_6NO_3^-$	5-Oxoproline	1.05E+06 ± 1.09E+06	1.5E+06 ± 1.27E+06	↑	0.0795
163.09980	162.09253	$C_{10}H_{13}NO$	$C_{10}H_{12}NO^-$	N-Acetyl-phenylethyl-amine	1.5E+04 ± 1.48E+05	1.49E+05 ± 4.66E+05	↑	0.0578
172.14637	171.13910	$C_{10}H_{20}O_2$	$C_{10}H_{19}O_2^-$	Decanoic acid	4.69E+04 ± 2.64E+05	2.38E+05 ± 6.42E+05	↑	0.0116
188.01433	187.00705	$C_7H_8O_4S$	$C_7H_7O_4S^-$	p-cresol sulfate	5.74E+04 ± 3.23E+05	5.33E+05 ± 1.03E+06	↑	0.0002
188.14116	187.13389	$C_{10}H_{20}O_3$	$C_{10}H_{19}O_3^-$	10-Hydroxy-decanoic acid	1.67E+04 ± 1.64E+05	1.76E+05 ± 5.5E+05	↑	0.0129
186.06411	185.05684	$C_7H_{10}N_2O_4$	$C_7H_9N_2O_4^-$	S-AMPA	1.49E+05 ± 4.69E+05	0.0E+0 0± 0.0E+0.0	↓	0.2695

192.06343	191.05616	$C_7H_{12}O_6$	$C_7H_{11}O_6^-$	Quinic acid	6.30E+05 ± 1.02E+06	1.07E+06 ± 1.3E+06	↑	0.019
210.07402	209.06675	$C_7H_{14}O_7$	$C_7H_{13}O_7^-$	Sedo-heptulose	1.31E+06 ± 1.14E+06	8.06E+05 ± 9.76E+05	↓	0.0701
234.16207	233.15480	$C_{15}H_{22}O_2$	$C_{15}H_{21}O_2^-$	Valerenic acid	8.67E+05 ± 1.06E+06	1.23E+06 ±1.19E+06	↑	0.1567
260.02032	259.01305	$C_6H_{12}O_9S$	$C_6H_{11}O_9S^-$	D-Glucose-6-sulfate	4.1E+05 ± 8.18E+05	5.54E+05 ± 8.94E+05	↑	0.3258
268.07956	267.07228	$C_9H_{16}O_9$	$C_9H_{15}O_9^-$	α-mannosyl-glycerate	1.32E+06 ± 1.49E+06	1.78E+06 ± 1.78E+06	↑	0.1406
304.24043	303.23316	$C_{20}H_{32}O_2$	$C_{22}H_{31}O_2^-$	Arachidonic acid	4.01E+05 ± 8.42E+05	9.15E+05 ± 1.52E+06	↑	0.0494
306.25612	305.24885	$C_{20}H_{34}O_2$	$C_{20}H_{33}O_2^-$	Dihomo-γ-linolenic acid	6.61E+05 ± 1.28E+06	8.62E+05 ± 1.19E+06	↑	0.4911
622.55332	621.54604	$C_{39}H_{74}O_5$	$C_{39}H_{73}O_5^-$	DG (36:1)	1.73E+06 ± 2.23E+06	8.17E+05 ± 1.62E+06	↓	0.0677
747.61377	746.60650	$C_{42}H_{86}NO_7P$	$C_{42}H_{85}NO_7P^-$	PC/PE	1.58E+06 ± 1.29E+06	1.09E+06 ± 1.24E+06	↓	0.0291

The investigation of metabolic changes in neurodegeneration is essential, to unravel the mechanisms which are influenced due to the neurodegenerative disease PD. The use of CSF as sample matrix to investigate the metabolic alterations is very likely since it is the biofluids with closest contact to brain where the changes take place (Blennow *et al.*, 2010). Therefore, changes in brain metabolism might be reflected in CSF (Michalke and Berthele, 2011). The non-targeted FT-ICR-MS analysis was done without any prior hypothesis. A spectral profile comparison between healthy and diseased stated was done to create new hypothesis and to compare the obtained results with already known metabolic disturbances. As discussed in the introduction part (see chapter 1.2), none of the existing method is able to cover all metabolites (Wishart *et al.*, 2008). Therefore, the use of various techniques is mandatory to uncover as much metabolic alterations as possible. Several studies already investigated the unknown space of changes due to PD, but our approach using FT-ICR-MS was the first published metabolomic attempt using this technique in PD CSF analysis (Willkommen *et al.*, 2018b). As hypothesized, we found a couple of metabolites differing in PD compared to control. Specifically, metabolites belonging to the lipid/ fatty acid, glutathione, and energy metabolism revealed a strong alteration. Especially the increased level of the fatty acid arachidonic acid is associated with increased oxidative stress and neuroinflammation (Rapoport, 2008; Lee *et al.*, 2010; Ayala *et al.*, 2014). The influenced metabolic pathways are discussed in the following paragraphs.

Sophisticated statistical models sorted the most important masses and provided a group separation between CTR and PD. The assigned most important masses (listed in Table 17) revealed affected pathways in disease mechanisms. The metabolite 5-oxoproline belongs to the γ-glutamyl-cycle and thus it is implicated in glutathione (GSH) – metabolism. 5-oxoproline itself is an oxidation product and elevated levels of the metabolite are associated with oxidative stress (Cassol *et al.*, 2014). Within the γ-glutamyl-cycle the antioxidant compound GSH is synthesized. GSH can protect the organism against oxidative stress by oxidizing to glutathione disulfide (GSSG) with simultaneous reduction of H_2O_2 (Aoyama and Nakaki, 2013). Decreased levels of this essential antioxidant can increase the susceptibility of oxidative stress and the damages induced by reactive oxygen species (ROS). The loss of GSH is proven to be associated

with the aging process (Knight, 2000; Maher, 2005), but decreased levels of the metabolite were also found in neurodegenerative diseases or more specifically, in PD reduced GSH was detected in substantia nigra (Sian *et al.*, 1994a; Sian *et al.*, 1994b; Pearce *et al.*, 1997). Additionally, several metabolomic studies found GSH or its oxidized form GSSG in various body fluids. LeWitt et *al.* demonstrated reduced concentrations of GSSG in CSF of PD patients by use of LC-MS techniques (LeWitt *et al.*, 2013). Moreover, in plasma reduced amount of GSH in 60 patients with PD as compared to 25 CTRs was analyzed (Bogdanov *et al.*, 2008). Contrary to this reduced levels of GSH, increased concentration of GSH has been found in an early disease stage (Maher, 2005). In line with this increase and our findings, elevated levels of 5-oxoproline were found in plasma of 20 newly diagnosed PD patients in comparison to 20 CTRs (Trupp *et al.*, 2014). Moreover, Wu et al. investigated the urinary excretion of 5-oxoproline and found increased levels. They linked the increased excretion with reduced bioavailability of cysteine and glycine and therefore also lowered GSH biosynthesis in vivo (Wu *et al.*, 2004). An increase in the GSH synthesis, as demonstrated by our results, is associated with a higher need to remove ROS in an early disease state. Supposing that the increased GSH synthesis is insufficient or the synthesis is even decreased, ROS will accumulate after a short timeframe and cause neurodegenerative conditions. Although we were not able to detect GSH itself, the increased concentration of the γ-glutamyl-cycle metabolite 5-oxoproline seems to be associated with increased anti-oxidative characteristics in the early disease process.

Moreover, we found some metabolites which are involved in the energy metabolism. The metabolites D-glucose-6-sulfate and α-mannosylglycerate produced higher intensities in PD and the metabolite sedoheptulose showed lower intensity in CSF of PD-patients. The metabolite α-mannosylglycerate is involved in the fructose and mannose metabolism. The metabolites fructose and mannose were found increased in CSF of PD-patients, too (Trezzi *et al.*, 2017). Additionally, these compounds are part of the glycolysis (Izumi and Zorumski, 2009), an important metabolic process to produce nucleotide sugars. Glycolysis is enhanced in oxidative stress conditions in order to eliminate oxidative phosphorylation in mitochondria (Mazzio and Soliman, 2003). Moreover, Ahmed et al. found raised concentrations of sorbitol in plasma of PD-patients

(Ahmed *et al.*, 2009). Sorbitol is another metabolite involved in the fructose and mannose pathway. Apart from these sugar metabolites, several other monosaccharides presented increased serum-intensities in PD (Michell *et al.*, 2008). Although they could not further differentiate the monosaccharides, the results show the involvement of sugar compounds in the disease status. Additionally, metabolic changes were investigated in dopaminergic cells after exposure to environmental and mitochondrial toxins as a model for PD. The results showed enhanced concentrations of sedoheptulose as well as an increase of glucose and myoinositol (Lei *et al.*, 2014). Moreover, sedoheptulose can be converted to sedoheptulose-7-phosphate, an important metabolite of the pentose phosphate pathway. The oxidative pentose phosphate pathway is the major source for the synthesis of antioxidant enzymes like glutathione peroxidase and thioredoxin reductase (Bouzier-Sore and Bolanos, 2015). Therefore, decreased levels of sedoheptulose may reveal an enhanced turnover of the metabolite to produce antioxidant compounds. Additionally, the metabolite α-mannosylglycerate showed inhibitory effects on α-synuclein fibrillation. Since α-mannosylglycerate did not alter the expression level or the degradation rate of α-synuclein, the authors concluded that α-mannosylglycerate works as a chemical chaperone to complex the protein α-synuclein and inhibits the fibril formation (Faria *et al.*, 2013). Fibrillation of α-synuclein is a major hallmark of PD; therefore, the increase of α-mannosylglycerate levels in PD can be a sign of the effort to complex the protein and inhibit the formation of the toxic form. Our results show a clear shift in the three metabolites and with this indicates changes in energy metabolism, but also in other metabolic pathways like the pentose phosphate pathway. Changes in the energy metabolism due to PD are proven already in several studies and need further investigation to unravel mechanisms in neurodegeneration.

Apart from the already discussed metabolites, also several fatty acids showed significantly altered intensities in PD. The metabolites quinic acid, decanoic acid, 10-hydroxydecanoic acid, valerenic acid, arachidonic acid, and dihomo-γ-linolenic acid displayed enhanced intensities in PD. In contrast to this, the lipid metabolism compounds DG, PC, and PE showed lower intensities in PD. Several medium and long chain fatty acids (5-dodecanoate, 3-hydroxydecanoate, docosadienoate, and docosatrienoate) had elevated concentrations in plasma as well as in CSF of PD-

patients. The metabolomics investigations were done in a non-targeted manner (LeWitt *et al.*, 2017). Studies by Trupp et al. and Michell et al. in plasma and serum resulted in lower concentrations of C16 and C18 fatty acids as well as of octenoic acid (Michell *et al.*, 2008; Trupp *et al.*, 2014). Especially the polyunsaturated fatty acids (PUFA) arachidonic acid (ARA) and dihomo-γ-linolenic (DGLA) are in the focus of investigations in brain and associated body fluids in neurodegenerative diseases. This class of compounds is very susceptible to oxidative stress due to lipid peroxidation (Liu *et al.*, 2008; Ayala *et al.*, 2014). DGLA can be converted into the pro-inflammatory metabolite ARA, but can also form anti-inflammatory metabolites. ARA itself is bound to membranes in brain and can be release enzymatically due to inflammatory processes (Bazinet and Laye, 2014). The elevated levels of both metabolites in the PD-patients seem to be associated with pro-inflammatory features. The metabolism of ARA is rigorously regulated in brain, but misbalances induced by neurodegeneration like neuroinflammation or oxidative stress can influence the ARA metabolism (Bosetti, 2007). More specifically, processes like enzymatic oxidation of ARA can be elevated and with this multiple pro-inflammatory metabolites are synthesized (Bazinet and Laye, 2014). The fatty acid profile was determined in postmortem brains of PD patients and in parkinsonian monkeys with gas chromatography (Julien *et al.*, 2006). A significantly increased ARA concentration was found in the cortex of all brains after intake of the drug levodopa. Additionally, up-regulated cytosolic phospholipase A_2 was measured in cortex and putamen of rats with induced PD. This up-regulation indicates an increased neuroinflammatory status in the brains of PD-rats and is also associated with elevated ARA-signaling. Moreover, another study with induced PD in rats (by Mn-injection) resulted in an increased production of the inflammation markers prostaglandin B_1, 15-(S)-HETE, and Resolvin (Neth *et al.*, 2015b). The increased intensities of DGLA and ARA in CSF of PD-patients as found within our investigations (see Figure 1 F) seem therefore to be associated with elevated neuroinflammatory characteristics and with oxidative stress.

3.7.2 Mass difference enrichment analysis

Mass differences were originally used as a tool for feature annotation. Breitling et al. implemented two different concepts of application. On the one hand, mass differences can be used as networks to realize ab initio pathway detection. On the other hand, mass differences are suitable for feature identification if another metabolite is already known (Breitling *et al.*, 2006a; Breitling *et al.*, 2006b). This concept was further optimized by several publications (Rogers *et al.*, 2009; Morreel *et al.*, 2014). This extended approach enables an improved interpretability since it reveals unknown connections between different features. The mass difference enrichment analysis (MDEA) is building up networks starting from a reference mass. Within the network accurate m/z-features, molecular masses, or possible compounds are illustrated as nodes. These nodes are connected with the respective mass differences, the so-called edges. The mass differences or edges represent specific possible biochemical reactions. The MDEA then takes the network and estimates how many connections from each mass difference can be expected on the basis of the network. Afterwards, MDEA counts how many reactions of a given type were really found and calculates a Z-score. The results of this MDEA performed with the m/z-features of the FT-ICR-MS analysis in CSF-samples are illustrated within the following chapter.

Data analysis

The MDEA was done following the procedure described in (Moritz *et al.*, 2017). Shortly described, a set of mass difference building blocks are investigated for their enrichment with PD-markers. The list of these mass difference building blocks is attached to the publication and involves various important mass difference features (Moritz *et al.*, 2017). The analysis was performed with the whole set of features with molecular formula assignment obtained by FT-ICR-MS analysis and respective statistical data-pretreatment. The entire metabolome provides the chemical source to (bio-) synthesize the 243 most important masses, which were selected by the RelieF algorithm. The MDEA examines the mass differences which are linked to the remaining features to highlight suitable reactions of biomarker production (Moritz *et al.*, 2017; Kaling *et al.*, 2018). The mass differences describe specific biochemical reactions within the human

metabolism. To quantify the enrichment, Fisher´s exact test was performed, providing Z-scores and p-values. The Z-scores of $Z \approx 2$ and $Z \approx 2.5$ relate to $p \approx 0.05$ and $p \approx 0.01$, respectively. The network visualization was performed in the open source software Gephi (The Open Graph Viz Plat-form, http://gephi.github.io/).

Results and Discussion

Since we were only able to assign a small part of the m/z-features to respective compounds, the MDEA was meant to increase the size of information coming from the FT-ICR-MS measurements. As already presented, the MDEA analyses mass-differences between various m/z-features within a network and compares the prevalence of a certain reaction on the basis of the network with the real amount of this reaction. The schematic representation of the connection of two nodes through a biochemical reaction on basis of mass differences in the MS-spectra is illustrated in Fig. 3-16.
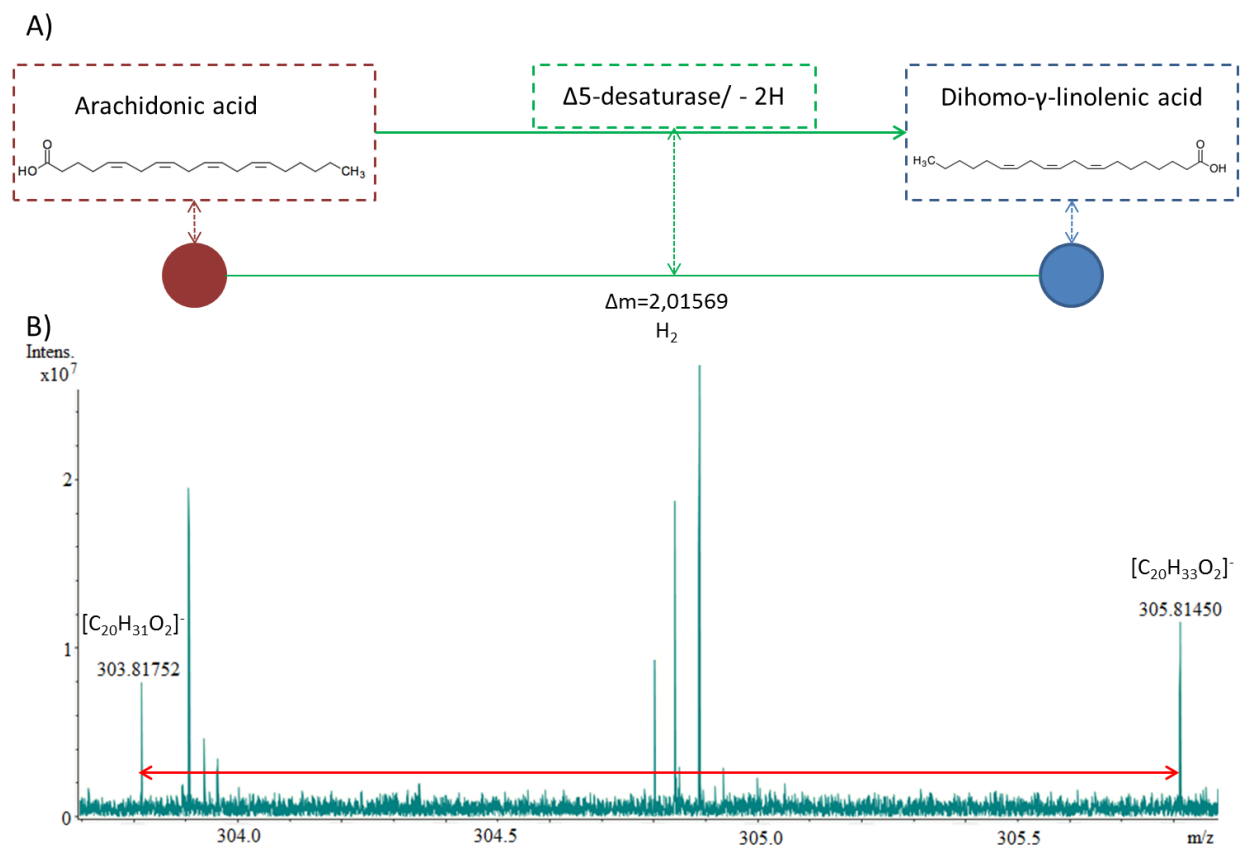
Figure 3-16: Schematic representation of MDEA. A) Connection of two compounds (nodes) by a specific mass difference representing a biochemical reaction (edge) and B) respective m/z-signals within spectra.

By the help of this mass differences and nodes a network was build up. Within this network the connection between ARA and DGLA, but also between other assigned m/z-features is shown. The mass differences are defined by Z-scores. These scores correspond to an increase or decreased of the occurrence of the respective mass difference. In Figure 3-17 the over-represented mass differences of significantly regulated metabolic features in PD are shown (the Z-scores of all mass differences are listed in Table S4 of (Willkommen *et al.*, 2018a)).
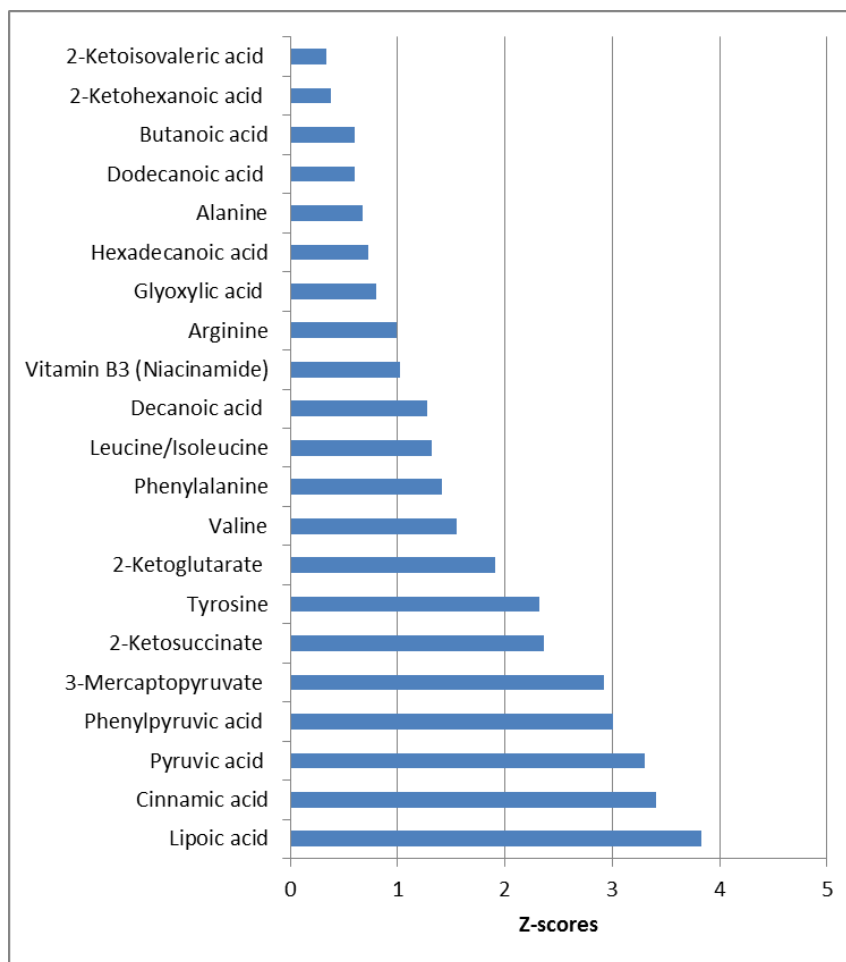
Figure 3-17: Over-represented mass differences obtained by MDEA. Z-scores > 2 correspond to p-values < 0.05.

The positive Z-scores imply that the mass difference of a reaction was found more often to produce markers than expected. This might be associated with an increased activity of the organism to build the investigated mass differences into its biomass. Several of the over-represented mass differences in PD are compounds, which are involved in the cellular respiration processes. Compounds like α-ketoglutarate and pyruvate belonging to the tricarboxylic acid (TCA) cycle exhibited positive Z-scores. Apart from that, also substrates and break-down products of TCA-cycle compounds were found over-represented as illustrated by the positive Z-scores indicating a mitochondrial dysfunction. Mitochondria produce a large proportion of the cellular energy by oxidative phosphorylation. A dysfunction of mitochondrial processes is already known to be

involved in PD (Schapira *et al.*, 1990; Anandhan *et al.*, 2017). In Figure 3-18 our findings of alterations in TCA cycle are illustrated. All mass differences/ compounds were found to be over-represented in PD. All direct participants of the TCA cycle are colored orange, precursors of TCA cycle compounds are colored red and break-down products of TCA cycle compounds are colored purple.
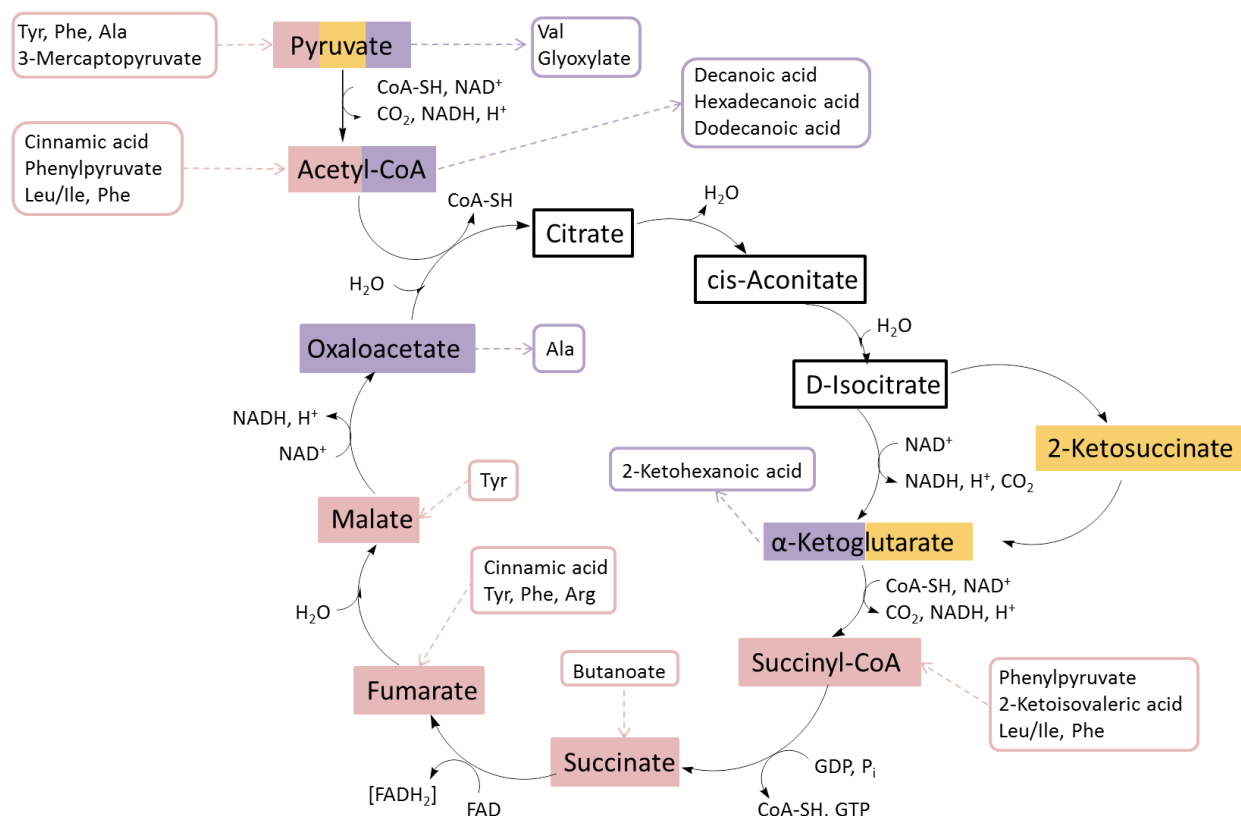
Figure 3-18: Over-represented mass differences which are associated with the TCA cycle. Color code: Metabolites found directly by MDEA involved in TCA cycle are colored orange; precursor-metabolites found by MDEA synthesizing TCA cycle compounds are colored red; break-down products of TCA cycle compounds found by MDEA are colored purple.

The primary cause of mitochondrial misbalance is ROS produced within the mitochondria. Moreover, metabolic dysregulation seems to be a contributor (Pieczenik and Neustadt, 2007; Moon and Paek, 2015). Alterations in the metabolic homeostasis of

TCA cycle was found within various studies. Increased amount of malate in plasma and citrate in CSF were found in PD-patients (Trupp *et al.*, 2014; Wu *et al.*, 2016). Contrary to this, decreased concentrations of citrate, malate, isocitrate, and succinate have been analyzed in plasma (Ahmed *et al.*, 2009). Differences in altered metabolites may be due to varying sample handling and storage, patients' age, gender, and medication, as well as different determination methods. Not only metabolites of the TCA cycle are affected, but also enzymes and proteins needed for mitochondrial processes. The compounds lipoic acid and vitamin B3 are essential for the proper functioning of pyruvate dehydrogenase which is catalyzing the oxidative decarboxylation of pyruvate. Additionally, the compounds fumarate, malate, oxaloacetate, α-ketoglutarate, citrate, and NAD, which are involved in TCA cycle, were found to be associated with Mn. These findings were obtained in CSF analysis by CZE hyphenated to ICP-MS (Michalke *et al.*, 2007). A variation of associated trace element to specific metabolites might be an intensifying influence for enhanced oxidative stress conditions in PD as well as for mitochondrial dysfunction. The significantly over-represented mass differences are not only belonging to TCA cycle but also to other metabolic processes. Another example, which was revealed by MDEA, is the over-representation of reactions with malondialdehyde (MDA) in PD. MDA is a sufficient marker for oxidative stress and a break-down product of PUFAs, but is not detectable by FT-ICR-MS. The reason for MDA to be not detectable in FT-ICR-MS is the small molecular weight (MW_{MDA} = 72,0636 g/mol) and the labile character of the compound. MDA is associated with lipid peroxidation and therefore already known as biomarker of PD (de Farias *et al.*, 2016). Increased levels of MDA were found in plasma and erythrocytes of PD-patients compared to CTR (Sanyal *et al.*, 2009; Sunday *et al.*, 2014). An overview of MDA metabolism is given in a recent review (Ayala *et al.*, 2014).

Conclusion

The non-targeted method FT-ICR-MS was used to get a comprehensive overview of changes in the metabolism due to PD. The metabolic profiles of each sample underwent sophisticated statistical procedures to extract information regarding the differentiation between CTR and PD. A set of 243 masses was found to separate both groups

according to sPLS-DA and OPLS-DA. Assigned masses are linked to fatty acid/ lipid metabolism and energy metabolism. Especially the fatty acid arachidonic acid is of interest since it is linked to oxidative stress and neuro-inflammatory conditions. Moreover, an MDEA showed an over-representation of mass differences associated with the TCA-cycle. Changes in TCA-cycle may be linked to mitochondrial dysfunction. Overall, the metabolomic investigation revealed several changes in the normal metabolism due to PD.

3.8   Specific PD-markers

3.8.1 AChE activity

Acetylcholinesterase (AChE) is an enzyme which specifically catalyzes the cleavage of acetylcholine to acetic acid and choline. The degradation process of acetylcholine is important for the forwarding of neuronal stimuli. This process is very rapid what is necessary for a fast forwarding of action potentials of the nerve cells. Therefore, AChE plays a critical role in the function of the nervous system. An impairment of the cholinergic neurotransmission has already been proven for several neurological diseases like AD (Kessler *et al.*, 2006; Herholz, 2008) and PD (Manyam *et al.*, 1990). Various chemical warfare agents and insecticides inhibit the activity of AChE which consequently results in the accumulation of acetylcholine in the synaptic cleft. This finally leads to a hyperstimulation of internal organs and can cause death. Since the activity of AChE is of paramount importance in the function of the CNS and obtained results in PD are contradictory, we decided to evaluate the activity of this specific enzyme. The results are presented in the following chapter.

Study participants and Method

For the measurement of AChE activity we used a set of 27 CSF-samples for analysis. Out of these samples, 13 originated from PD-patients (age ± SD: 65.5 ± 10.4 years; sex: 6 female, 7 male) and 14 samples were taken from neurologically healthy controls (age ± SD: 57.5 ± 15.2 years, sex: 5 female, 9 male).

For the determination of the AChE activity in CSF we used the AChE fluorescent activity Kit from Arbor Assays. Samples were diluted 1:10 with assay buffer prior to measurement. According to the assay protocol, 100 µL of each diluted sample and standard were pipetted into the 96-well plate (duplicate). Additionally, 50 µL of the provided reaction mixture was added to each well. After incubation for 20 minutes at room temperature, the fluorescent emission at 510 nm was measured after excitation at 370-410 nm with a plate reader (Safire2, Tecan).

Results and Discussion

By application of the used Fluorescent kit we were able to quantify AChE activity in CSF of PD patients and respective CTRs. The results of this investigation are shown in Fig. 3-19. The executed standard calibration curve resulted in a high coefficient of determination as shown in Fig 3-19 A. Moreover, in Fig. 3-19 B the results of the comparison between CTR and PD for AChE activity in CSF are illustrated.
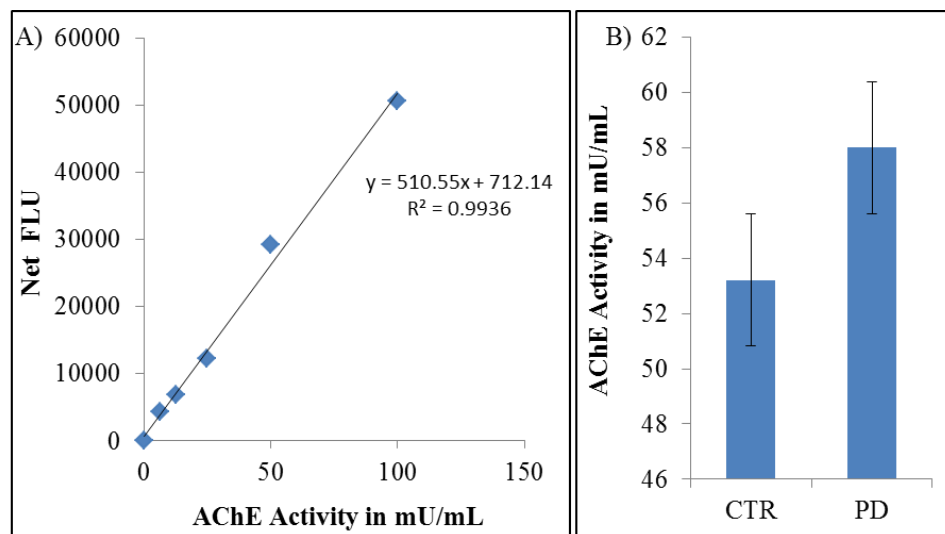
Figure 3-19: Results of the Acetylcholinesterase fluorescent activity kit. A) Standard calibration curve showed high linearity und good coefficient of determination. B) Comparison of the means ± SD of AChE activity in CTR and PD did not reveal a significant difference.

A Student´s t-test indicated an insignificant shift (p = 0.594) of the AChE activity. In PD the activity of the enzyme is slightly increased. This finding is in agreement with (Ruberg

99

et al., 1986; Zubenko *et al.*, 1986; Sirviö *et al.*, 1987; Manyam *et al.*, 1990). Although an insignificant shift towards higher AChE activity in PD was observed. Increased AChE activity was observed as reaction to Mn-induced oxidative stress in a rat model (Fernsebner *et al.*, 2014). Additionally, due to oxidative stress the activity of AChE activity has been found enhanced in cultured cells. Within this model AChE activity was especially enlarged inside and around amyloid plaques which are present in AD brain (Melo *et al.*, 2003). Another study found AChE to be directly linked to the conversion of β-amyloid into insoluble plaques (Rees and Brimijoin, 2003). A similar involvement is conceivable in the fibrillation of α-synuclein, the protein involved in the development of PD, but no literature is available supporting this thesis. Additionally, the AChE activity is increased in SN of PD brains compared to normal brains (Rinne *et al.*, 1973). Again significantly increased activity of AChE was discovered in the salivary flow of PD-patients in contrast to CTR (Fedorova *et al.*, 2015). They hypothesized, that increased AChE activity in saliva is the consequence of increasing α-synuclein deposition, but need further experiments to prove their hypothesis. Moreover, AChE inhibitors showed an improvement of some PD-symptoms (Farah *et al.*, 2018). In line with this finding, increased AChE expression seems to have a role in neuronal cell death what is associated with PD (Zhang *et al.*, 2013).

Therefore, the analyzed slight increase of AChE activity within the investigated PD samples might be linked to increased oxidative stress in PD and higher rate of neuronal cell death.

3.8.2 α-Synuclein

The protein α-synuclein is a natively unfolded soluble 14 kDa protein. The aggregation of α-synuclein is the pathological hallmark of PD. The protein can be converted through a toxic oligomeric intermediate into an insoluble aggregate which is the major constituent of Lewy bodies (Bharathi *et al.*, 2008). α-synuclein is a presynaptic protein which is found in several brain regions (Maroteaux *et al.*, 1988; Jakes *et al.*, 1994). The structure of the protein is divided into three main parts. The residues 1-60 are the N-terminal, amphiphilic part with four imperfect repeats of eleven amino acids. This first part is shaped like an α-helix. The non-amyloid β-component (NAC)-region of residues

61-95 is hydrophobic and is primarily involved in the aggregation process. The last C-terminal part contains the highly charged residues 96-140 (Fink, 2006). The protein has several possible functions, but not all physiological functions are completely known. It is involved in the vesicle release and trafficking (Fink, 2006), in the dopamine synthesis and regulation (Perez *et al.*, 2002; Post *et al.*, 2018), and it elevates the formation of the soluble NSF attachment protein receptor (SNARE) complex (Burré *et al.*, 2010). Additionally, α-synuclein showed to act as a cellular ferrireductase with Cu and NADH as co-factors to reduce $Fe(III)$ to $Fe(II)$ (Davies *et al.*, 2011; McDowall *et al.*, 2017). The involvement of α-synuclein in the PD-etiology is widely accepted. Therefore, we determined the amount of the protein in CSF by a commercially available enzyme-linked immunosorbent assay (ELISA).

Study participants and Method

For the measurement of total α-synuclein concentration we used a set of 24 CSF-samples for analysis. Out of these samples, 12 originated from PD-patients (age ± SD: 67.1 ± 9.1 years; sex: 6 female, 6 male) and 12 samples were taken from neurologically healthy controls (age ± SD: 58.1 ± 13.1 years, sex: 4 female, 8 male).

For the determination of α-synuclein in human CSF we used the "hSyn total ELISA-Enzyme immunoassay for quantitative determination" from Analytik Jena. The samples were diluted 1:4 directly in the plate. According to the assay protocol, 75 µL of a 1:20 diluted horseradish peroxidase (HRP) conjugate (anti- α-synuclein antibody concentrate) was pipetted per well onto the plate. Additionally, 25 µL of the provided standards, blank, quality standard, and samples were pipetted per well (in duplicate) and mixed 2-3 times using the pipet. The plate was covered with a tape and incubated at 6 °C for 22 h. Afterwards, the cover was removed and each well was washed nine times with 300 µL of wash solution. Immediately after the washing procedure 100 µL of staining solution were added to each well. The plate incubated again for 15 min in the dark at 22 °C. Finally, 150 µL of stop solution was added to each well. The plate was shaken for 3 s and settled down for 5 s before the optical density (O.D.) was measured at 450 nm and 620 nm as reference wave length with a plate reader (Safire2, Tecan).

Results and Discussion

The protein α-synuclein is involved in the pathological processes which are associated with PD. Therefore, the determination of the concentration of total α-synuclein was of crucial importance for the comprehensive characterization of CSF samples. We have used the "hSyn total ELISA-Enzyme immunoassay for quantitative determination" of total α-synuclein concentrations. The results of calibration of delivered standards as well as the comparison of α-synuclein concentrations in CSF of CTR and PD patients are illustrated in Fig. 3-20. The juxtaposition of the mean concentrations with respective SD showed an insignificant shift of α-synuclein in PD patients ($p = 0.705$) towards slightly higher concentrations.
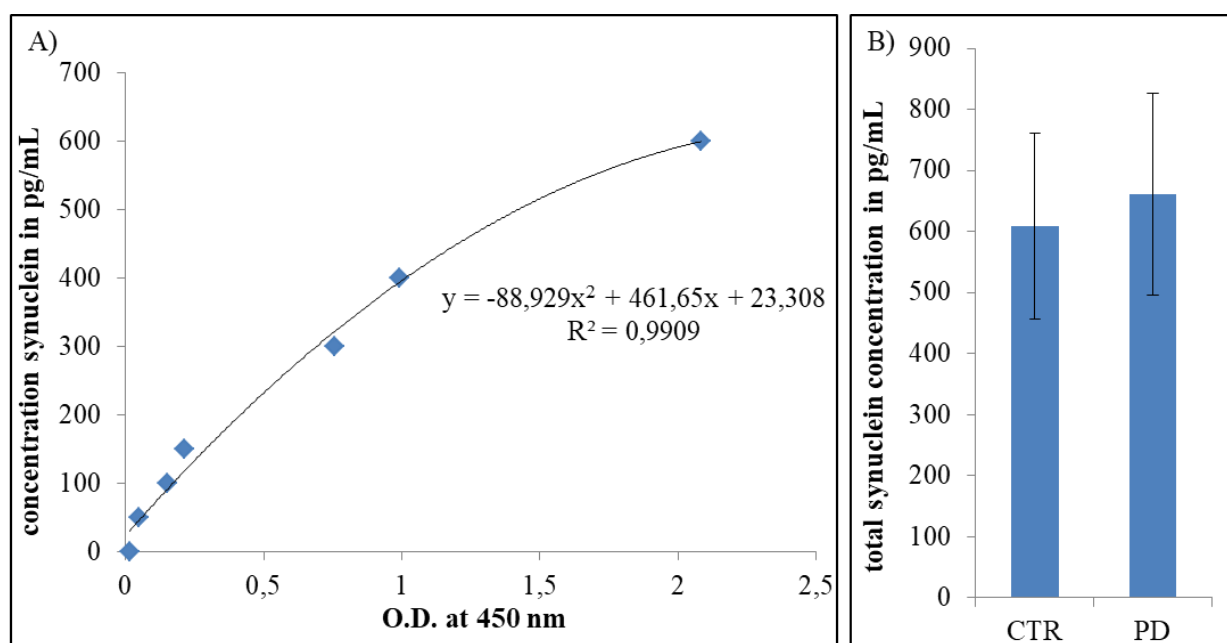
A) The equation shown is $y = -88{,}929x^2 + 461{,}65x + 23{,}308$ with $R^2 = 0{,}9909$.

Figure 3-20: Results of the hSyn total ELISA-Enzyme immunoassay for quantitative determination of α-Synuclein in human CSF. A) Standard calibration curve showed a good coefficient of determination with quadratic equation. B) Comparison of the means ± SD of total α-Synuclein in CTR and PD did not reveal a significant difference.

Several studies already determined the shift of α-Synuclein in CSF of PD patients. A study comparing PD and atypical parkinsonism revealed no significant differences between both groups. An adjustment for age didn´t have any influence on the outcome,

indicating α-Synuclein as an unsuitable biomarker (Aerts *et al.*, 2012). Another investigation determined the levels of total α-Synuclein, oligomeric α-Synuclein, phosphorylated α-Synuclein, and oligomeric phosphorylated α-Synuclein in the ventricular CSF of post mortem samples. They compared the CSF samples of 20 CTRs against 76 patients (39x PD, 17x dementia with Lewy bodies (DLB), 12x progressive supranuclear palsy (PSP), and 8x multiple system atrophy (MSA)). For the comparison between CTR and PD only insignificant changes have been found for the four determined α-Synuclein species (Foulds *et al.*, 2012). Moreover, Hong et al. analyzed the amount of total α-Synuclein in CSF of 117 PD patients and 132 CTR (also of 50 AD patients). The level of α-Synuclein decreased significantly in PD, but increased (although insignificant) in AD (Hong *et al.*, 2010). Additionally, they found an influence of age on the α-Synuclein concentration mainly in CTR and also of blood contaminations in the CSF samples. An association with gender was not proved. In concordance with these findings, significantly lower amounts of α-Synuclein were found in 63 PD patients compared to 39 CTRs. The decreased levels were associated with increased motor severity in PD and significant correlations with the total level of the protein tau and its phosphorylated modification (Kang *et al.*, 2013). Moreover, significantly reduced α-Synuclein levels were found in PD CSF by various studies (Tokuda *et al.*, 2006; Parnetti *et al.*, 2011; Mollenhauer *et al.*, 2013; Mondello *et al.*, 2014; Parnetti *et al.*, 2014a; Stewart *et al.*, 2014; van Dijk *et al.*, 2014). In contrast to the reduced α-Synuclein levels, Park et *al.* couldn´t find a significant difference in total α-Synuclein amount in CSF of 23 untreated PD patients as compared to 29 age- and sex-matched CTRs. They demonstrated significantly higher amounts of oligomeric α-Synuclein in CSF of PD patients (Park *et al.*, 2011). A more recent study tried to discriminate PD patients and CTR through quantification of α-Synuclein in CSF by the use of two detection kits. They found for neither of the kits a significantly difference in the total α-Synuclein (Forland *et al.*, 2018).

In concordance with Park et *al.*, Foulds et *al.*, and Forland et *al.*, we didn´t find a significant change in the amount of total α-Synuclein in CSF comparing PD patients with controls. Since we have analyzed slightly increasing values for α-Synuclein, our results are in contrast to the cited literature indicating decreased concentrations of α-Synuclein

in PD. Differences in the findings may be associated with varying procedures of analysis, differences in samples size and comparability between PD patients and CTR, age differences and sample pretreatment. Our samples stood up to 6 h at room temperature and therefore, changes in the structure of α-Synuclein are possible. The oligomeric form of α-Synuclein was suggested to be the most toxic one, an increase of this species was found in CSF of PD patients (Tokuda *et al.*, 2006; Park *et al.*, 2011; Parnetti *et al.*, 2014a; Parnetti *et al.*, 2014b). Our performed analysis revealed the concentration of total α-Synuclein without differentiation in oligomeric and monomeric form of α-Synuclein. However, α-Synuclein fibrillation and aggregation can be enhanced by interaction with various metals (Fink, 2006; Bharathi *et al.*, 2008; Carboni and Lingor, 2015; Lingor *et al.*, 2017). Interactions of α-Synuclein with Cu (Paik *et al.*, 1999; Anandhan *et al.*, 2015), Fe (Li *et al.*, 2010a; Peng *et al.*, 2010), Zn (Tõugu and Palumaa, 2012; Valiente-Gabioud *et al.*, 2012), and Mn (Cai *et al.*, 2010; Li *et al.*, 2010b; Ducic *et al.*, 2015) were found. Thereby, increased level of total α-Synuclein finally also lead to enhanced levels of fibrillation (Uversky *et al.*, 2001).

Therefore, the slightly increased amount of α-Synuclein in CSF of PD patients may be associated with increased aggregated forms of α-Synuclein. This aggregation can be induced or enhanced by the also elevated levels of Cu, Fe, and Zn as described in chapter 3.2.

Conclusion

The AChE activity and the amount of α-synuclein were determined by specific kits with fluorescent emission or optical density, respectively. Both parameters are already known influencing factors in PD and contribute to the comprehensive investigations of CSF in PD. For AChE a slightly increased activity was found in PD which might be associated with increased oxidative stress and higher rate of neuronal cell death. As for AChE activity, α-synuclein was slightly increased in PD, but without significance. For a more sophisticated statement regarding α-synuclein, the specific forms need to be analyzed (e.g. oligomeric form). Since oligomeric α-synuclein is the most toxic form of the protein an increase of this form would be most deleterious.

3.9 Data integration of metallomics with metabolomics results[4]

Within data integration different types of datasets can be matched together (Ni *et al.*, 2019). This is of great importance to find mutual connections between different datasets. The integration of different parameters can deliver even more informative relations than is available from the individual datasets separately (Jansson *et al.*, 2009; Maier *et al.*, 2017). This might help to increase knowledge about ongoing processes in disease investigations. Within this thesis the linkage between the metallomic and metabolomic measurements were analyzed to identify the interaction between both. In many metabolic processes enzymes with trace elements in the catalytic center are involved. Therefore, links between metals and metabolites will arise and the knowledge of these connections will help to uncover the mechanisms of disease onset and progression.

Data analysis

The metallomic data presented in chapter 3.2, 3.3, 3.4, and 3.6.2 and the metabolomic results shown in chapter 3.7 were integrated together. Therefore, the metallomic and metabolomic datasets were integrated by a vertical integration method (Yu and Zeng, 2018) to get for each sample a metallomic and a metabolomic typology. Furthermore, the resulting dataset was scaled with unite variance and was analyzed by a Block-sPLS-DA. This analysis is appropriate for the integration of datasets (MixOmics package, RStudio Version 1.0.136 - © 2009-2016 RStudio, Inc.). The applied model imposed sparseness throughout the latent components. Additionally, the model improved the selection of variables, reduced the dimensions, and allowed the aggregation of the two different datasets (Wold, 1966; Tenenhaus, 1998; Tenenhaus and Tenenhaus, 2011). The classification performance was determined by a 7-fold cross validation and the performance was calculated by BER. This rate is suitable for an unbalanced amount of samples per class since it estimates the average proportion of wrongly classified samples in each class (Rohart *et al.*, 2017). Various metallomic and metabolomic variables showed a relation to each other as characterized by strong

---

[4] The following chapter has been partially prepublished in (Lucio *et al.*, 2019)

correlations. For the metabolomics data we concentrated on the assigned m/z-features presented in Table 17. We evaluated lists of connected features showing a differentiation in PD, and they mainly drove the separation between PD and CTR. Additionally, for these connected features a GLM was run to compute the respective p-values with the confounding variables age and gender. The p-values were adjusted with Benjamini-Hochberg test. Since having an unbalanced experimental study design, we calculated the least square means that is equal to the specific effects for the linear predictor part of the model. These calculations were done in SAS version 9.3 (SAS Institute Inc., Cary, NC, USA).

Results and Discussion

The results of metallomics investigations as well as of metabolomics investigations presented within this work, already showed some quite interesting results. These results substantiated existing studies on Parkinson´s disease and added new knowledge. Moreover, the task of this work was to combine different variables determined throughout this work to add in-depth expertise. More specifically, we tried to integrate the results of metallomics investigations as presented in chapters 3.2, 3.3, 3.6.2 and metabolomic investigations as discussed in chapter 3.7. Statistical models were used to identify significant interrelations and the biological meaning is discussed.

The data integration was built up between the list of "most important masses" (see Table 17) and the elemental information total elemental concentrations of Cu, Fe, Mn and Zn, species characterization, and the metal-determination within the amino acid fractions. Although, the datasets were already statistically reduced and had diverse typology, the calculated correlation value of 47% between the two datasets is acceptable. The interrelation between the two datasets as calculated by the integration of metallomic and metabolomic datasets, with the respective correlation value, is represented in Fig. 3-21.
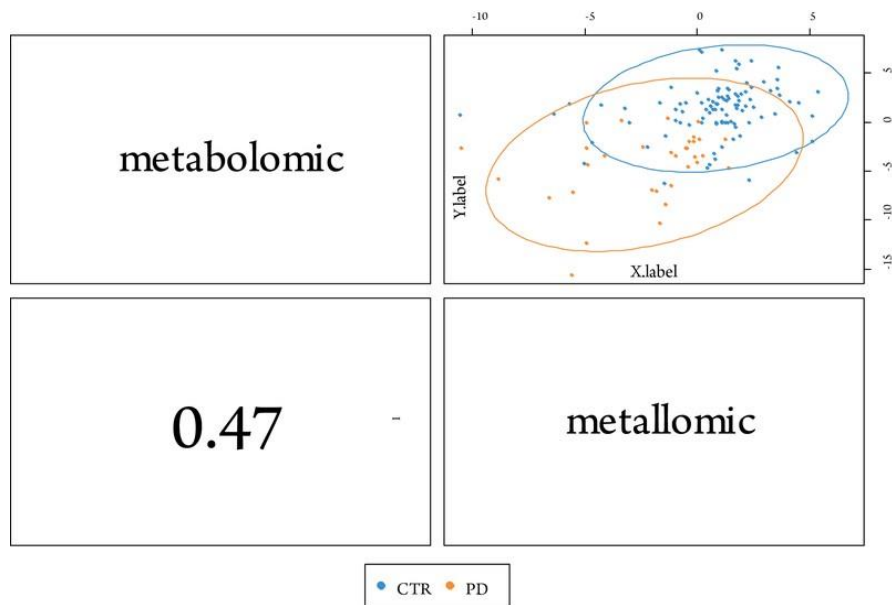
Figure 3-21: Illustration of the interrelation between metallomic and metabolomic data out of the same sample set with respective correlation value.

The two investigated blocks of metabolomics and metallomics as well as their separation efficiency is illustrated by a Block sPLS-DA analysis in Fig. 3-22 A. The analysis has three valid components, absorbing 25% of the metabolomic dataset and 23% of the metallomic dataset. The various variables used within the two blocks were ranked according to their importance and the variables with the highest ranking score were used to specify the structure of this connection. In Fig. 3-22 B the ranking of the variables in both blocks is shown. Additionally, in Fig. 3-22 C the classification model and validity of the test is exemplified.
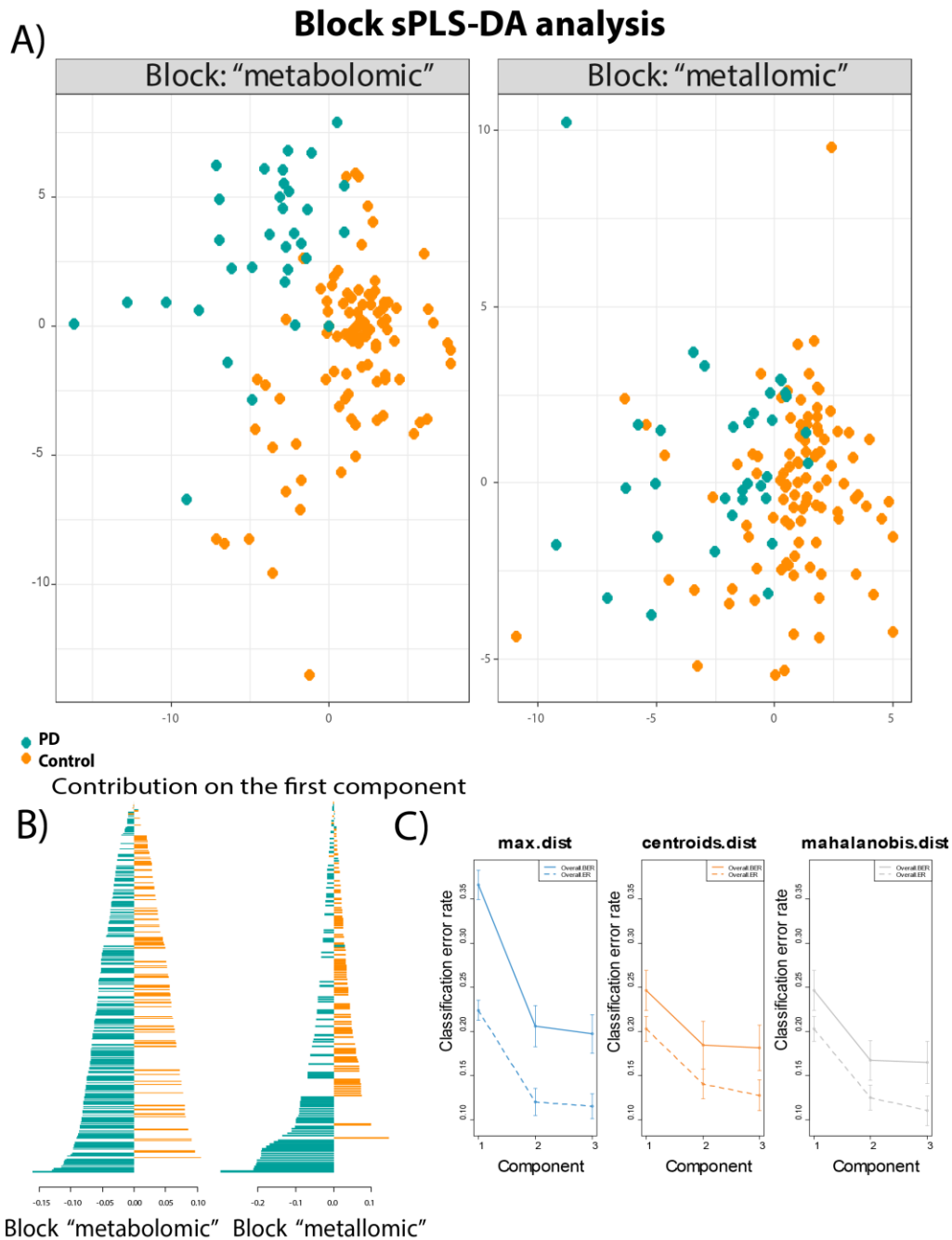
Figure 3-22: Statistical analysis of metallomic and metabolomic parameters. A) Block sPLS-DA analysis of metabolomic and metallomic parameters showing increased concentrations/ ratios for either PD or CTR; B) the correlations values for the PD patients and CTR for the metabolomic and metallomic block and C) classification performance of the model showing a stabilization of the error rates after the second component.

Finally, the analysis of the associations revealed two different groups of interrelations as shown in Fig. 3-23. Within the yellow box the variables in the 95th percentile of the most important variables are located. The second group within the orange box contains the connected variables in the 50th to 95th percentile of the most important variables. The metallomic variables are presented as green dots, whereas red dots represent metabolomic parameters.
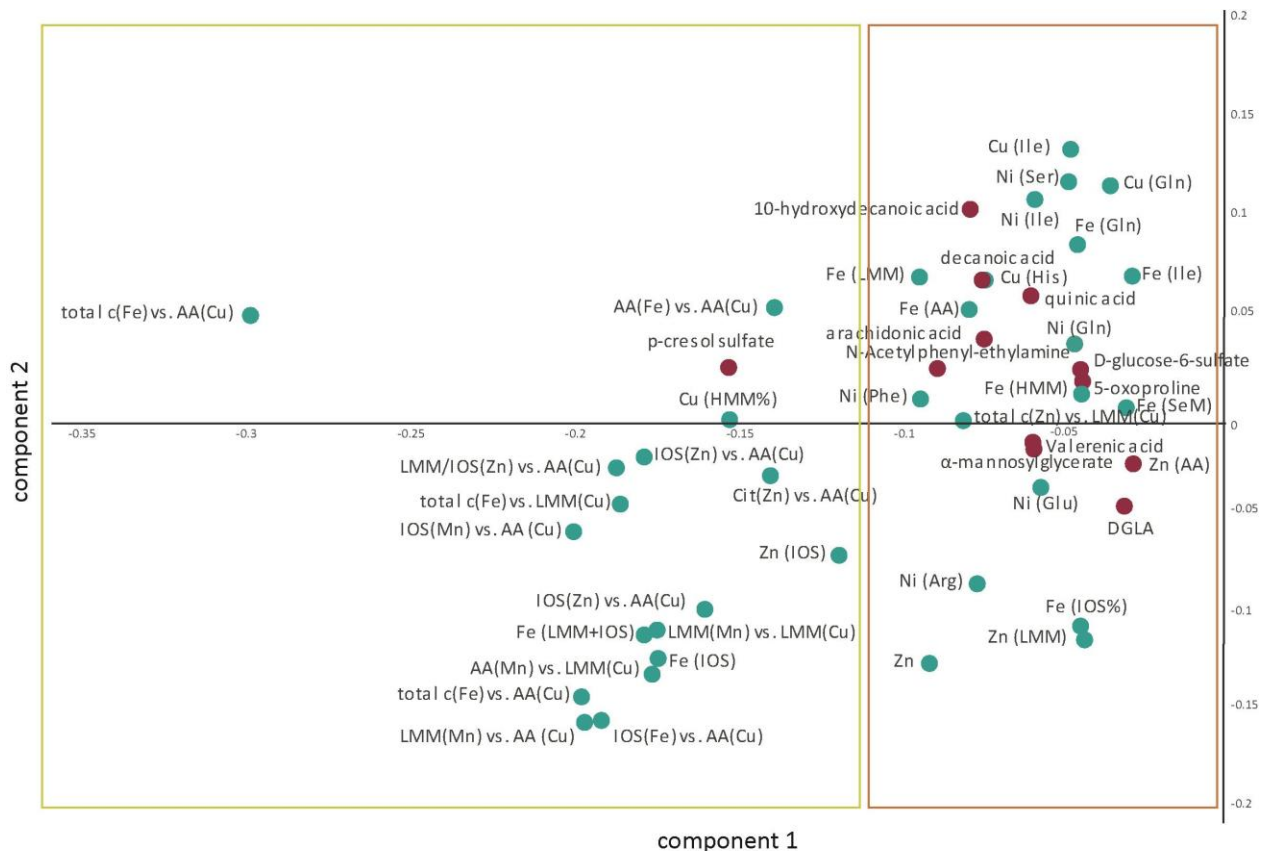
Figure 3-23: Loadings plot of the most important metallomic (green) related to the metabolomic biomarkers (red) in the first and second component. All depicted parameters are enhanced in PD. In the yellow box are the variables presented in Table 18, in the orange one the variables listed in Table 19. AA-amino acid, Arg-arginine, Cit-citrate, DGLA-dihomo-γ-linoleic acid, Gln-glutamine, Glu-glutamic acid, His-histidine, HMM-high molecular mass, Ile-isoleucine, IOS-inorganic species, LMM-low molecular mass, Phe-phenylalanine, SeM-selenomethionine, Ser-serine.

Within the first defined block of connected variables (95th percentile, yellow block in Fig.3-23) mainly metallomic values are concerned. A list of the variables involved in this first block is presented in Table 18 together with the p-values. The calculated p-values included the confounding factors age and gender for elimination of these influences on the connected variables. The highly significant variables arose mainly between the ratios of size fractions as calculated out of the fractions of SEC-analysis (see chapter 3.3.2). Moreover, some specific fractions of SEC-analysis like Fe (IOS) and Cu (HMM%) are involved in the interactions. The ratios had a close relation due to the involvement of the LMM-fraction of Cu in 13 of the listed ratios. As already described earlier, the LMM-Cu fraction or more specifically the AA-fraction of Cu in the SEC-analysis showed up to be the major factor in the significantly differentiating ratios. All the listed ratios with a Cu-fraction in denominator showed an increased value in PD. Besides Cu, also the important role of the trace element Fe and its involvement in redox-processes in disease progression is underlined. The metal Fe is involved in many of the ratios, too, and these ratios show increased values. The trace elements Fe and Cu are able to form ROS by Fenton reaction and therefore, can be toxic within human body. The cascade of Fenton reaction and the emerging damage was already discussed. Since ratios are involved in the interrelations, the concept of dyshomeostatic element balances is underlined. Trace elements like Cu and Fe can on the one hand side contribute to the redox-balance through their activity in metallo-enzymes. On the other hand side they are known to contribute to toxic processes like protein aggregation in neurodegeneration (Gaeta and Hider, 2009). The impaired balance of several metals seems to be a major attributor in disease development and progression. To keep brain functions appropriate, a strict regulation of elemental ratios was already established (Ahmed and Santosh, 2010; Zheng and Monnot, 2012; Zhao *et al.*, 2013). Within this first block of correlations only one metabolomic variable is involved. The metabolic waste product p-cresol sulfate shows a strong connection with the various shifted ratios within Table 18. The metabolite was already measured in CSF (Cassol *et al.*, 2014) and showed a connection to several neurological diseases like multiple sclerosis and AD (Cao *et al.*, 2000; Nedergaard, 2013). Metabolic waste products are a hallmark of various age-associated neurodegenerative diseases since they have increased

accumulation in diseased persons (Nedergaard, 2013). The metabolomic investigation within our sample set pointed to raised concentrations of p-cresol sulfate in the CSF of PD patients (see also chapter 3.7.1). In the degradation process of the amino acids tyrosine and phenylalanine the metabolite p-cresol sulfate is one of the products. Due to this fact, the close connection of the metabolite with the amino acid size fraction and the respective ratios is obvious. The increase of the amino acids in CSF is collateral to the increased production of metabolic waste or more specifically of p-cresol sulfate.

Table 18: The first block of related variables between metallomics and metabolomics. The variables are located within the 95th percentile of the most important variables. The p-values were calculated with the confounding variables age and gender and were adjusted with Benjamini-Hochberg.

Type of measurement	Variables	Adjusted p-value
Metallomics	Zn (IOS)	0.0146
Metallomics	$AA_{(Fe)}$ vs. $AA_{(Cu)}$	0.0199
Metallomics	$Cit_{(Zn)}$ vs. $AA_{(Cu)}$	0.6381
Metallomics	Cu (HMM%)	0.1081
Metabolomics	p-cresol sulfate	0.0006
Metallomics	$IOS_{(Zn)}$ vs. $AA_{(Cu)}$	0.1781
Metallomics	Fe (IOS)	0.6447
Metallomics	$LMM_{(Mn)}$ vs. $LMM_{(Cu)}$	0.0261
Metallomics	$AA_{(Mn)}$ vs. $LMM_{(Cu)}$	0.3393
Metallomics	Fe (LMM+IOS)	0.7717
Metallomics	$IOS_{(Zn)}$ vs. $AA_{(Cu)}$	0.5994
Metallomics	total $c_{(Fe)}$ vs. $LMM_{(Cu)}$	0.0069
Metallomics	$LMM/IOS_{(Zn)}$ vs. $AA_{(Cu)}$	0.3438
Metallomics	$LMM_{(Mn)}$ vs. $AA_{(Cu)}$	0.0223
Metallomics	$IOS_{(Fe)}$ vs. $AA_{(Cu)}$	0.1049
Metallomics	total $c_{(Fe)}$ vs. $AA_{(Cu)}$	0.0245
Metallomics	$IOS_{(Mn)}$ vs. $AA_{(Cu)}$	0.0278
Metallomics	total $c_{(Fe)}$ vs. $AA_{(Cu)}$	0.1349

Except for the ratios of various elemental balances, we identified a second block of variables correlating together. These variables of the second block are listed in Table 19. The interrelations arose between the fatty acid metabolites arachidonic acid, decanoic acid, 10-hydroxydecanoic acid, valerenic acid, and quinic acid with various parameters of metallomic measurements, especially with metals within amino acid fractions. The fatty acids are closely related among each other through the lipid metabolism within human biology. Moreover, a linkage of these metabolites to the redox-active metals Cu and Fe exists. As already mentioned several times, Cu and Fe are essential trace elements in human metabolism, but in excess may evolve hazardous effects to the body through e.g. ROS (Gaeta and Hider, 2009). The influence of fatty acids in PD was previously discussed in detail (see chapter 3.7.1); all found fatty acids had enhanced concentrations in PD. Interestingly, a study where neuronal cells were exposed to decanoic acid presented increased catalase activity after six days of exposure (Hughes *et al.*, 2014). The compound catalase is an antioxidant enzyme removing hydrogen peroxide which is produced by SOD (Scibior and Czeczot, 2006). The metallo-enzyme SOD protects the organism against oxidative stress conditions and exists in human in three different forms. One of the three forms of existing SOD is Cu-Zn-SOD. Table 19 shows the close connection of Cu associated with histidine and the raised concentration of decanoic acid. The Cu-histidine might be a part of SOD and the close linkage to decanoic acid seems to be sign of increased oxidative stress conditions in PD. Moreover, the essential trace element Ni is involved in the connections with the fatty acids, too. The panel of metals measured was extended in the measurement of amino acid fractions (see chapter 3.6.2). Ni is one of the added metals and like Cu and Fe, is part of various metallo-enzymes. In metallo-enzymes, like SOD (Ryan *et al.*, 2015) and acetyl-CoA-synthase (Boer *et al.*, 2014; Can *et al.*, 2014; Manesis *et al.*, 2017), it acts as catalytic center and evolves it´s redox activity. A special emphasis is placed to the metallo-enzyme acetyl-CoA-synthase since it is a building block in fatty acid synthesis (Ikeda *et al.*, 2001). Therefore, the connection between Ni and fatty acids is of major interest and needs further investigation to uncover the influence of this connection to PD. The concentration of Ni in differing bio-fluids was already measured several times in PD and respective CTR-samples. An elemental fingerprint was

measured in CSF samples, but without a significant difference in concentrations. Nonetheless, the trace metal Ni was identified among others for sufficient classification between PD and control (Maass *et al.*, 2018). Moreover, significantly enhanced Ni concentrations were determined in blood and serum in PD patients (Forte *et al.*, 2005). Taken together, our results with increased Ni concentrations underline the findings of both mentioned studies and identified the trace element Ni as a possible contributor to PD development and progression. Especially the connection between Ni-enzymes and the fatty acid synthesis in PD needs further investigation.

Table 19: The second block of related variables between metallomics and metabolomics. The variables are located within the 50th and 95th percentile of the most important variables. The p-values were calculated with the confounding variables age and gender and were adjusted with Benjamini-Hochberg.

Type of measurement	Parameter	Significance of correlation (p-value)
Metallomics	Ni (Glu)	0.6634
Metallomics	Ni (Ile)	0.3033
Metabolomics	valerenic acid	0.1180
Metabolomics	mannosylglycerate	0.4745
Metabolomics	quinic acid	0.0291
Metallomics	Cu (His)	<.0001
Metabolomics	arachidonic acid	0.0013
Metabolomics	decanoic acid	0.7490
Metallomics	Ni (Arg)	0.1524
Metabolomics	10-hydroxydecanoic acid	0.0125

Conclusion

The integration of metallomic and metabolomic datasets revealed that results of the stand-alone investigations evolve even higher significance in the interrelation study. Additionally, the data integration even enhanced the knowledge of causative processes ongoing in PD. By the use of sophisticated statistical models we identified two blocks of closely linked metallomic and metabolomic variables. The interrelations exposed with this statistical model gave a more detailed overview and showed the relevance of such integrative approaches.

4. Conclusion and Perspectives

The task of this work was a comprehensive investigation of *Metallomics* and *Metabolomics* in CSF of PD-patients and respective CTRs. Therefore, the first part of the thesis (chapters 3.2 – 3.5) addresses various investigations regarding essential trace elements. Additionally, in the second part of this thesis specific compound classes and the metabolism itself have been investigated. Finally, the results of *Metallomics* and *Metabolomics* were integrated to obtain more in-depth information. A summary of the most important results is illustrated in Fig. 4-1.
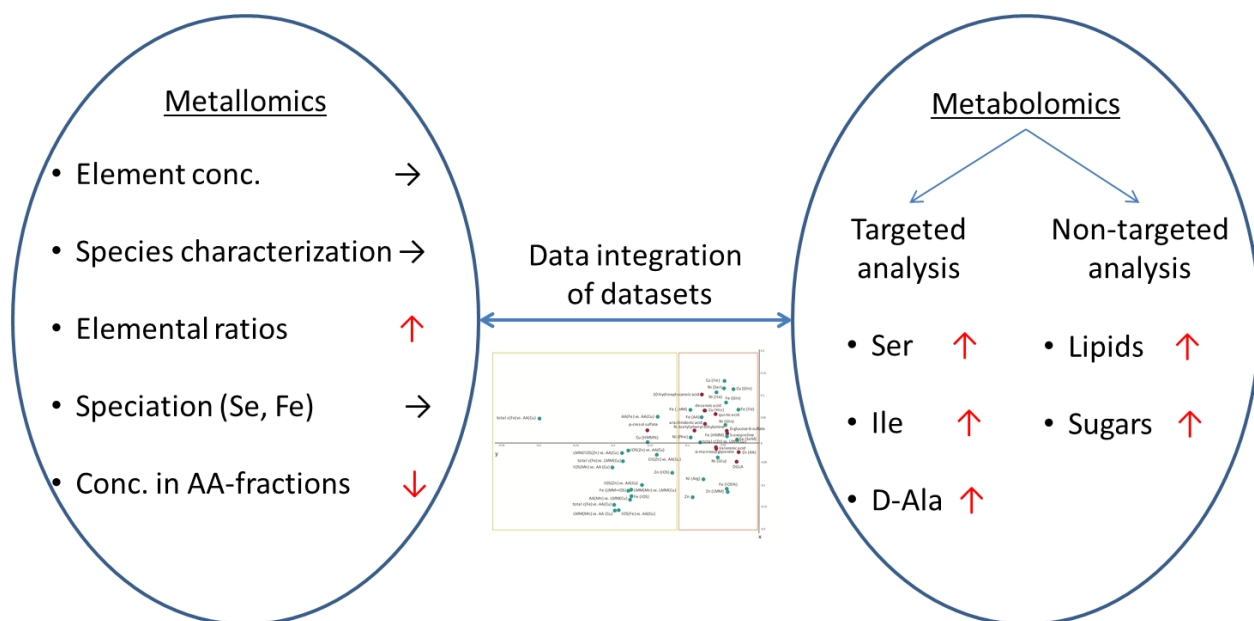
Figure 4-1: Schematic representation of the results of the thesis. All of the investigation parts, namely metallomics, metabolomics, and the integration of both data-sets revealed significant changes for some metals and metabolites.

The investigations gave some new insights into PD development and progression. Some of the obtained results turned out to be of particular interest; whereas others didn´t have the power to discriminate between diseased and healthy state. The *Metallomic* investigations mainly revealed misbalanced ratios of several species to be highly significantly affected. Moreover, differences in the metal-proportion of amino acid

fractions were ascertained, especially for Cu, Fe, Mg, and Sr. The remaining parameters of *Metallomics* investigation, i.e. concentration of Cu, Fe, Mn, and Zn in CSF, species characterization by SEC-ICP-MS, Se-speciation, and redox-speciation of Fe, indicated some shifts, but they were not suitable for differentiation between the groups. For the investigation of the metabolism and the metabolites involved, on the one hand, amino acids were examined, and on the other side a non-targeted investigation with FT-ICR-MS was performed. The analysis of amino acids showed an enhanced serine concentration in PD, as well as in the age group 40-60 an increase of isoleucine. The more detailed analysis of the amino acids and the separation of D- and L-amino acids showed an increase in D-alanine concentration in PD compared to CTR. The non-targeted analysis by FT-ICR-MS showed a set of metabolites to be affected through disease. The assigned compounds belong to different metabolic pathways, especially fatty acid/ lipid metabolism and energy metabolism. Almost all of the changes found within this thesis may be related to increased oxidative stress conditions in PD. Finally, the results of metallomic and metabolomic investigations were integrated to find possible connections between both datasets. The data integration identified two blocks of strongly connected variables. Especially, the importance of the dyshomestatic elemental ratios was underlined. Moreover, an interrelation between the trace element Ni and the fatty acids was identified and needs further investigation.

With these investigations existing knowledge of PD could be confirmed. Moreover, due to the first-time application of some investigations like SEC-ICP-MS, IC-ICP-MS, ESI-FT-ICR-MS, and die investigation of D-/L-amino acids in CSF of PD-patients new insights of disease mechanisms were revealed.

The investigations already revealed several changes due to disease. Based on these findings, future research should include more homogeneous patient- and CTR-groups (e.g. age, sex, medication, duration of disease) to have higher comparability. Moreover, the SEC-ICP-MS already showed interesting results for the Cu-separation. A more detailed speciation analysis of these Cu-species might be of high interest in PD-research. Additionally, targeted metabolomic investigations of fatty acids and other compound classes might lead to reliable markers for the disease. To reveal the

116

underlying mechanism in Parkinson´s disease and to find markers of the pre-symptomatic phase of the disease, long-term studies of various body fluids (serum, CSF, blood, salvia) are necessary.

5. Literature

Aerts MB, Esselink RA, Abdo WF, Bloem BR, Verbeek MM. CSF alpha-synuclein does not differentiate between parkinsonian disorders. Neurobiol Aging 2012; 33(2): 430 e1-3.

Aguilar MV, Jimenez-Jimenez FJ, Molina JA, Meseguer I, Mateos-Vega CJ, Gonzales-Munos MJ*, et al.* Cerebrospinal fluid selenium and chromium levels in patients with Parkinson´s disease. J Neural Transm 1998; 105: 1245-51.

Ahmed SS, Santosh W. Metallomic profiling and linkage map analysis of early Parkinson's disease: a new insight to aluminum marker for the possible diagnosis. PLoS One 2010; 5(6): e11252.

Ahmed SS, Santosh W, Kumar S, Christlet HT. Metabolic profiling of Parkinson's disease: evidence of biomarker from gene expression analysis and rapid neural network detection. Journal of biomedical science 2009; 16: 63.

Alexander GE, Crutcher MD. Functional architecture of basal ganglia circuits: neural substrates of parallel processing. Trends Neurosci 1990; 13(7): 266-71.

Alimonti A, Bocca B, Pino A, Ruggieri F, Forte G, Sancesario G. Elemental profile of cerebrospinal fluid in patients with Parkinson's disease. J Trace Elem Med Biol 2007; 21(4): 234-41.

Altun Ö, Bilcen S. Spectroscopic characterization of Cu(II) complex of l-phenylalanine and d,l-tryptophan. Spectrochim Acta A 2010; 75(2): 789-93.

Anandhan A, Jacome MS, Lei S, Hernandez-Franco P, Pappa A, Panayiotidis MI*, et al.* Metabolic Dysfunction in Parkinson's Disease: Bioenergetics, Redox Homeostasis and Central Carbon Metabolism. Brain Res Bull 2017; 133: 12-30.

Anandhan A, Rodriguez-Rocha H, Bohovych I, Griggs AM, Zavala-Flores L, Reyes-Reyes EM*, et al.* Overexpression of alpha-synuclein at non-toxic levels increases dopaminergic cell death induced by copper exposure via modulation of protein degradation pathways. Neurobiol Dis 2015; 81: 76-92.

Andersen AD, Binzer M, Stenager E, Gramsbergen JB. Cerebrospinal fluid biomarkers for Parkinson's disease – a systematic review. Acta Neurol Scand 2017; 135(1): 34-56.

Ansari MA, Ahmad AS, Ahmad M, Salim S, Yousuf S, Ishrat T*, et al.* Selenium protects cerebral ischemia in rat brain mitochondria. Biol Trace Elem Res 2004; 101(1): 73-86.

Aoyama K, Nakaki T. Impaired glutathione synthesis in neurodegeneration. Int J Mol Sci 2013; 14(10): 21021-44.

Apostoli P, Cornelis JD, Hoet P, Lison D, Templeton D. Elemental speciation in human health risk assessment World Health Organization. Dept. of Protection of the Human Environment; International Programme on Chemical Safety; 2006.

Arnal N, Cristalli DO, de Alaniz MJ, Marra CA. Clinical utility of copper, ceruloplasmin, and metallothionein plasma determinations in human neurodegenerative patients and their first-degree relatives. Brain Res 2010; 1319: 118-30.

Ayala A, Munoz MF, Arguelles S. Lipid peroxidation: production, metabolism, and signaling mechanisms of malondialdehyde and 4-hydroxy-2-nonenal. Oxid Med Cell Longev 2014; 2014: 360438.

Banerjee S, Mazumdar S. Electrospray Ionization Mass Spectrometry: A Technique to Access the Information beyond the Molecular Weight of the Analyte. International Journal of Analytical Chemistry 2012; 2012: 40.

Barbariga M, Curnis F, Andolfo A, Zanardi A, Lazzaro M, Conti A, *et al.* Ceruloplasmin functional changes in Parkinson's disease-cerebrospinal fluid. Mol Neurodegener 2015; 10: 59.

Barneo-Caragol C, Martínez-Morillo E, Rodríguez-González S, Lequerica-Fernández P, Vega-Naredo I, Álvarez Menéndez FV. Strontium and oxidative stress in normal pregnancy. Journal of Trace Elements in Medicine and Biology 2018; 45: 57-63.

Batista-Nascimento L, Pimentel C, Menezes RA, Rodrigues-Pousada C. Iron and neurodegeneration: from cellular homeostasis to disease. Oxid Med Cell Longev 2012; 2012: 128647.

Bazinet RP, Laye S. Polyunsaturated fatty acids and their metabolites in brain function and disease. Nat Rev Neurosci 2014; 15(12): 771-85.

Bernheimer H, Birkmayer W, Hornykiewicz O, Jellinger K, Seitelberger F. Brain dopamine and the syndromes of Parkinson and Huntington Clinical, morphological and neurochemical correlations. Journal of the Neurological Sciences 1973; 20(4): 415-55.

Bharathi P, Nagabhushan P, Rao KS. Mathematical approach to understand the kinetics of alpha-synuclein aggregation: relevance to Parkinson's disease. Comput Biol Med 2008; 38(10): 1084-93.

Bhatt MH, Elias MA, Mankodi AK. Acute and reversible parkinsonism due to organophosphate pesticide intoxication. Five cases 1999; 52(7): 1467-.

Blennow K, Hampel H, Weiner M, Zetterberg H. Cerebrospinal fluid and plasma biomarkers in Alzheimer disease. Nat Rev Neurol 2010; 6(3): 131-44.

Boer JL, Mulrooney SB, Hausinger RP. Nickel-dependent metalloenzymes. Archives of Biochemistry and Biophysics 2014; 544: 142–152.

Bocca B, Alimonti A, Senofonte O, Pino A, Violante N, Petrucci F, *et al.* Metal changes in CSF and peripheral compartments of parkinsonian patients. J Neurol Sci 2006; 248(1-2): 23-30.

Bogdanov M, Matson WR, Wang L, Matson T, Saunders-Pullman R, Bressman SS, *et al.* Metabolomic profiling to develop blood biomarkers for Parkinson's disease. Brain 2008; 131(2): 389-96.

Bolognin S, Messori L, Zatta P. Metal ion physiopathology in neurodegenerative disorders. Neuromolecular Med 2009; 11(4): 223-38.

Bosetti F. Arachidonic Acid Metabolism in Brain Physiology and Pathology: Lessons from Genetically Altered Mouse Models. J Neurochem 2007; 102(3): 577-86.

Botas A, Campbell HM, Han X, Maletic-Savatic M. Metabolomics of Neurodegenerative Diseases. Int Rev Neurobiol 2015; 122: 53-80.

Bouzier-Sore AK, Bolanos JP. Uncertainties in pentose-phosphate pathway flux assessment underestimate its contribution to neuronal glucose consumption: relevance for neurodegeneration and aging. Front Aging Neurosci 2015; 7: 89.

Bowman AB, Kwakye GF, Herrero Hernandez E, Aschner M. Role of manganese in neurodegenerative diseases. J Trace Elem Med Biol 2011; 25(4): 191-203.

Braak H, Ghebremedhin E, Rub U, Bratzke H, Del Tredici K. Stages in the development of Parkinson's disease-related pathology. Cell Tissue Res 2004; 318(1): 121-34.

Braak H, Rub U, Gai WP, Del Tredici K. Idiopathic Parkinson's disease: possible routes by which vulnerable neuronal types may be subject to neuroinvasion by an unknown pathogen. J Neural Transm 2003; 110(5): 517-36.

Breitling R, Pitt AR, Barrett MP. Precision mapping of the metabolome. Trends Biotechnol 2006a; 24(12): 543-8.

Breitling R, Ritchie S, Goodenowe D, Stewart ML, Barrett MP. Ab initio prediction of metabolic networks using Fourier transform mass spectrometry data. Metabolomics 2006b; 2(3): 155-64.

Broe GA, Akhtar AJ, Andrews GR, Caird FI, Gilmore AJ, McLennan WJ. Neurological disorders in the elderly at home. Journal of neurology, neurosurgery, and psychiatry 1976; 39(4): 362-6.

Brouwer M, Koeman T, van den Brandt PA, Kromhout H, Schouten LJ, Peters S*, et al.* Occupational exposures and Parkinson's disease mortality in a prospective Dutch cohort. Occup Environ Med 2015; 72(6): 448-55.

Brown RJC, Milton MJT. Analytical techniques for trace element analysis: an overview. TrAC Trends in Analytical Chemistry 2005; 24(3): 266-74.

Bruker. maXis - User manual. 2008.

Burré J, Sharma M, Tsetsenis T, Buchman V, Etherton MR, Südhof TC. Alpha-synuclein promotes SNARE-complex assembly in vivo and in vitro. Science (New York, NY) 2010; 329(5999): 1663-7.

Burté F, Houghton D, Lowes H, Pyle A, Nesbitt S, Yarnall A*, et al.* metabolic profiling of Parkinson's disease and mild cognitive impairment. Mov Disord 2017; 32(6): 927-32.

Buszewski B, Noga S. Hydrophilic interaction liquid chromatography (HILIC)—a powerful separation technique. Analytical and Bioanalytical Chemistry 2012; 402(1): 231-47.

Byrne LA, Hynes MJ, Connolly CD, Murphy RA. Analytical determination of apparent stability constants using a copper ion selective electrode. Journal of inorganic biochemistry 2011; 105(12): 1656-61.

Byrns CN, Pitts MW, Gilman CA, Hashimoto AC, Berry MJ. Mice lacking selenoprotein P and selenocysteine lyase exhibit severe neurological dysfunction, neurodegeneration, and audiogenic seizures. The Journal of biological chemistry 2014; 289(14): 9662-74.

Cai T, Yao T, Zheng G, Chen Y, Du K, Cao Y*, et al.* Manganese induces the overexpression of α-synuclein in PC12 cells via ERK activation. Brain Research 2010; 1359: 201-7.

Callixte K-T, Clet TB, Jacques D, Faustin Y, François DJ, Maturin T-T. The pattern of neurological diseases in elderly people in outpatient consultations in Sub-Saharan Africa. BMC research notes 2015; 8: 159-.

Can M, Armstrong FA, Ragsdale SW. Structure, function, and mechanism of the nickel metalloenzymes, CO dehydrogenase, and acetyl-CoA synthase. Chem Rev 2014; 114(8): 4149-74.

Cannata-Andía JB, Rodríguez-García M, Gómez-Alonso C. Mecanismo de acción del ranelato de estroncio. Rev Osteoporos Metab Miner 2010; 2: 85-9.

Cao L, Kirk MC, Coward LU, Jackson P, Whitaker JN. p-Cresol sulfate is the dominant component of urinary myelin basic protein like material. Arch Biochem Biophys 2000; 377(1): 9-21.

Capo CR, Arciello M, Squitti R, Cassetta E, Rossini PM, Calabrese L*, et al.* Features of ceruloplasmin in the cerebrospinal fluid of Alzheimer's disease patients. Biometals 2008; 21(3): 367-72.

Carboni E, Lingor P. Insights on the interaction of alpha-synuclein and metals in the pathophysiology of Parkinson's disease. Metallomics 2015; 7(3): 395-404.

Casale A, De Robertis A, De Stefano C, Gianguzza A, Patanè G, Rigano C*, et al.* Thermodynamic parameters for the formation of glycine complexes with magnesium(II), calcium(II), lead(II), manganese(II), cobalt(II), nickel(II), zinc(II) and cadmium(II) at different temperatures and ionic strengths, with particular reference to natural fluid conditions. Thermochim Acta 1995; 255(Supplement C): 109-41.

Cassol E, Misra V, Dutta A, Morgello S, Gabuzda D. Cerebrospinal fluid metabolomics reveals altered waste clearance and accelerated aging in HIV patients with neurocognitive impairment. AIDS 2014; 28(11): 1579-91.

Cech NB, Enke CG. Practical implications of some recent studies in electrospray ionization fundamentals. Mass Spectrom Rev 2001; 20(6): 362-87.

Chen RL, Preston JE. Changes in kinetics of amino acid uptake at the ageing ovine blood–cerebrospinal fluid barrier. Neurobiology of Aging 2012; 33(1): 121-33.

Chervyakov AV, Gulyaeva NV, Zakharova MN. D-amino acids in normal ageing and pathogenesis of neurodegenerative diseases. Neurochemical Journal 2011; 5(2): 100-14.

Chinta SJ, Andersen JK. Redox imbalance in Parkinson's disease. Biochimica et biophysica acta 2008; 1780(11): 1362-7.

Chwiej J, Adamek D, Szczerbowska-Boruchowska M, Krygowska-Wajs A, Wojcik S, Falkenberg G*, et al.* Investigations of differences in iron oxidation state inside single neurons from substantia nigra of Parkinson's disease and control patients using the micro-XANES technique. JBIC J Biol Inorg Chem 2007; 12(2): 204-11.

Collins JF. Gene chip analyses reveal differential genetic responses to iron deficiency in rat duodenum and jejunum. Biological research 2006; 39(1): 25-37.

Corso G, Cristofano A, Sapere N, la Marca G, Angiolillo A, Vitale M*, et al.* Serum Amino Acid Profiles in Normal Subjects and in Patients with or at Risk of Alzheimer Dementia. Dementia and Geriatric Cognitive Disorders EXTRA 2017; 7(1): 143-59.

Cowan DM, Fan Q, Zou Y, Shi X, Chen J, Aschner M*, et al.* Manganese exposure among smelting workers: blood manganese-iron ratio as a novel tool for manganese exposure assessment. Biomarkers 2009; 14(1): 3-16.

Crossgrove J, Zheng W. Manganese toxicity upon overexposure. NMR Biomed 2004; 17(8): 544-53.

Cuajungco MP, Lees GJ. Zinc metabolism in the brain: relevance to human neurodegenerative disorders. Neurobiol Dis 1997; 4(3-4): 137-69.

D'Aniello A, Fisher G, Migliaccio N, Cammisa G, D'Aniello E, Spinelli P. Amino acids and transaminases activity in ventricular CSF and in brain of normal and Alzheimer patients. Neuroscience Letters 2005; 388(1): 49-53.

Danysz W, Parsons CG. Glycine and N-methyl-D-aspartate receptors: physiological significance and possible therapeutic applications. Pharmacol Rev 1998; 50(4): 597-664.

Davies Katherine M, Mercer Julian FB, Chen N, Double Kay L. Copper dyshomoeostasis in Parkinson's disease: implications for pathogenesis and indications for novel therapeutics. Clinical Science 2016; 130(8): 565-74.

Davies P, Moualla D, Brown DR. Alpha-Synuclein Is a Cellular Ferrireductase. PLOS ONE 2011; 6(1): e15814.

de Farias CC, Maes M, Bonifácio KL, Bortolasci CC, de Souza Nogueira A, Brinholi FF, *et al.* Highly specific changes in antioxidant levels and lipid peroxidation in Parkinson's disease and its progression: Disease and staging biomarkers and new drug targets. Neurosci Lett 2016; 617(Supplement C): 66-71.

del Hoyo P, Garcia-Redondo A, de Bustos F, Molina JA, Sayed Y, Alonso-Navarro H, *et al.* Oxidative stress in skin fibroblasts cultures from patients with Parkinson's disease. BMC neurology 2010; 10: 95.

Demirelli H, Köseoĝlu F. Equilibrium Studies of Schiff Bases and Their Complexes with Ni(II), Cu(II) and Zn(II) derived from Salicylaldehyde and Some α-Amino Acids. J Solution Chem 2005; 34(5): 561-77.

Dick FD, De Palma G, Ahmadi A, Scott NW, Prescott GJ, Bennett J, *et al.* Environmental risk factors for Parkinson's disease and parkinsonism: the Geoparkinson study. Occup Environ Med 2007; 64(10): 666-72.

Diederich J, Brielmeier M, Schwerdtle T, Michalke B. Manganese and iron species in Sprague–Dawley rats exposed with $MnCl_2 \cdot 4H_2O$ (i.v.). Microchem J 2012; 105: 115-23.

Diederich J, Michalke B. Enhanced extract preperation of native manganese and iron species from brain and liver tissue. Anal Bioanal Chem 2011; 399: 1799-806.

Doi M, Yamaoka I, Fukunaga T, Nakayama M. Isoleucine, a potent plasma glucose-lowering amino acid, stimulates glucose uptake in C2C12 myotubes. Biochem Biophys Res Commun 2003; 312(4): 1111-7.

Dringen R, Scheiber IF, Mercer JF. Copper metabolism of astrocytes. Front Aging Neurosci 2013; 5: 9.

Ducic T, Carboni E, Lai B, Chen S, Michalke B, Lazaro DF, *et al.* Alpha-Synuclein Regulates Neuronal Levels of Manganese and Calcium. ACS Chem Neurosci 2015; 6(10): 1769-79.

Dudzik D, Barbas-Bernardos C, García A, Barbas C. Quality assurance procedures for mass spectrometry untargeted metabolomics. a review. J Pharm Biomed Anal 2018; 147: 149-73.

Eggert K, Berg D. Früherkennung und Kohortenstudien. Das Kompetenznetz Parkinson und die Deutsche Parkinson Gesellschaft 2015.

Ellwanger JH, Franke SI, Bordin DL, Pra D, Henriques JA. Biological functions of selenium and its potential influence on Parkinson's disease. An Acad Bras Cienc 2016; 88(3 Suppl): 1655-74.

Farah R, Haraty H, Salame Z, Fares Y, Ojcius DM, Said Sadier N. Salivary biomarkers for the diagnosis and monitoring of neurological diseases. Biomedical Journal 2018; 41(2): 63-87.

Faria C, Jorge CD, Borges N, Tenreiro S, Outeiro TF, Santos H. Inhibition of formation of alpha-synuclein inclusions by mannosylglycerate in a yeast model of Parkinson's disease. Biochimica et biophysica acta 2013; 1830(8): 4065-72.

Farrall AJ, Wardlaw JM. Blood-brain barrier: ageing and microvascular disease--systematic review and meta-analysis. Neurobiol Aging 2009; 30(3): 337-52.

Fedorova T, Knudsen CS, Mouridsen K, Nexo E, Borghammer P. Salivary Acetylcholinesterase Activity Is Increased in Parkinson´s Disease: A Potential Marker of Parasympathetic Dysfunction. Parkinson´s Disease 2015; 2015: 7.

Fernsebner K, Zorn J, Kanawati B, Walker A, Michalke B. Manganese leads to an increase in markers of oxidative stress as well as to a shift in the ratio of Fe(II)/(III) in rat brain tissue. Metallomics 2014; 6(4): 921-31.

Ferraro TN, Hare TA. Free and conjugated amino acids in human CSF: influence of age and sex. Brain Res 1985; 338(1): 53-60.

Fink AL. The aggregation and fibrillation of alpha-synuclein. Acc Chem Res 2006; 39(9): 628-34.

Finkelstein MM, Jerrett M. A study of the relationships between Parkinson's disease and markers of traffic-derived and environmental manganese air pollution in two Canadian cities. Environ Res 2007; 104(3): 420-32.

Fisher G, Lorenzo N, Abe H, Fujita E, Frey WH, Emory C, *et al.* Free D- and L-amino acids in ventricular cerebrospinal fluid from Alzheimer and normal subjects. Amino Acids 1998; 15(3): 263-9.

Fisher GH, D'Aniello A, Vetere A, Padula L, Cusano GP, Man EH. Free D-aspartate and D-alanine in normal and Alzheimer brain. Brain Res Bull 1991; 26(6): 983-5.

Forcisi S, Moritz F, Lucio M, Lehmann R, Stefan N, Schmitt-Kopplin P. Solutions for low and high accuracy mass spectrometric data matching: a data-driven annotation strategy in nontargeted metabolomics. Anal Chem 2015; 87(17): 8917-24.

Forland MG, Ohrfelt A, Dalen I, Tysnes OB, Blennow K, Zetterberg H, *et al.* Evolution of cerebrospinal fluid total alpha-synuclein in Parkinson's disease. Parkinsonism Relat Disord 2018; 49: 4-8.

Forte G, Alimonti A, Pino A, Stanzione P, Brescianini S, Brusa L, *et al.* Metals and oxidative stress in patients with Parkinson's disease. Ann Ist Super Sanita 2005; 41(2): 189-95.

Forte G, Bocca B, Senofonte O, Petrucci F, Brusa L, Stanzione P, *et al.* Trace and major elements in whole blood, serum, cerebrospinal fluid and urine of patients with Parkinson's disease. J Neural Transm 2004; 111(8): 1031-40.

Foulds PG, Yokota O, Thurston A, Davidson Y, Ahmed Z, Holton J, *et al.* Post mortem cerebrospinal fluid alpha-synuclein levels are raised in multiple system atrophy and distinguish this from the other alpha-synucleinopathies, Parkinson's disease and Dementia with Lewy bodies. Neurobiol Dis 2012; 45(1): 188-95.

Frederickson CJ, Koh J-Y, Bush AI. The neurobiology of zinc in health and disease. Nat Rev Neurosci 2005; 6: 449.

Gaeta A, Hider RC. The crucial role of metal ions in neurodegeneration: the basis for a promising therapeutic strategy. Br J Pharmacol 2005; 146(8): 1041-59.

Gaeta A, Hider RC. The crucial role of metal ions in neurodegeneration: the basis for a promising therapeutic strategy: Crucial role of metal ions in neurodegeneration. British Journal of Pharmacology 2009; 146: 1041–1059.

Galazka-Friedman J, Bauminger ER, Friedman A, Barcikowska M, Hechel D, Nowik I. Iron in parkinsonian and control substantia nigra--a Mossbauer spectroscopy study. Mov Disord 1996; 11(1): 8-16.

Gazzaniga GC, Ferraro B, Camerlingo M, Casto L, Viscardi M, Mamoli A. A case control study of CSF copper, iron and manganese in Parkinson disease. Ital J Neurol Sci 1992; 13: 239-43.

Gonzalez-Riano C, Garcia A, Barbas C. Metabolomics studies in brain tissue: A review. J Pharm Biomed Anal 2016; 130: 141-68.

González-Weller D, Rubio C, Gutiérrez ÁJ, González GL, Mesa JMC, Gironés CR*, et al.* Dietary intake of barium, bismuth, chromium, lithium, and strontium in a Spanish population (Canary Islands, Spain). Food and Chemical Toxicology 2013; 62: 856-68.

Gorboletova GG, Metlin AA. Thermodynamics of the formation of copper(II) complexes with L-histidine in aqueous solution. Russ J Phys Chem A 2015; 89(2): 218-23.

Gorell JM, A. PB, Johnson CC, Peterson E. Occupational Metal Exposure and the Risk of Parkinson´s Disease. Neuroepidemiology 1999; 18: 303-8.

Gorell JM, Peterson EL, Rybicki BA, Johnson CC. Multiple risk factors for Parkinson's disease. J Neurol Sci 2004; 217(2): 169-74.

Hamase K, Inoue T, Morikawa A, Konno R, Zaitsu K. Determination of free D-proline and D-leucine in the brains of mutant mice lacking D-amino acid oxidase activity. Anal Biochem 2001; 298(2): 253-8.

Hamase K, Konno R, Morikawa A, Zaitsu K. Sensitive determination of D-amino acids in mammals and the effect of D-amino-acid oxidase activity on their amounts. Biological & pharmaceutical bulletin 2005; 28(9): 1578-84.

Hamase K, Morikawa A, Zaitsu K. d-Amino acids in mammals and their diagnostic value. Journal of Chromatography B 2002; 781(1): 73-91.

Hancock DB, Martin ER, Mayhew GM, Stajich JM, Jewett R, Stacy MA*, et al.* Pesticide exposure and risk of Parkinson's disease: a family-based case-control study. BMC neurology 2008; 8: 6.

Hatano T, Saiki S, Okuzumi A, Mohney RP, Hattori N. Identification of novel biomarkers for Parkinson's disease by metabolomic technologies. J Neurol Neurosurg Psychiatr 2016; 87(3): 295-301.

Havelund J, Heegaard N, Færgeman N, Gramsbergen J. Biomarker Research in Parkinson's Disease Using Metabolite Profiling. Metabolites 2017; 7(3): 42.

Hebbrecht G, Maenhaut W, Reuck JD. Brain trace elements and aging. Nuclear Instruments and Methods in Physics Research Section B: Beam Interactions with Materials and Atoms 1999; 150(1): 208-13.

Herholz K. Acetylcholine esterase activity in mild cognitive impairment and Alzheimer's disease. European Journal of Nuclear Medicine and Molecular Imaging 2008; 35(1): 25-9.

Hill KE, Zhou J, McMahan WJ, Motley AK, Atkins JF, Gesteland RF*, et al.* Deletion of Selenoprotein P Alters Distribution of Selenium in the Mouse. Journal of Biological Chemistry 2003; 278(16): 13640-6.

Hoehn MM, Yahr MD. Parkinsonism: onset, progression, and mortality. 1967. Neurology 2001; 57(10 Suppl 3): S11-26.

Hong Z, Shi M, Chung KA, Quinn JF, Peskind ER, Galasko D*, et al.* DJ-1 and alpha-synuclein in human cerebrospinal fluid as biomarkers of Parkinson's disease. Brain 2010; 133(Pt 3): 713-26.

Hou X, Amais RS, Jones BT, Donati GL. Inductively Coupled Plasma Optical Emission Spectrometry. In: Meyers RA, editor. Encyclopedia of Analytical Chemistry 2016.

Hozumi I, Hasegawa T, Honda A, Ozawa K, Hayashi Y, Hashimoto K*, et al.* Patterns of levels of biological metals in CSF differ among neurodegenerative diseases. J Neurol Sci 2011; 303(1-2): 95-9.

Hu L, He B, Wang Y, Jiang G, Sun H. Metallomics in environmental and health related research: Current status and perspectives. Chin Sci Bull 2013; 58(2): 169-76.

Hughes AJ, Daniel SE, Kilford L, Lees AJ. Accuracy of clinical diagnosis of idiopathic Parkinson's disease: a clinico-pathological study of 100 cases. Journal of Neurology, Neurosurgery & Psychiatry 1992; 55(3): 181-4.

Hughes SD, Kanabus M, Anderson G, Hargreaves IP, Rutherford T, Donnell MO, et al. The ketogenic diet component decanoic acid increases mitochondrial citrate synthase and complex I activity in neuronal cells. J Neurochem 2014; 129: 426–433.

Hung YH, Bush AI, Cherny RA. Copper in the brain and Alzheimer's disease. J Biol Inorg Chem 2010a; 15(1): 61-76.

Hung YH, Bush AI, Cherny RA. Copper in the brain and Alzheimer's disease. J Biol Inorg Chem 2010b; 15(1): 61-76.

Ikeda Y, Yamamoto J, Okamura M, Fujino T, Takahashi S, Takeuchi K*, et al.* Transcriptional regulation of the murine acetyl-CoA synthetase 1 gene through multiple clustered binding sites for sterol regulatory element-binding proteins and a single neighboring site for Sp1. J Biol Chem 2001; 276(36): 34259-69.

Izumi Y, Zorumski CF. Glial–neuronal interactions underlying fructose utilization in rat hippocampal slices. Neuroscience 2009; 161(3): 847-54.

Jakes R, Spillantini MG, Goedert M. Identification of two distinct synucleins from human brain. FEBS Lett 1994; 345(1): 27-32.

Jankovic J. Parkinson's disease: clinical features and diagnosis. J Neurol Neurosurg Psychiatr 2008; 79(4): 368-76.

Jansson J, Willing B, Lucio M, Fekete A, Dicksved J, Halfvarson J, et al. Metabolomics Reveals Metabolic Biomarkers of Crohn's Disease. PLoS ONE 2009; 4: e6386.

Ji SG, Weiss JH. Zn2+-induced disruption of neuronal mitochondrial function: Synergism with Ca2+, critical dependence upon cytosolic Zn2+ buffering, and contributions to neuronal injury. Experimental Neurology 2018; 302: 181-95.

Jimenez-Jimenez FJ, Alonso-Navarro H, Garcia-Martin E, Agundez JA. Cerebrospinal fluid biochemical studies in patients with Parkinson's disease: toward a potential search for biomarkers for this disease. Front Cell Neurosci 2014; 8: 369.

Jiménez-Jiménez FJ, Molina J, Vargas C, Gómez P, Navarro J, Benito-Leon J*, et al.* Neurotransmitter amino acids in cerebrospinal fluid of patients with Parkinson's disease. J Neurol Sci 1996; 141(1–2): 39-44.

Jimenez-Jimenez FJ, Molina JA, Aguilar MV, Meseguer I, Mateos-Vega CJ, Gonzales-Munos MJ*, et al.* Cerebrospinal fluid levels of transition metals in patients with Parkinson´s disease. J Neural Transm 1998; 105: 497-505.

Jomova K, Vondrakova D, Lawson M, Valko M. Metals, oxidative stress and neurodegenerative disorders. Mol Cell Biochem 2010; 345(1-2): 91-104.

Julien C, Berthiaume L, Hadj-Tahar A, Rajput AH, Bedard PJ, Di Paolo T*, et al.* Postmortem brain fatty acid profile of levodopa-treated Parkinson disease patients and parkinsonian monkeys. Neurochem Int 2006; 48(5): 404-14.

Kalíková K, Šlechtová T, Tesařová E. Enantiomeric Ratio of Amino Acids as a Tool for Determination of Aging and Disease Diagnostics by Chromatographic Measurement. Separations 2016; 3(4): 30.

Kaling M, Schmidt A, Moritz F, Rosenkranz M, Witting M, Kasper K*, et al.* Mycorrhiza-Triggered Transcriptomic and Metabolomic Networks Impinge on Herbivore Fitness. Plant Physiology 2018; 176(4): 2639-56.

Kang JH, Irwin DJ, Chen-Plotkin AS, Siderowf A, Caspell C, Coffey CS*, et al.* Association of cerebrospinal fluid beta-amyloid 1-42, T-tau, P-tau181, and alpha-synuclein levels with clinical features of drug-naive patients with early Parkinson disease. JAMA Neurol 2013; 70(10): 1277-87.

Katsuki H, Nonaka M, Shirakawa H, Kume T, Akaike A. Endogenous D-serine is involved in induction of neuronal death by N-methyl-D-aspartate and simulated ischemia in rat cerebrocortical slices. The Journal of pharmacology and experimental therapeutics 2004; 311(2): 836-44.

Kera Y, Aoyama H, Matsumura H, Hasegawa A, Nagasaki H, Yamada R. Presence of free D-glutamate and D-aspartate in rat tissues. Biochim Biophys Acta 1995; 1243(2): 283-6.

Kessler H, Pajonk FG, Meisser P, Schneider-Axmann T, Hoffmann KH, Supprian T, *et al.* Cerebrospinal fluid diagnostic markers correlate with lower plasma copper and ceruloplasmin in patients with Alzheimer's disease. J Neural Transm 2006; 113(11): 1763-9.

Khoronenkova SV, Tishkov VI. D-Amino acid oxidase: Physiological role and applications. Biochemistry (Moscow) 2008; 73(13): 1511-8.

Kim YH, Kim EY, Gwag BJ, Sohn S, Koh JY. Zinc-induced cortical neuronal death with features of apoptosis and necrosis: mediation by free radicals. Neuroscience 1999; 89(1): 175-82.

Knight JA. The biochemistry of aging. Advances in clinical chemistry 2000; 35: 1-62.

Koplik R, Borkova M, Mestek O, Kominkova J, Suchanek M. Application of size-exclusion chromatography-inductively coupled plasma mass spectrometry for fractionation of element species in seeds of legumes. J Chromatogr B Analyt Technol Biomed Life Sci 2002; 775(2): 179-87.

Kozlowski H, Luczkowski M, Remelli M, Valensin D. Copper, zinc and iron in neurodegenerative diseases (Alzheimer's, Parkinson's and prion diseases). Coordin Chem Rev 2012; 256(19-20): 2129-41.

Kubáň P, Guchardi R, Hauser PC. Trace-metal analysis with separation methods. TrAC Trends in Analytical Chemistry 2005; 24(3): 192-8.

Lakke JP, Teelken AW, vd Voet H, Wolthers BG. Amino acid abnormalities in cerebrospinal fluid and blood serum of patients with Parkinson's disease, other heredodegenerative disorders and head injuries. Advances in neurology 1987; 45: 243-7.

Lakke JPWF, Teelken AW. Amino acid abnormalities in cerebrospinal fluid of patients with parkinsonism and extrapyramidal disorders. Neurology 1976; 26(5): 489-.

Lan J, Jiang DH. Excessive iron accumulation in the brain: a possible potential risk of neurodegeneration in Parkinson's disease. J Neural Transm 1997; 104(6-7): 649-60.

Lazzer S, Bedogni G, Lafortuna CL, Marazzi N, Busti C, Galli R, *et al.* Relationship Between Basal Metabolic Rate, Gender, Age, and Body Composition in 8,780 White Obese Subjects. Obesity 2010; 18(1): 71-8.

Lee HJ, Bazinet RP, Rapoport SI, Bhattacharjee AK. Brain arachidonic acid cascade enzymes are upregulated in a rat model of unilateral Parkinson disease. Neurochem Res 2010; 35(4): 613-9.

Lei S, Zavala-Flores L, Garcia-Garcia A, Nandakumar R, Huang Y, Madayiputhiya N, *et al.* Alterations in Energy/Redox Metabolism Induced by Mitochondrial and Environmental Toxins: A Specific Role for

Glucose-6-Phosphate-Dehydrogenase and the Pentose Phosphate Pathway in Paraquat Toxicity. ACS Chemical Biology 2014; 9(9): 2032-48.

Levine J, Panchalingam K, McClure RJ, Gershon S, Pettegrew JW. Stability of CSF metabolites measured by proton NMR. Journal of neural transmission (Vienna, Austria : 1996) 2000; 107(7): 843-8.

LeWitt PA, Li J, Lu M, Beach TG, Adler CH, Guo L*, et al.* 3-hydroxykynurenine and other Parkinson's disease biomarkers discovered by metabolomic analysis. Mov Disord 2013; 28(12): 1653-60.

LeWitt PA, Li J, Lu M, Guo L, Auinger P. Metabolomic biomarkers as strong correlates of Parkinson disease progression. Neurology 2017; 88(9): 862-9.

Li GJ, Choi BS, Wang X, Liu J, Waalkes MP, Zheng W. Molecular mechanism of distorted iron regulation in the blood-CSF barrier and regional blood-brain barrier following in vivo subchronic manganese exposure. Neurotoxicology 2006; 27(5): 737-44.

Li W-J, Jiang H, Song N, Xie J-X. Dose- and time-dependent α-synuclein aggregation induced by ferric iron in SK-N-SH cells. Neuroscience Bulletin 2010a; 26(3): 205-10.

Li Y, Sun L, Cai T, Zhang Y, Lv S, Wang Y*, et al.* α-Synuclein overexpression during manganese-induced apoptosis in SH-SY5Y neuroblastoma cells. Brain Research Bulletin 2010b; 81(4): 428-33.

Lill R, Dutkiewicz R, Elsasser HP, Hausmann A, Netz DJ, Pierik AJ*, et al.* Mechanisms of iron-sulfur protein maturation in mitochondria, cytosol and nucleus of eukaryotes. Biochim Biophys Acta 2006; 1763(7): 652-67.

Lin C-H, Yang H-T, Chiu C-C, Lane H-Y. Blood levels of D-amino acid oxidase vs. D-amino acids in reflecting cognitive aging. Scientific Reports 2017; 7(1): 14849.

Lingor P, Carboni E, Koch JC. Alpha-synuclein and iron: two keys unlocking Parkinson's disease. J Neural Transm 2017; 124(8): 973-81.

Liu X, Yamada N, Maruyama W, Osawa T. Formation of dopamine adducts derived from brain polyunsaturated fatty acids: mechanism for Parkinson disease. The Journal of biological chemistry 2008; 283(50): 34887-95.

Liu Y, Smirnov K, Lucio M, Gougeon RD, Alexandre H, Schmitt-Kopplin P. MetICA: independent component analysis for high-resolution mass-spectrometry based non-targeted metabolomics. BMC Bioinformatics 2016; 17(1): 114.

Loeffler DA, DeMaggio AJ, Juneau PL, Brickman CM, Mashour GA, Finkelman JH*, et al.* Ceruloplasmin is increased in Cerebrospinal Fluid in Alzheimer´s but not Parkinson´s Disease. Alzheimer Dis Assoc Disord 1994; 8(3): 190-7.

Lohner S, Fekete K, Marosvolgyi T, Decsi T. Gender differences in the long-chain polyunsaturated fatty acid status: systematic review of 51 publications. Annals of nutrition & metabolism 2013; 62(2): 98-112.

Lucchini RG, Albini E, Benedetti L, Borghesi S, Coccaglio R, Malara EC*, et al.* High prevalence of Parkinsonian disorders associated to manganese exposure in the vicinities of ferroalloy industries. Am J Ind Med 2007; 50(11): 788-800.

Lucchini RG, Martin CJ, Doney BC. From manganism to manganese-induced parkinsonism: a conceptual model based on the evolution of exposure. Neuromolecular Med 2009; 11(4): 311-21.

Lucio M, Fekete A, Frommberger M, Schmitt-Kopplin P. Metabolomics: High-Resolution Tools Offer to Follow Bacterial Growth on a Molecular Level. Handbook of Molecular Microbial Ecology I: John Wiley & Sons, Inc.; 2011. p. 683-95.

Maass F, Michalke B, Leha A, Boerger M, Zerr I, Koch J-C*, et al.* Elemental fingerprint as a cerebrospinal fluid biomarker for the diagnosis of Parkinson's disease. J Neurochem 2018: n/a-n/a.

Maher P. The effects of stress and aging on glutathione metabolism. Ageing Res Rev 2005; 4(2): 288-314.

Jansson J, Willing B, Lucio M, Fekete A, Dicksved J, Halfvarson J, et al. Metabolomics Reveals Metabolic Biomarkers of Crohn's Disease. PLoS ONE 2009; 4: e6386.

Lucio M, Willkommen D, Schroeter M, Sigaroudi A, Schmitt-Kopplin P, Michalke B. Integrative Metabolomic and Metallomic Analysis in a Case–Control Cohort With Parkinson's Disease. Front Aging Neurosci 2019; 11: 331.

Maier TV, Lucio M, Lee LH, VerBerkmoes NC, Brislawn CJ, Bernhardt J, et al. Impact of Dietary Resistant Starch on the Human Gut Microbiome, Metaproteome, and Metabolome. mBio 2017; 8: e01343-17, /mbio/8/5/e01343-17.atom.

Michalke B, Willkommen D, Venkataramani V. Iron Redox Speciation Analysis Using Capillary Electrophoresis Coupled to Inductively Coupled Plasma Mass Spectrometry (CE-ICP-MS). Front Chem 2019; 7: 136.

Moritz F, Forcisi S, Harir M, Kanawati B, Lucio M, Tziotis D, et al. The Potential of Ultrahigh Resolution MS (FTICR-MS) in Metabolomics. In: Lämmerhofer M, Weckwerth W, editor(s). Metabolomics in Practice. Weinheim, Germany: Wiley-VCH Verlag GmbH & Co. KGaA; 2013. p. 117–36

Müller C, Harir M, Hertkorn N, Kanawati B, Tziotis D, Schmitt-Kopplin P. Using Ultrahigh-Resolution Mass Spectrometry to Unravel the Chemical Space of Complex Natural Product Mixtures. In: Havlíček V, Spížek J, editor(s). Natural Products Analysis. Hoboken, NJ: John Wiley & Sons, Inc; 2014. p. 545–72

Ni Y, Yu G, Chen H, Deng Y, Wells PM, Steves CJ, et al. M 2 IA: a Web Server for Microbiome and Metabolome Integrative Analysis [Internet]. Bioinformatics; 2019[cited 2019 Nov 24] Available from: http://biorxiv.org/lookup/doi/10.1101/678813

Thermo Scientific. AAA-Direct System - Product Manual [Internet]. 2018Available from: https://assets.thermofisher.com/TFS-Assets/CMD/manuals/Man-031481-AAA-Direct-Man031481-EN.pdf

Willkommen D, Lucio M, Moritz F, Forcisi S, Kanawati B, Smirnov KS, et al. Metabolomic investigations in cerebrospinal fluid of Parkinson's disease. PLoS ONE 2018; 13: e0208752.

Willkommen D, Lucio M, Schmitt-Kopplin P, Gazzaz M, Schroeter M, Sigaroudi A, et al. Species fractionation in a case-control study concerning Parkinson's disease: Cu-amino acids discriminate CSF of PD from controls. Journal of Trace Elements in Medicine and Biology 2018; 49: 164–70.

Mally J, Szalai G, Stone TW. Changes in the concentration of amino acids in serum and cerebrospinal fluid of patients with Parkinson's disease. J Neurol Sci 1997; 151(2): 159-62.

Mandal R, Guo AC, Chaudhary KK, Liu P, Yallou FS, Dong E, et al. Multi-platform characterization of the human cerebrospinal fluid metabolome: a comprehensive and quantitative update. Genome Med 2012; 4(4): 38.

Mandrioli J, Michalke B, Solovyev N, Grill P, Violi F, Lunetta C, et al. Elevated Levels of Selenium Species in Cerebrospinal Fluid of Amyotrophic Lateral Sclerosis Patients with Disease-Associated Gene Mutations. Neurodegener Dis 2017; 17(4-5): 171-80.

Manesis AC, O'Connor MJ, Schneider CR, Shafaat HS. Multielectron Chemistry within a Model Nickel Metalloprotein: Mechanistic Implications for Acetyl-CoA Synthase. J Am Chem Soc 2017; 139(30): 10328-38.

Manyam BV, Giacobini E, Colliver JA. Cerebrospinal fluid choline levels are decreased in Parkinson's disease. Annals of neurology 1990; 27(6): 683-5.

Maret W. Metallothionein/disulfide interactions, oxidative stress, and the mobilization of cellular zinc. Neurochem Int 1995; 27(1): 111-7.

Mariani S, Ventriglia M, Simonelli I, Donno S, Bucossi S, Vernieri F, et al. Fe and Cu do not differ in Parkinson's disease: a replication study plus meta-analysis. Neurobiol Aging 2013; 34(2): 632-3.

Maroteaux L, Campanelli JT, Scheller RH. Synuclein: a neuron-specific protein localized to the nucleus and presynaptic nerve terminal. J Neurosci 1988; 8(8): 2804-15.

Martin RB. Peptide bond characteristics. Met Ions Biol Syst 2001; 38: 1-23.

Martineau M, Baux G, Mothet J-P. d-Serine signalling in the brain: friend and foe. Trends in Neurosciences 2006; 29(8): 481-91.

May TW, Wiedmeyer RH. A table of polyatomic interferences in ICP-MS. At Spectrom 1998; 19(5): 150-5.

Mazzio E, Soliman KFA. The Role of Glycolysis and Gluconeogenesis in the Cytoprotection of Neuroblastoma Cells against 1-Methyl 4-Phenylpyridinium Ion Toxicity. NeuroToxicology 2003; 24(1): 137-47.

McDowall JS, Ntai I, Honeychurch KC, Hart JP, Colin P, Schneider BL, *et al.* Alpha-synuclein ferrireductase activity is detectible in vivo, is altered in Parkinson's disease and increases the neurotoxicity of DOPAL. Molecular and Cellular Neuroscience 2017; 85: 1-11.

Meermann B, Sperling M. Hyphenated techniques as tools for speciation analysis of metal-based pharmaceuticals: developments and applications. Anal Bioanal Chem 2012; 403(6): 1501-22.

Meiser J, Delcambre S, Wegner A, Jager C, Ghelfi J, d'Herouel AF, *et al.* Loss of DJ-1 impairs antioxidant response by altered glutamine and serine metabolism. Neurobiol Dis 2016; 89: 112-25.

Melo JB, Agostinho P, Oliveira CR. Involvement of oxidative stress in the enhancement of acetylcholinesterase activity induced by amyloid beta-peptide. Neurosci Res 2003; 45(1): 117-27.

Mertz W. The essential trace elements. Science 1981; 213(4514): 1332-8.

Michalke B. Element speciation definitions, analytical methodology, and some examples. Ecotoxicol Environ Saf 2003; 56(1): 122-39.

Michalke B. Capillary electrophoresis-inductively coupled plasma-mass spectrometry: A report on technical principles and problem solutions, potential, and limitations of this technology as well as on examples of application. Electrophoresis 2005; 26(7-8): 1584-97.

Michalke B, Berthele A. Contribution to selenium speciation in cerebrospinal fluid samples. J Anal At Spectrom 2011; 26(1): 165-70.

Michalke B, Berthele A, Mistriotis P, Ochsenkühn-Petropoulou M, Halbach S. Manganese speciation in human cerebrospinal fluid using CZE coupled to inductively coupled plasma MS. Electrophoresis 2007; 28(9): 1380-6.

Michalke B, Halbach S, Nischwitz V. JEM spotlight: metal speciation related to neurotoxicity in humans. J Environ Monit 2009; 11(5): 939-54.

Michalke B, Nischwitz V. Review on metal speciation analysis in cerebrospinal fluid-current methods and results: a review. Anal Chim Acta 2010; 682(1-2): 23-36.

Michalke B, Willkommen D, Drobyshev E, Solovyev N. The importance of speciation analysis in neurodegeneration research. Trends Analyt Chem 2017.

Michalke B, Willkommen D, Venkataramani V. Iron Redox Speciation Analysis Using Capillary Electrophoresis Coupled to Inductively Coupled Plasma Mass Spectrometry (CE-ICP-MS). Front Chem 2019; 7: 136.

Michell AW, Mosedale D, Grainger DJ, Barker RA. Metabolomic analysis of urine and serum in Parkinson's disease. Metabolomics 2008; 4(3): 191.

Miličević A, Raos N. A model to estimate stability constants of amino acid chelates with Cu(II) and Ni(II) at different ionic strengths. J Mol Liq 2012; 165(Supplement C): 139-42.

Miyoshi Y, Hamase K, Okamura T, Konno R, Kasai N, Tojo Y, *et al.* Simultaneous two-dimensional HPLC determination of free d-serine and d-alanine in the brain and periphery of mutant rats lacking d-amino-acid oxidase. Journal of Chromatography B 2011; 879(29): 3184-9.

Moldovan A-S, Groiss SJ, Elben S, Südmeyer M, Schnitzler A, Wojtecki L. The treatment of Parkinson's disease with deep brain stimulation: current issues. Neural Regeneration Research 2015; 10(7): 1018-22.

Molina JA, Jimenez-Jimenez FJ, Gomez P, Vargas C, Navarro JA, Orti-Pareja M, *et al.* Decreased cerebrospinal fluid levels of neutral and basic amino acids in patients with Parkinson's disease. J Neurol Sci 1997; 150(2): 123-7.

Molina JA, Jiménez-Jiménez FJ, Vargas C, Gómez P, de Bustos F, Ortí-Pareja M, *et al.* Cerebrospinal fluid levels of non-neurotransmitter amino acids in patients with Alzheimer's disease. Journal of neural transmission 1998; 105(2): 279-86.

Mollenhauer B, Trautmann E, Taylor P, Manninger P, Sixel-Doring F, Ebentheuer J, *et al.* Total CSF alpha-synuclein is lower in de novo Parkinson patients than in healthy subjects. Neurosci Lett 2013; 532: 44-8.

Molnar D, Schutz Y. The effect of obesity, age, puberty and gender on resting metabolic rate in children and adolescents. European journal of pediatrics 1997; 156(5): 376-81.

Mondello S, Constantinescu R, Zetterberg H, Andreasson U, Holmberg B, Jeromin A. CSF alpha-synuclein and UCH-L1 levels in Parkinson's disease and atypical parkinsonian disorders. Parkinsonism Relat Disord 2014; 20(4): 382-7.

Monnot AD, Behl M, Ho S, Zheng W. Regulation of brain copper homeostasis by the brain barrier systems: effects of Fe-overload and Fe-deficiency. Toxicol Appl Pharmacol 2011; 256(3): 249-57.

Moon HE, Paek SH. Mitochondrial Dysfunction in Parkinson's Disease. Exp Neurobiol 2015; 24(2): 103-16.

Moritz F, Forcisi S, Harir M, Kanawati B, Lucio M, Tziotis D, et al. The Potential of Ultrahigh Resolution MS (FTICR-MS) in Metabolomics. In: Lämmerhofer M, Weckwerth W, editor(s). Metabolomics in Practice. Weinheim, Germany: Wiley-VCH Verlag GmbH & Co. KGaA; 2013. p. 117–136

Moritz F, Kaling M, Schnitzler JP, Schmitt-Kopplin P. Characterization of poplar metabotypes via mass difference enrichment analysis. Plant Cell Environ 2017; 40(7): 1057-73.

Morreel K, Saeys Y, Dima O, Lu F, Van de Peer Y, Vanholme R*, et al.* Systematic structural characterization of metabolites in Arabidopsis via candidate substrate-product pair networks. The Plant cell 2014; 26(3): 929-45.

Mortadza SS, Sim JA, Stacey M, Jiang LH. Signalling mechanisms mediating Zn 2+ -induced TRPM2 channel activation and cell death in microglial cells. Scientific Reports 2017; 7.

Mounicou S, Szpunar J, Lobinski R. Metallomics: the concept and methodology. Chem Soc Rev 2009; 38(4): 1119-38.

Müller C, Fonseca JR, Rock TM, Krauss-Etschmann S, Schmitt-Kopplin P. Enantioseparation and selective detection of D-amino acids by ultra-high-performance liquid chromatography/mass spectrometry in analysis of complex biological samples. Journal of Chromatography A 2014; 1324: 109-14.

Müller C, Harir M, Hertkorn N, Kanawati B, Tziotis D, Schmitt-Kopplin P. Using Ultrahigh-Resolution Mass Spectrometry to Unravel the Chemical Space of Complex Natural Product Mixtures. In: Havlíček V, Spížek J, editor(s). Natural Products Analysis. Hoboken, NJ: John Wiley & Sons, Inc; 2014. p. 545–572

Nedergaard M. Garbage Truck of the Brain. Science 2013; 340: 1529–1530.

Neth K, Lucio M, Walker A, Kanawati B, Zorn J, Schmitt-Kopplin P*, et al.* Diverse Serum Manganese Species Affect Brain Metabolites Depending on Exposure Conditions. Chem Res Toxicol 2015a; 28(7): 1434-42.

Neth K, Lucio M, Walker A, Zorn J, Schmitt-Kopplin P, Michalke B. Changes in Brain Metallome/Metabolome Pattern due to a Single i.v. Injection of Manganese in Rats. PLoS One 2015b; 10(9): e0138270.

Ni Y, Yu G, Chen H, Deng Y, Wells PM, Steves CJ, et al. M 2 IA: a Web Server for Microbiome and Metabolome Integrative Analysis [Internet]. Bioinformatics; 2019[cited 2019 Nov 24] Available from: http://biorxiv.org/lookup/doi/10.1101/678813

Nikam S, Nikam P, Ahaley SK, Sontakke AV. Oxidative stress in Parkinson's disease. Indian J Clin Biochem 2009; 24(1): 98-101.

Nikolaev EN, Boldin IA, Jertz R, Baykut G. Initial experimental characterization of a new ultra-high resolution FTICR cell with dynamic harmonization. J Am Soc Mass Spectrom 2011; 22(7): 1125-33.

Nischwitz V, Berthele A, Michalke B. Speciation analysis of selected metals and determination of their total contents in paired serum and cerebrospinal fluid samples: An approach to investigate the permeability of the human blood-cerebrospinal fluid-barrier. Anal Chim Acta 2008; 627(2): 258-69.

Nishitani S, Takehana K, Fujitani S, Sonaka I. Branched-chain amino acids improve glucose metabolism in rats with liver cirrhosis. American journal of physiology Gastrointestinal and liver physiology 2005; 288(6): G1292-300.

Öhman A, Forsgren L. NMR metabonomics of cerebrospinal fluid distinguishes between Parkinson's disease and controls. Neurosci Lett 2015; 594: 36-9.

Oliver SG, Winson MK, Kell DB, Baganz F. Systematic functional analysis of the yeast genome. Trends in Biotechnology 1998; 16(9): 373-8.

Ozcelik D, Uzun H. Copper Intoxication; Antioxidant Defenses and Oxidative Damage in Rat Brain. Biological Trace Element Research 2009; 127(1): 45-52.

Paik SR, Shin HJ, Lee JH, Chang CS, Kim J. Copper(II)-induced self-oligomerization of alpha-synuclein. Biochem J 1999; 340: 821-8.

Park KH, Kim MS, Baek SJ, Bae IH, Seo S-W, Kim J, et al. Simultaneous molecular formula determinations of natural compounds in a plant extract using 15 T Fourier transform ion cyclotron resonance mass spectrometry. Plant Methods 2013; 9: 15-.

Park MJ, Cheon SM, Bae HR, Kim SH, Kim JW. Elevated levels of alpha-synuclein oligomer in the cerebrospinal fluid of drug-naive patients with Parkinson's disease. J Clin Neurol 2011; 7(4): 215-22.

Parkinson J. An essay on the shaking palsy. 1817. J Neuropsychiatry Clin Neurosci 2002; 14(2): 223-36; discussion 2.

Parnetti L, Castrioto A, Chiasserini D, Persichetti E, Tambasco N, El-Agnaf O*, et al.* Cerebrospinal fluid biomarkers in Parkinson disease. Nat Rev Neurol 2013; 9(3): 131-40.

Parnetti L, Chiasserini D, Bellomo G, Giannandrea D, De Carlo C, Qureshi MM*, et al.* Cerebrospinal fluid Tau/alpha-synuclein ratio in Parkinson's disease and degenerative dementias. Mov Disord 2011; 26(8): 1428-35.

Parnetti L, Chiasserini D, Persichetti E, Eusebi P, Varghese S, Qureshi MM*, et al.* Cerebrospinal fluid lysosomal enzymes and alpha-synuclein in Parkinson's disease. Mov Disord 2014a; 29(8): 1019-27.

Parnetti L, Farotti L, Eusebi P, Chiasserini D, De Carlo C, Giannandrea D*, et al.* Differential role of CSF alpha-synuclein species, tau, and Abeta42 in Parkinson's Disease. Front Aging Neurosci 2014b; 6: 53.

Pearce RKB, Owen A, Daniel S, Jenner P, Marsden CD. Alterations in the distribution of glutathione in the substantia nigra in Parkinson's disease. Journal of neural transmission 1997; 104(6): 661-77.

Peng Y, Wang C, Xu HH, Liu YN, Zhou F. Binding of alpha-synuclein with Fe(III) and with Fe(II) and biological implications of the resultant complexes. J Inorg Biochem 2010; 104(4): 365-70.

Perez RG, Waymire JC, Lin E, Liu JJ, Guo F, Zigmond MJ. A role for alpha-synuclein in the regulation of dopamine biosynthesis. J Neurosci 2002; 22(8): 3090-9.

Perkin E. NexION 350 ICP-MS-manual. 2015.

Persechini A, McMillan K, Masters BS. Inhibition of nitric oxide synthase activity by Zn2+ ion. Biochemistry 1995; 34(46): 15091-5.

Pieczenik SR, Neustadt J. Mitochondrial dysfunction and molecular pathways of disease. Exp Mol Pathol 2007; 83(1): 84-92.

Pivovarova NB, Stanika RI, Kazanina G, Villanueva I, Andrews SB. The interactive roles of zinc and calcium in mitochondrial dysfunction and neurodegeneration. J Neurochem 2014; 128(4): 592-602.

Post MR, Lieberman OJ, Mosharov EV. Can Interactions Between α-Synuclein, Dopamine and Calcium Explain Selective Neurodegeneration in Parkinson's Disease? Frontiers in Neuroscience 2018; 12(161).

Powers R, Lei S, Anandhan A, Marshall DD, Worley B, Cerny RL*, et al.* Metabolic Investigations of the Molecular Mechanisms Associated with Parkinson's Disease. Metabolites 2017; 7(2).

Prashanth L, Kattapagari K, Chitturi R, Baddam V, Prasad L. A review on role of essential trace elements in health and disease. Journal of Dr NTR University of Health Sciences 2015; 4(2): 75-85.

Pyreu D, Bedenko J. Thermodynamics of Ternary Complex Formation of Copper(II) and Nickel Iminodiacetates with Histidine in Solution. J Solution Chem 2017; 46(3): 633-42.

Quintana C, Bellefqih S, Laval JY, Guerquin-Kern JL, Wu TD, Avila J*, et al.* Study of the localization of iron, ferritin, and hemosiderin in Alzheimer's disease hippocampus by analytical microscopy at the subcellular level. J Struct Biol 2006; 153(1): 42-54.

Qureshi GA, Qureshi AA, Memon SA, Parvez SH. Impact of selenium, iron, copper and zinc in on/off Parkinson´s patients on L-dopa therapy. J Neural Transm 2006; 71: 229-36.

Racette BA, Criswell SR, Lundin JI, Hobson A, Seixas N, Kotzbauer PT*, et al.* Increased risk of parkinsonism associated with welding exposure. Neurotoxicology 2012; 33(5): 1356-61.

Ramos P, Santos A, Pinto NR, Mendes R, Magalhaes T, Almeida A. Iron levels in the human brain: a post-mortem study of anatomical region differences and age-related changes. J Trace Elem Med Biol 2014; 28(1): 13-7.

Rapoport SI. Arachidonic Acid and the Brain. J Nutr 2008; 138(12): 2515-20.

Rees TM, Brimijoin S. The role of acetylcholinesterase in the pathogenesis of Alzheimer's disease. Drugs of today (Barcelona, Spain : 1998) 2003; 39(1): 75-83.

Richarz AN, Bratter P. Speciation analysis of trace elements in the brains of individuals with Alzheimer's disease with special emphasis on metallothioneins. Anal Bioanal Chem 2002; 372(3): 412-7.

Riederer P, Sofic E, Rausch W-D, Schmidt B, Reynolds GP, Jellinger K*, et al.* Transition Metals, Ferritin, Glutathione, and Ascorbic Acid in Parkinsonian Brains. J Neurochem 1989; 52(2): 515-20.

Rinne UK, Riekkinen P, Sonninen V, Laaksonen H. BRAIN ACETYLCHOLINESTERASE IN PARKINSON'S DISEASE. Acta neurologica Scandinavica 1973; 49(2): 215-26.

Rogers S, Scheltema RA, Girolami M, Breitling R. Probabilistic assignment of formulas to mass peaks in metabolomics experiments. Bioinformatics (Oxford, England) 2009; 25(4): 512-8.

Rohart F, Gautier B, Singh A, Lê Cao K-A. mixOmics: An R package for 'omics feature selection and multiple data integration. PLOS Computational Biology 2017; 13(11): e1005752.

Rouault TA. The role of iron regulatory proteins in mammalian iron homeostasis and disease. Nat Chem Biol 2006; 2(8): 406-14.

Rowinska-Zyrek M, Salerno M, Kozlowski H. Neurodegenerative diseases - Understanding their molecular bases and progress in the development of potential treatments. Coordin Chem Rev 2015; 284: 298-312.

Ruberg M, Rieger F, Villageois A, Bonnet AM, Agid Y. Acetylcholinesterase and butyrylcholinesterase in frontal cortex and cerebrospinal fluid of demented and non-demented patients with Parkinson's disease. Brain Research 1986; 362(1): 83-91.

Ryan KC, Guce AI, Johnson OE, Brunold TC, Cabelli DE, Garman SC*, et al.* Nickel superoxide dismutase: structural and functional roles of His1 and its H-bonding network. Biochemistry 2015; 54(4): 1016-27.

Salvador GA. Iron in neuronal function and dysfunction. Biofactors 2010; 36(2): 103-10.

Samakashvili S, Ibáñez C, Simó C, Gil-Bea FJ, Winblad B, Cedazo-Mínguez A*, et al.* Analysis of chiral amino acids in cerebrospinal fluid samples linked to different stages of Alzheimer disease. ELECTROPHORESIS 2011; 32(19): 2757-64.

Sanyal J, Ahmed SSSJ, Ng HKT, Naiya T, Ghosh E, Banerjee TK*, et al.* Metallomic Biomarkers in Cerebrospinal fluid and Serum in patients with Parkinson's disease in Indian population. Scientific Reports 2016; 6: 35097.

Sanyal J, Bandyopadhyay SK, Banerjee TK, Mukherjee SC, Chakraborty DP, Ray BC*, et al.* Plasma levels of lipid peroxides in patients with Parkinson's disease. Eur Rev Med Pharmacol Sci 2009; 13(2): 129-32.

Sasabe J, Suzuki M. Distinctive Roles of D-Amino Acids in the Homochiral World: Chirality of Amino Acids Modulates Mammalian Physiology and Pathology. The Keio Journal of Medicine 2018; advpub.

Sayre LM, Perry G, Smith MA. Redox metals and neurodegenerative disease. Curr Opin Chem Biol 1999; 3(2): 220-5.

Schapira AHV, Cooper JM, Dexter D, Clark JB, Jenner P, Marsden CD. Mitochondrial Complex I Deficiency in Parkinson's Disease. J Neurochem 1990; 54(3): 823-7.

Scibior D, Czeczot H. [Catalase: structure, properties, functions]. Postepy Hig Med Dosw (Online) 2006; 60: 170–180.

Shimazaki Y, Takani M, Yamauchi O. Metal complexes of amino acids and amino acid side chain groups. Structures and properties. Dalton Trans 2009(38): 7854-69.

Shimazaki Y, Yajima T, Yamauchi O. Properties of the indole ring in metal complexes. A comparison with the phenol ring. Journal of inorganic biochemistry 2015; 148: 105-15.

Sian J, Dexter DT, Lees AJ, Daniel S, Agid Y, Javoy-Agid F, *et al.* Alterations in glutathione levels in Parkinson's disease and other neurodegenerative disorders affecting basal ganglia. Ann Neurol 1994a; 36(3): 348-55.

Sian J, Dexter DT, Lees AJ, Daniel S, Jenner P, Marsden CD. Glutathione-related enzymes in brain in Parkinson's disease. Ann Neurol 1994b; 36(3): 356-61.

Sirviö J, Soininen HS, Kutvonen R, Hyttinen J-M, Helkala E-L, Riekkinen PJ. Acetyl- and butyrylcholinesterase activity in the cerebrospinal fluid of patients with Parkinson's disease. Journal of the Neurological Sciences 1987; 81(2): 273-9.

Skjorringe T, Moller LB, Moos T. Impairment of interrelated iron- and copper homeostatic mechanisms in brain contributes to the pathogenesis of neurodegenerative disorders. Front Pharmacol 2012; 3: 169.

Sofic E, Riederer P, Heinsen H, Beckmann H, Reynolds GP, Hebenstreit G, *et al.* Increased iron (III) and total iron content in post mortem substantia nigra of parkinsonian brain. J Neural Transm 1988; 74(3): 199-205.

Solovyev N, Berthele A, Michalke B. Selenium speciation in paired serum and cerebrospinal fluid samples. Anal Bioanal Chem 2013; 405(6): 1875-84.

Solovyev N, Vinceti M, Grill P, Mandrioli J, Michalke B. Redox speciation of iron, manganese, and copper in cerebrospinal fluid by strong cation exchange chromatography - sector field inductively coupled plasma mass spectrometry. Anal Chim Acta 2017.

Sovago I, Kiss T, Gergely A. Critical survey of the stability constants of complexes of aliphatic amino acids (Technical Report). Pure and Applied Chemistry; 1993. p. 1029.

Stewart T, Liu C, Ginghina C, Cain KC, Auinger P, Cholerton B, *et al.* Cerebrospinal fluid alpha-synuclein predicts cognitive decline in Parkinson disease progression in the DATATOP cohort. Am J Pathol 2014; 184(4): 966-75.

Stoessel D, Schulte C, Teixeira dos Santos MC, Scheller D, Rebollo-Mesa I, Deuschle C, *et al.* Promising Metabolite Profiles in the Plasma and CSF of Early Clinical Parkinson's Disease. Frontiers in Aging Neuroscience 2018; 10(51).

Subramaniam SR, Chesselet MF. Mitochondrial dysfunction and oxidative stress in Parkinson's disease. Prog Neurobiol 2013; 106-107: 17-32.

Suhre K, Schmitt-Kopplin P. MassTRIX: mass translator into pathways. Nucleic Acids Res 2008; 36(suppl_2): W481-W4.

Sun H, Chai Z-F. Metallomics: An integrated science for metals in biology and medicine. Annual Reports Section "A" (Inorganic Chemistry) 2010; 106: 20.

Sun Y, Pham AN, Waite TD. Elucidation of the interplay between Fe(II), Fe(III), and dopamine with relevance to iron solubilization and reactive oxygen species generation by catecholamines. Journal of Neurochemistry 2016; 137(6): 955-68.

Sunday O, Adekunle M, Temitope O, Richard A, Samuel A, Olufunminyi A, *et al.* Alteration in antioxidants level and lipid peroxidation of patients with neurodegenerative diseases {Alzheimer's disease and Parkinson disease}. Int J Nutr Pharm Neurol Dis 2014; 4(3): 146-52.

Szpunar-Łobińska J, Witte C, Łobinski R, Adams FC. Separation techniques in speciation analysis for organometallic species. Fresenius J Anal Chem 1995; 351(4): 351-77.

Szpunar J. Bio-inorganic speciation analysis by hyphenated techniques. Analyst 2000a; 125(5): 963-88.

Szpunar J. Trace element speciation analysis of biomaterials by high-performance liquid chromatography with inductively coupled plasma mass spectrometric detection. Trends Analyt Chem 2000b; 19(2): 127-37.

Taylor JM, Main BS, Crack PJ. Neuroinflammation and oxidative stress: Co-conspirators in the pathology of Parkinson's disease. Neurochem Int 2013; 62(5): 803-19.

Tenenhaus A, Tenenhaus M. Regularized Generalized Canonical Correlation Analysis. Psychometrika 2011; 76: 257.

Tenenhaus M. La regression PLS: theorie et pratique. Paris: Editions Technic; 1998

Thermo FS. Element2/XR - Hardware manual.

Thermo Scientific. AAA-Direct System - Product Manual [Internet]. 2018, Available from: https://assets.thermofisher.com/TFS-Assets/CMD/manuals/Man-031481-AAA-Direct-Man031481-EN.pdf

Timerbaev AR. Element speciation analysis using capillary electrophoresis: twenty years of development and applications. Chem Rev 2013; 113(1): 778-812.

Timerbaev AR, Pawlak K, Aleksenko SS, Foteeva LS, Matczuk M, Jarosz M. Advances of CE-ICP-MS in speciation analysis related to metalloproteomics of anticancer drugs. Talanta 2012; 102: 164-70.

Titchenal CA, Rogers QR, Indrieri RJ, Morris JG. Threonine Imbalance, Deficiency and Neurologic Dysfunction in the Kitten. The Journal of Nutrition 1980; 110(12): 2444-59.

Tokuda T, Salem SA, Allsop D, Mizuno T, Nakagawa M, Qureshi MM*, et al.* Decreased alpha-synuclein in cerebrospinal fluid of aged individuals and subjects with Parkinson's disease. Biochem Biophys Res Commun 2006; 349(1): 162-6.

Tõugu V, Palumaa P. Coordination of zinc ions to the key proteins of neurodegenerative diseases: Aβ, APP, α-synuclein and PrP. Coordin Chem Rev 2012; 256(19): 2219-24.

Trezzi JP, Galozzi S, Jaeger C, Barkovits K, Brockmann K, Maetzler W*, et al.* Distinct metabolomic signature in cerebrospinal fluid in early parkinson's disease. Mov Disord 2017; 32(10): 1401-8.

Trupp M, Jonsson P, Ohrfelt A, Zetterberg H, Obudulu O, Malm L*, et al.* Metabolite and peptide levels in plasma and CSF differentiating healthy controls from patients with newly diagnosed Parkinson's disease. J Parkinsons Dis 2014; 4(3): 549-60.

Tuchsen F, Jensen AA. Agricultural work and the risk of Parkinson's disease in Denmark, 1981-1993. Scandinavian journal of work, environment & health 2000; 26(4): 359-62.

Tziotis D, Hertkorn N, Schmitt-Kopplin P. Kendrick-analogous network visualisation of ion cyclotron resonance Fourier transform mass spectra: improved options for the assignment of elemental compositions and the classification of organic molecular complexity. Eur J Mass Spectrom 2011; 17(4): 415-21.

Uversky VN, Li J, Bower K, Fink AL. Synergistic effects of pesticides and metals on the fibrillation of alpha-synuclein: implications for Parkinson's disease. Neurotoxicology 2002; 23(4-5): 527-36.

Uversky VN, Li J, Fink AL. Metal-triggered Structural Transformations, Aggregation, and Fibrillation of Human α-Synuclein: A POSSIBLE MOLECULAR LINK BETWEEN PARKINSON′S DISEASE AND HEAVY METAL EXPOSURE. Journal of Biological Chemistry 2001; 276(47): 44284-96.

Valdez CE, Smith QA, Nechay MR, Alexandrova AN. Mysteries of Metals in Metalloenzymes. Accounts of Chemical Research 2014; 47(10): 3110-7.

Valiente-Gabioud AA, Torres-Monserrat V, Molina-Rubino L, Binolfi A, Griesinger C, Fernández CO. Structural basis behind the interaction of Zn2+ with the protein α-synuclein and the Aβ peptide: A comparative analysis. Journal of inorganic biochemistry 2012; 117: 334-41.

van Dijk KD, Bidinosti M, Weiss A, Raijmakers P, Berendse HW, van de Berg WD. Reduced alpha-synuclein levels in cerebrospinal fluid in Parkinson's disease are unrelated to clinical and imaging measures of disease severity. Eur J Neurol 2014; 21(3): 388-94.

Van Sande M, Caers J, Lowenthal A. Cerebrospinal fluid amino acids in extrapyramidal disorders before and after L-DOPA treatment. Z Neurol 1971; 199(1): 24-9.

Vinceti M, Chiari A, Eichmuller M, Rothman KJ, Filippini T, Malagoli C*, et al.* A selenium species in cerebrospinal fluid predicts conversion to Alzheimer's dementia in persons with mild cognitive impairment. Alzheimers Res Ther 2017; 9(1): 100.

Vinceti M, Solovyev N, Mandrioli J, Crespi CM, Bonvicini F, Arcolin E*, et al.* Cerebrospinal fluid of newly diagnosed amyotrophic lateral sclerosis patients exhibits abnormal levels of selenium species including elevated selenite. NeuroToxicology 2013; 38: 25-32.

Wagele B, Witting M, Schmitt-Kopplin P, Suhre K. MassTRIX reloaded: combined analysis and visualization of transcriptome and metabolome data. PLoS One 2012; 7(7): e39860.

Wakabayashi K, Tanji K, Mori F, Takahashi H. The Lewy body in Parkinson's disease: molecules implicated in the formation and degradation of alpha-synuclein aggregates. Neuropathology : official journal of the Japanese Society of Neuropathology 2007; 27(5): 494-506.

Wang X, Li GJ, Zheng W. Efflux of iron from the cerebrospinal fluid to the blood at the blood-CSF barrier: effect of manganese exposure. Exp Biol Med 2008; 233(12): 1561-71.

Ward RJ, Zucca FA, Duyn JH, Crichton RR, Zecca L. The role of iron in brain ageing and neurodegenerative disorders. Lancet Neurol 2014; 13(10): 1045-60.

Williams RJP. Chemical selection of elements by cells. Coordin Chem Rev 2001; 216-217(Supplement C): 583-95.

Willis AW, Evanoff BA, Lian M, Galarza A, Wegrzyn A, Schootman M*, et al.* Metal emissions and urban incident Parkinson disease: a community health study of Medicare beneficiaries by using geographic information systems. Am J Epidemiol 2010; 172(12): 1357-63.

Willkommen D, Lucio M, Moritz F, Forcisi S, Kanawati B, Smirnov KS*, et al.* Metabolomic investigations in cerebrospinal fluid of Parkinson's disease. PLOS ONE 2018a; 13(12): e0208752.

Willkommen D, Lucio M, Schmitt-Kopplin P, Gazzaz M, Schroeter M, Sigaroudi A*, et al.* Species fractionation in a case-control study concerning Parkinson's disease: Cu-amino acids discriminate CSF of PD from controls. J Trace Elem Med Biol 2018b.

Wilm M. Principles of Electrospray Ionization. Molecular & cellular proteomics : MCP 2011; 10(7): M111.009407.

Wirdefeldt K, Adami HO, Cole P, Trichopoulos D, Mandel J. Epidemiology and etiology of Parkinson's disease: a review of the evidence. Eur J Epidemiol 2011; 26 Suppl 1: S1-58.

Wishart DS. Current Progress in computational metabolomics. Briefings in Bioinformatics 2007; 8(5): 279-93.

Wishart DS, Lewis MJ, Morrissey JA, Flegel MD, Jeroncic K, Xiong Y, *et al.* The human cerebrospinal fluid metabolome. Journal of Chromatography B 2008; 871(2): 164-73.

Wishart DS, Tzur D, Knox C, Eisner R, Guo AC, Young N, *et al.* HMDB: the Human Metabolome Database. Nucleic Acids Research 2007; 35(suppl_1): D521-D6.

Witten IH, Frank E, Hall MA, Pal C. Data mining : practical machine learning tools and techniques. Fourth Edition. ed. Amsterdam: Elsevier; 2017.

Wojcieszek J, Szpunar J, Lobinski R. Speciation of technologically critical elements in the environment using chromatography with element and molecule specific detection. Trends Analyt Chem 2017.

Wold H. Estimation of principal components and related models by iterative least squares. In: Multivariate Analysis. N.Y.: Academic Press; 1966. p. 391–420

Wörmann K, Walker A, Moritz F, Forcisi S, Tziotis D, Lucio M, *et al.* Revolution in der Diabetesdiagnostik dank -omics - Biomarker mittels Metabolomics; 2012.

Wu G, Fang Y-Z, Yang S, Lupton JR, Turner ND. Glutathione Metabolism and Its Implications for Health. J Nutr 2004; 134(3): 489-92.

Wu J, Wuolikainen A, Trupp M, Jonsson P, Marklund SL, Andersen PM, *et al.* NMR analysis of the CSF and plasma metabolome of rigorously matched amyotrophic lateral sclerosis, Parkinson's disease and control subjects. Metabolomics 2016; 12(6): 101.

Wuolikainen A, Jonsson P, Ahnlund M, Antti H, Marklund SL, Moritz T, *et al.* Multi-platform mass spectrometry analysis of the CSF and plasma metabolomes of rigorously matched amyotrophic lateral sclerosis, Parkinson's disease and control subjects. Mol Biosyst 2016; 12(4): 1287-98.

Xu J, Jia Z, Knutson MD, Leeuwenburgh C. Impaired iron status in aging research. Int J Mol Sci 2012; 13(2): 2368-86.

Yang MS, Wong HF, Yung KL. Determination of endogenous trace metal contents in various mouse brain regions after prolonged oral administration of aluminum chloride. J Toxicol Environ Health A 1998; 55(6): 445-53.

Yekkala R, Meers C, Van Schepdael A, Hoogmartens J, Lambrichts I, Willems G. Racemization of aspartic acid from human dentin in the estimation of chronological age. Forensic science international 2006; 159 Suppl 1: S89-94.

Yokel RA. Blood-brain barrier flux of aluminium, manganese, iron and other metals suspected to contribute zo metal-induced neurodegernation. J Alzheimers Dis 2006; 10: 223-53.

Yokel RA, Crossgrove J. Manganese Toxicokinetics at the Blood–Brain Barrier. Res Rep Health Eff Inst 2004; 119: 7-58.

Yokoyama M, Koh J, Choi DW. Brief exposure to zinc is toxic to cortical neurons. Neuroscience Letters 1986; 71(3): 351-5.

Yoshii F, Barker WW, Chang JY, Loewenstein D, Apicella A, Smith D, et al. Sensitivity of Cerebral Glucose Metabolism to Age, Gender, Brain Volume, Brain Atrophy, and Cerebrovascular Risk Factors. Journal of Cerebral Blood Flow & Metabolism 1988; 8(5): 654-61.

Yu X-T, Zeng T. Integrative Analysis of Omics Big Data. In: Huang T, editor(s). Computational Systems Biology. New York, NY: Springer New York; 2018. p. 109–135

Zawisza I, Rozga M, Bal W. Affinity of copper and zinc ions to proteins and peptides related to neurodegenerative conditions (A beta, APP, alpha-synuclein, PrP). Coordin Chem Rev 2012; 256(19-20): 2297-307.

Zecca L, Stroppolo A, Gatti A, Tampellini D, Toscani M, Gallorini M, et al. The role of iron and copper molecules in the neuronal vulnerability of locus coeruleus and substantia nigra during aging. Proc Natl Acad Sci U S A 2004a; 101(26): 9843-8.

Zecca L, Youdim MB, Riederer P, Connor JR, Crichton RR. Iron, brain ageing and neurodegenerative disorders. Nat Rev Neurosci 2004b; 5(11): 863-73.

Zhang J, Zhang Y, Wang J, Cai P, Luo C, Qian Z, et al. Characterizing iron deposition in Parkinson's disease using susceptibility-weighted imaging: an in vivo MR study. Brain Res 2010; 1330: 124-30.

Zhang X, Lu L, Liu S, Ye W, Wu J, Zhang X. Acetylcholinesterase deficiency decreases apoptosis in dopaminergic neurons in the neurotoxin model of Parkinson's disease. The International Journal of Biochemistry & Cell Biology 2013; 45(2): 265-72.

Zhao HW, Lin J, Wang XB, Cheng X, Wang JY, Hu BL, et al. Assessing plasma levels of selenium, copper, iron and zinc in patients of Parkinson's disease. PLoS One 2013; 8(12): e83060.

Zheng W, Monnot AD. Regulation of brain iron and copper homeostasis by brain barrier systems: Implication in neurodegenerative diseases. Pharmacology & Therapeutics 2012; 133: 177–188.

Zheng W, Zhao Q, Slavkovich V, Aschner M, Graziano JH. Alteration of iron homeostasis following chronic exposure to manganese in rats. Brain research 1999; 833(1): 125-32.

Zubenko GS, Marquis JK, Volicer L, Direnfeld LK, Langlais PJ, Nixon RA. Cerebrospinal fluid levels of angiotensin- converting enzyme, acetylcholinesterase, and dopamine metabolites in dementia associated with Alzheimer's disease and Parkinson's disease: A correlative study. Biological Psychiatry 1986; 21(14): 1365-81.

Zucca FA, Segura-Aguilar J, Ferrari E, Munoz P, Paris I, Sulzer D, *et al.* Interactions of iron, dopamine and neuromelanin pathways in brain aging and Parkinson's disease. Prog Neurobiol 2017; 155: 96-119.

6. Appendix

6.1 Supplementary tables and figures

6.1.1 Characterization by means of SEC-ICP-MS
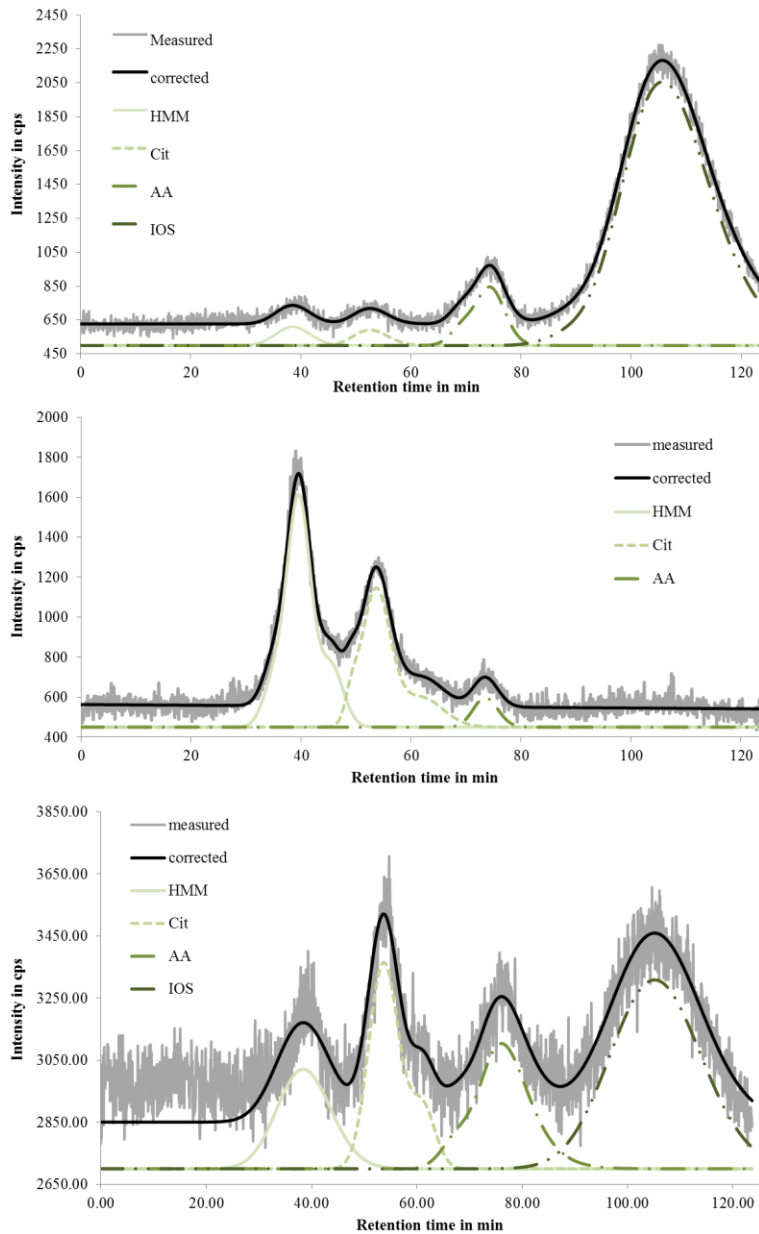
Figure A1: Observed SEC-ICP-MS-chromatogram (, with graphical off-set) of A) Fe, B) Cu, and C) Zn in CSF with fractions aligned (—— , aligned chromatogram, with graphical off-set) by use of PeakFit^{TM} software. Species detected are „HMM" (——), „Citrate" (---), „Amino acids" (-··-) and „Inorganic species" (—··—).

6.1.2 Determination of amino acids

Table A1: SD of the measured metal concentrations of Cu, Fe, Mg, Mn, Ni, Sr, and Zn in the amino acid fractions in CSF for CTR- and PD-samples.

		$c_{(Cu)}$ in µg/L	$c_{(Fe)}$ in µg/L	$c_{(Mg)}$ in µg/L	$c_{(Mn)}$ in µg/L	$c_{(Ni)}$ in µg/L	$c_{(Sr)}$ in µg/L	$c_{(Zn)}$ in µg/L
Arg	CTR	43.19	80.49	77.11	1.04	6.18	1.72	19.11
	PD	13.48	264.12	48.22	2.23	54.19	2.44	25.04
Gln	CTR	8.26	196.37	37.40	14.46	13.13	2.93	27.11
	PD	23.04	645.72	38.81	1.95	25.47	0.99	215.54
Ala	CTR	16.12	190.63	32.38	2.15	10.84	2.28	43.84
	PD	1.91	39.58	14.83	1.46	2.95	0.48	9.64
Gly	CTR	498.10	146.76	71.40	4.51	26.40	3.89	126.20
	PD	13.70	161.51	80.16	1.01	2.01	1.97	39.93
Ser	CTR	12.03	107.07	58.93	1.34	31.50	2.12	151.73
	PD	4.72	69.95	13.73	0.56	141.04	0.84	37.49
Ile	CTR	10.58	73.31	77.60	0.95	7.04	3.06	32.12

	PD	33.75	85.68	41.13	0.53	43.98	1.04	25.17
Leu	CTR	13.71	77.93	40.47	1.12	4.79	1.54	34.87
	PD	12.43	93.71	13.92	0.41	1.54	1.95	44.46
SeM	CTR	13.13	50.49	62.00	0.47	2.15	0.87	66.24
	PD	3.85	57.06	5.72	0.32	0.65	1.15	34.77
His	CTR	5.99	77.84	28.27	0.68	24.57	3.33	14.26
	PD	29.91	129.38	20.29	0.37	6.01	1.11	15.83
Phe	CTR	184.38	108.36	81.94	0.66	1.31	5.13	26.02
	PD	19.98	107.79	24.38	0.44	4.40	2.82	47.79
Glu	CTR	27.53	90.93	32.82	0.42	4.35	7.01	34.92
	PD	11.67	17.38	52.64	0.34	6.77	6.43	41.81
Tyr	CTR	26.05	75.97	100.19	1.11	54.89	7.24	86.17
	PD	8.82	112.95	21.97	0.68	4.82	7.86	74.93

6.1.3 Metabolic profiling

Table A2: Listed are all 243 core masses which significantly differentiate CTR and PD with respective mean intensity, SD, alteration in PD, SEN, SPE, positive predictive value (PPV), and negative predictive value (NPV).

No.	theoretical molecular ion formula	Mean intensity		SD		Alteration in PD	SEN	SPE	PPV	NPV
		CTR	PD	CTR	PD					
165	128.0353394	1.05E+06	1.50E+06	1.08E+06	1.25E+06	↑	0.484	0.711	0.349	0.812
143	134.0612035	1.69E+04	1.55E+05	1.65E+05	4.76E+05	↑	0.097	0.99	0.75	0.774
113	142.9987223	1.50E+04	1.47E+05	1.47E+05	4.48E+05	↑	0.097	0.99	0.75	0.774
83	144.1142933	1.50E+04	1.97E+05	1.47E+05	5.12E+05	↑	0.129	1	1	0.782
126	145.077232	0.00E+00	1.56E+05	0.00E+00	4.80E+05	↑	0.097	1	1	0.776
150	162.0925267	1.50E+04	1.49E+05	1.47E+05	4.58E+05	↑	0.097	0.99	0.75	0.774
136	171.139099	4.69E+04	2.38E+05	2.63E+05	6.31E+05	↑	0.129	0.99	0.8	0.78
147	180.9730968	2.54E+05	3.80E+05	6.26E+05	7.08E+05	↑	0.226	0.856	0.333	0.776
200	183.0275384	1.29E+06	1.78E+06	1.03E+06	1.08E+06	↑	0.742	0.515	0.329	0.862
56	183.0542765	3.05E+05	4.98E+04	7.94E+05	2.73E+05	↓	-	-	-	0.758
59	185.0568361	1.49E+05	0.00E+00	4.67E+05	0.00E+00	↓	-	-	-	0.758
92	187.0070548	5.74E+04	5.33E+05	3.22E+05	1.01E+06	↑	0.258	0.969	0.727	0.803
186	187.1338897	1.67E+04	1.76E+05	1.63E+05	5.41E+05	↑	0.097	1	1	0.776
105	191.0561635	6.30E+05	1.07E+06	1.02E+06	1.28E+06	↑	0.419	0.825	0.433	0.816
153	197.0043989	1.61E+05	3.34E+05	5.07E+05	6.83E+05	↑	0.194	0.928	0.462	0.783
90	207.1641247	1.54E+04	1.56E+05	1.51E+05	4.78E+05	↑	0.097	1	1	0.776
44	209.0667466	1.31E+06	8.06E+05	1.13E+06	9.60E+05	↓	-	-	-	0.758
97	220.0075213	1.55E+04	1.53E+05	1.52E+05	4.69E+05	↑	0.097	1	1	0.776
124	226.0391043	0.00E+00	1.52E+05	0.00E+00	4.64E+05	↑	0.097	1	1	0.776
201	226.9995545	1.74E+06	1.95E+06	1.52E+06	1.18E+06	↑	0.742	0.443	0.299	0.843

50	229.06944	4.89E+05	2.51E+05	9.20E+05	6.60E+05	↓	-	-	-	0.758
102	230.0646569	5.60E+04	2.46E+05	3.16E+05	6.41E+05	↑	0.129	0.979	0.667	0.779
93	232.0015517	1.60E+04	1.73E+05	1.57E+05	5.31E+05	↑	0.097	1	1	0.776
84	232.0133892	1.58E+04	2.15E+05	1.55E+05	5.60E+05	↑	0.129	1	1	0.782
236	232.9973025	3.62E+05	6.29E+05	7.85E+05	8.56E+05	↑	0.355	0.825	0.393	0.8
51	233.0279831	7.66E+05	5.54E+05	1.05E+06	8.77E+05	↓	-	-	-	0.758
127	233.1548034	8.67E+05	1.23E+06	1.06E+06	1.17E+06	↑	0.419	0.825	0.433	0.816
180	234.9837203	5.57E+05	7.84E+05	9.94E+05	1.01E+06	↑	0.323	0.825	0.37	0.792
94	239.030494	3.17E+05	5.20E+05	7.01E+05	8.24E+05	↑	0.29	0.856	0.391	0.79
145	243.0599553	4.86E+05	5.91E+05	8.89E+05	8.73E+05	↑	0.323	0.763	0.303	0.779
152	247.170377	2.83E+05	6.29E+05	6.41E+05	8.61E+05	↑	0.355	0.856	0.44	0.806
129	251.1287615	0.00E+00	1.81E+05	0.00E+00	5.69E+05	↑	0.097	1	1	0.776
142	254.9793135	7.39E+05	1.27E+06	9.98E+05	1.05E+06	↑	0.548	0.784	0.447	0.844
134	259.0130499	4.10E+05	5.54E+05	8.14E+05	8.79E+05	↑	0.29	0.794	0.31	0.778
104	260.2019043	1.78E+04	1.66E+05	1.74E+05	5.07E+05	↑	0.097	0.99	0.75	0.774
174	264.1486338	1.63E+04	1.84E+05	1.59E+05	5.69E+05	↑	0.097	0.99	0.75	0.774
156	267.0722849	1.32E+06	1.78E+06	1.48E+06	1.75E+06	↑	0.548	0.66	0.34	0.821
222	273.0593342	3.94E+05	6.98E+05	7.93E+05	8.89E+05	↑	0.387	0.794	0.375	0.802
100	275.0551273	6.88E+04	2.23E+05	3.33E+05	5.82E+05	↑	0.129	0.979	0.667	0.779
115	277.0810517	1.77E+04	1.55E+05	1.74E+05	4.75E+05	↑	0.097	0.99	0.75	0.774
163	279.0600541	1.85E+05	4.94E+05	5.99E+05	9.38E+05	↑	0.226	0.928	0.5	0.789
30	281.0547614	1.66E+06	1.23E+06	1.54E+06	1.40E+06	↓	-	-	-	0.758
33	289.1941332	6.89E+05	2.56E+05	1.09E+06	8.03E+05	↓	0.065	0.948	0.286	0.76
108	289.9477164	8.01E+05	9.48E+05	1.03E+06	1.01E+06	↑	0.355	0.784	0.344	0.792
148	291.9448085	5.75E+05	7.74E+05	8.95E+05	9.26E+05	↑	0.419	0.701	0.31	0.791
69	293.0491942	5.01E+05	2.48E+05	9.86E+05	6.53E+05	↓	-	-	-	0.758
87	296.8702688	0.00E+00	1.61E+05	0.00E+00	4.92E+05	↑	0.097	1	1	0.776
205	303.2331566	3.95E+05	9.15E+05	8.44E+05	1.49E+06	↑	0.387	0.876	0.5	0.817
214	305.2488453	6.61E+05	8.62E+05	1.28E+06	1.17E+06	↑	0.387	0.763	0.343	0.796

16	310.9028977	3.70E+06	2.74E+06	2.97E+06	3.01E+06	↓	0.097	0.928	0.3	0.763
74	312.8563631	7.61E+05	5.46E+05	1.07E+06	8.67E+05	↓	0.097	0.907	0.25	0.759
189	312.9445937	1.76E+04	1.69E+05	1.73E+05	5.19E+05	↑	0.097	0.99	0.75	0.774
139	316.2414787	6.37E+05	1.17E+06	1.09E+06	1.75E+06	↑	0.258	0.938	0.571	0.798
101	320.8849807	4.15E+05	7.90E+05	8.56E+05	1.03E+06	↑	0.387	0.804	0.387	0.804
232	321.0182229	4.60E+05	6.94E+05	8.40E+05	9.46E+05	↑	0.323	0.814	0.357	0.79
155	321.0805514	1.55E+06	2.23E+06	1.40E+06	1.52E+06	↑	0.71	0.515	0.319	0.847
79	325.8516718	8.31E+05	3.62E+05	1.82E+06	9.85E+05	↓	0.129	0.887	0.267	0.761
49	326.9165308	5.08E+05	3.18E+05	8.87E+05	7.38E+05	↓	0.032	0.979	0.333	0.76
95	326.9633437	2.32E+05	3.86E+05	6.24E+05	7.15E+05	↑	0.226	0.887	0.389	0.782
132	330.2206635	2.22E+04	2.20E+05	2.18E+05	6.93E+05	↑	0.097	0.99	0.75	0.774
128	332.236467	3.20E+05	1.68E+06	1.78E+06	4.60E+06	↑	0.29	0.959	0.692	0.809
98	332.9295205	7.41E+05	1.34E+06	1.05E+06	1.16E+06	↑	0.613	0.649	0.358	0.84
123	332.9350046	2.57E+05	5.79E+05	7.03E+05	9.26E+05	↑	0.29	0.897	0.474	0.798
167	334.8851498	1.96E+05	2.75E+05	6.69E+05	6.27E+05	↑	0.161	0.918	0.385	0.774
172	334.9037847	1.31E+06	1.48E+06	1.48E+06	1.03E+06	↑	0.71	0.515	0.319	0.847
242	337.2056849	8.43E+06	9.22E+06	9.74E+06	8.82E+06	↑	0.806	0.371	0.291	0.857
229	338.8720683	4.33E+06	5.42E+06	2.83E+06	2.86E+06	↑	0.581	0.701	0.383	0.84
66	338.9455472	8.30E+05	4.87E+05	1.54E+06	1.11E+06	↓	0.032	0.969	0.25	0.758
144	340.1726107	3.54E+04	2.36E+05	2.44E+05	6.16E+05	↑	0.129	0.979	0.667	0.779
206	340.9135907	3.60E+05	5.72E+05	8.40E+05	9.97E+05	↑	0.258	0.856	0.364	0.783
34	340.9790916	3.04E+06	2.51E+06	3.10E+06	2.80E+06	↓	0.452	0.691	0.318	0.798
178	342.8225347	7.90E+05	1.18E+06	1.25E+06	1.43E+06	↑	0.355	0.876	0.478	0.81
39	342.8927861	1.26E+06	7.39E+05	1.18E+06	1.02E+06	↓	-	-	-	0.758
183	344.1353778	7.20E+05	1.16E+06	1.13E+06	1.08E+06	↑	0.484	0.742	0.375	0.818
166	346.2157277	7.39E+04	3.34E+05	7.24E+05	1.11E+06	↑	0.097	0.99	0.75	0.774
8	347.0475828	1.77E+06	1.12E+06	1.50E+06	1.52E+06	↓	0.032	0.979	0.333	0.76
162	354.8782063	5.44E+05	1.36E+06	1.22E+06	1.90E+06	↑	0.452	0.804	0.424	0.821
208	356.9480971	1.35E+06	1.69E+06	1.25E+06	1.26E+06	↑	0.613	0.557	0.306	0.818

159	358.9193727	2.03E+05	3.70E+05	6.04E+05	7.65E+05	↑	0.161	0.938	0.455	0.778
120	359.1142318	5.39E+05	8.08E+05	9.70E+05	1.15E+06	↑	0.355	0.784	0.344	0.792
43	360.8953222	1.26E+06	8.74E+05	1.04E+06	1.04E+06	↓	0.032	0.979	0.333	0.76
158	360.9194921	1.30E+06	1.95E+06	1.43E+06	1.25E+06	↑	0.71	0.567	0.344	0.859
185	361.1354767	2.29E+06	3.18E+06	1.78E+06	2.19E+06	↑	0.581	0.67	0.36	0.833
103	362.8792155	1.63E+05	5.58E+05	5.49E+05	9.67E+05	↑	0.226	0.959	0.636	0.795
137	362.9165982	6.22E+05	1.07E+06	1.05E+06	1.08E+06	↑	0.516	0.742	0.39	0.828
196	364.2263848	1.87E+05	5.45E+05	1.83E+06	1.94E+06	↑	0.097	0.99	0.75	0.774
67	368.8826316	1.73E+06	1.43E+06	1.45E+06	1.38E+06	↓	0.258	0.814	0.308	0.775
73	368.8907008	1.86E+06	1.21E+06	1.74E+06	1.32E+06	↓	-	-	-	0.758
76	369.1348519	3.34E+06	2.74E+06	3.69E+06	2.76E+06	↓	0.516	0.598	0.291	0.795
18	370.8724695	4.98E+05	1.89E+05	9.89E+05	5.80E+05	↓	-	-	-	0.758
169	370.9450999	1.89E+05	3.73E+05	6.07E+05	7.72E+05	↑	0.194	0.907	0.4	0.779
75	372.9034148	3.01E+06	2.77E+06	1.45E+06	1.40E+06	↓	0.613	0.485	0.275	0.797
89	373.1982155	0.00E+00	1.81E+05	0.00E+00	5.54E+05	↑	0.097	1	1	0.776
45	374.8746664	1.16E+06	7.20E+05	1.45E+06	1.08E+06	↓	-	-	-	0.758
223	374.9900792	1.20E+06	1.29E+06	1.75E+06	1.23E+06	↑	0.452	0.722	0.341	0.805
38	378.8251053	2.23E+06	1.13E+06	3.67E+06	2.17E+06	↓	-	-	-	0.758
225	379.0393135	3.26E+05	5.62E+05	7.86E+05	9.94E+05	↑	0.226	0.897	0.412	0.784
131	379.9455675	5.78E+05	1.19E+06	9.63E+05	1.31E+06	↑	0.452	0.856	0.5	0.83
209	385.9456179	2.27E+05	4.61E+05	7.06E+05	8.63E+05	↑	0.226	0.897	0.412	0.784
212	392.8852387	1.17E+06	1.60E+06	1.25E+06	1.29E+06	↑	0.452	0.804	0.424	0.821
48	392.9062042	1.52E+06	1.43E+06	1.18E+06	1.31E+06	↓	0.258	0.825	0.32	0.777
135	392.9927234	9.61E+04	2.45E+05	4.15E+05	6.37E+05	↑	0.129	0.979	0.667	0.779
235	397.1274018	1.22E+06	1.21E+06	2.06E+06	1.60E+06	↓	0.452	0.66	0.298	0.79
52	398.8753993	1.11E+06	6.46E+05	2.02E+06	1.39E+06	↓	-	-	-	0.758
216	399.862614	5.64E+05	7.08E+05	1.18E+06	1.06E+06	↑	0.29	0.866	0.409	0.792
110	400.9379077	4.57E+05	6.52E+05	8.91E+05	9.52E+05	↑	0.323	0.825	0.37	0.792
187	401.9041454	4.85E+04	3.24E+05	3.38E+05	7.49E+05	↑	0.161	0.979	0.714	0.785

233	401.9147215	1.47E+06	1.93E+06	1.87E+06	1.21E+06	↑	0.806	0.526	0.352	0.895
243	405.000662	7.80E+05	1.00E+06	1.15E+06	1.14E+06	↑	0.452	0.67	0.304	0.793
230	408.9221852	2.09E+05	3.20E+05	7.16E+05	7.41E+05	↑	0.161	0.918	0.385	0.774
19	410.9199507	1.64E+06	1.07E+06	1.57E+06	1.40E+06	↓	0.032	0.969	0.25	0.758
116	411.9071325	3.07E+05	6.20E+05	7.57E+05	9.96E+05	↑	0.29	0.856	0.391	0.79
220	412.1463854	9.43E+05	1.22E+06	1.47E+06	1.32E+06	↑	0.516	0.68	0.34	0.815
80	414.8413507	1.47E+06	7.51E+05	1.77E+06	1.11E+06	↓	-	-	-	0.758
63	414.8525409	7.28E+05	4.76E+05	1.09E+06	8.99E+05	↓	-	-	-	0.758
68	414.8703841	1.79E+06	1.11E+06	2.22E+06	1.68E+06	↓	-	-	-	0.758
226	415.9222332	1.38E+06	2.16E+06	1.45E+06	1.62E+06	↑	0.742	0.474	0.311	0.852
241	416.8674134	1.47E+06	9.86E+05	2.20E+06	1.70E+06	↓	-	-	-	0.758
181	416.8780538	4.54E+05	6.78E+05	9.61E+05	1.13E+06	↑	0.29	0.825	0.346	0.784
141	416.9038998	7.89E+05	1.06E+06	1.14E+06	1.24E+06	↑	0.452	0.67	0.304	0.793
7	416.936107	7.74E+05	4.33E+05	1.15E+06	8.06E+05	↓	-	-	-	0.758
171	417.0323016	3.17E+05	7.31E+05	7.88E+05	1.01E+06	↑	0.355	0.856	0.44	0.806
122	417.9878313	1.24E+05	3.80E+05	4.87E+05	7.79E+05	↑	0.194	0.959	0.6	0.788
3	418.8102933	4.25E+06	3.55E+06	1.83E+06	2.04E+06	↓	0.032	0.99	0.5	0.762
58	418.9331433	6.99E+05	5.03E+05	1.09E+06	9.41E+05	↓	0.161	0.866	0.278	0.764
218	424.8442351	1.78E+05	3.45E+05	6.03E+05	7.96E+05	↑	0.161	0.938	0.455	0.778
36	425.0293776	1.12E+06	5.26E+05	1.71E+06	1.04E+06	↓	-	-	-	0.758
219	426.9067738	1.54E+06	2.15E+06	1.63E+06	1.75E+06	↑	0.677	0.629	0.368	0.859
204	430.9008325	2.27E+04	2.06E+05	2.23E+05	6.30E+05	↑	0.097	0.99	0.75	0.774
161	432.8702677	6.45E+05	1.16E+06	1.25E+06	1.31E+06	↑	0.419	0.845	0.464	0.82
227	435.9071505	4.55E+05	8.12E+05	9.62E+05	1.13E+06	↑	0.355	0.814	0.379	0.798
234	440.8682797	2.32E+06	2.84E+06	2.28E+06	2.05E+06	↑	0.677	0.505	0.304	0.831
240	441.2532148	5.58E+06	6.20E+06	7.70E+06	6.83E+06	↑	0.871	0.258	0.273	0.862
221	442.8653013	7.63E+05	1.15E+06	1.26E+06	1.24E+06	↑	0.484	0.732	0.366	0.816
190	442.9017812	1.53E+06	2.11E+06	1.64E+06	1.10E+06	↑	0.645	0.66	0.377	0.853
211	443.9512175	5.33E+05	7.87E+05	1.06E+06	1.09E+06	↑	0.355	0.794	0.355	0.794

175	448.8469297	1.16E+06	2.03E+06	1.43E+06	1.43E+06	↑	0.71	0.629	0.379	0.871
57	452.8004743	1.62E+06	8.85E+05	1.76E+06	1.15E+06	↓	-	-	-	0.758
27	452.8263734	6.40E+05	7.15E+04	1.16E+06	3.91E+05	↓	-	-	-	0.758
78	452.9337442	7.51E+05	4.97E+05	1.31E+06	1.05E+06	↓	0.065	0.959	0.333	0.762
213	456.9174466	2.69E+05	5.29E+05	7.79E+05	9.89E+05	↑	0.226	0.907	0.438	0.786
237	457.8682539	4.51E+05	7.31E+05	9.00E+05	1.08E+06	↑	0.29	0.887	0.45	0.796
191	460.8937338	9.05E+05	1.09E+06	1.23E+06	1.15E+06	↑	0.484	0.639	0.3	0.795
164	464.899465	1.15E+06	1.52E+06	1.29E+06	1.25E+06	↑	0.581	0.649	0.346	0.829
238	466.3082054	8.62E+05	1.16E+06	1.66E+06	1.76E+06	↑	0.387	0.784	0.364	0.8
81	466.8339179	2.51E+05	0.00E+00	7.10E+05	0.00E+00	↓	-	-	-	0.758
77	472.8290468	8.38E+05	5.10E+05	1.49E+06	1.11E+06	↓	-	-	-	0.758
118	473.8809276	5.65E+05	1.23E+06	9.80E+05	1.36E+06	↑	0.419	0.845	0.464	0.82
202	474.8947818	2.15E+06	2.23E+06	1.69E+06	1.28E+06	↑	0.742	0.474	0.311	0.852
96	474.9906003	2.37E+05	8.46E+05	6.68E+05	1.09E+06	↑	0.387	0.887	0.522	0.819
199	476.9064531	2.62E+06	3.28E+06	1.44E+06	1.32E+06	↑	0.516	0.732	0.381	0.826
198	478.9574898	1.55E+06	2.09E+06	1.56E+06	1.39E+06	↑	0.645	0.66	0.377	0.853
114	480.9077269	1.54E+05	3.85E+05	5.61E+05	7.87E+05	↑	0.194	0.948	0.545	0.786
140	486.928065	1.96E+05	4.04E+05	6.57E+05	8.35E+05	↑	0.194	0.918	0.429	0.781
149	499.8260416	8.30E+05	9.86E+05	1.30E+06	1.20E+06	↑	0.419	0.691	0.302	0.788
146	500.8708781	1.49E+06	1.75E+06	1.55E+06	1.20E+06	↑	0.71	0.557	0.338	0.857
173	510.7770559	1.03E+06	1.41E+06	1.35E+06	1.35E+06	↑	0.548	0.608	0.309	0.808
55	510.7852623	8.52E+05	3.34E+05	1.16E+06	7.65E+05	↓	-	-	-	0.758
239	512.8831979	2.95E+06	3.73E+06	1.66E+06	1.61E+06	↑	0.258	0.938	0.571	0.798
182	514.8575213	3.98E+05	6.58E+05	8.74E+05	1.06E+06	↑	0.29	0.825	0.346	0.784
106	514.8808046	0.00E+00	1.97E+05	0.00E+00	6.07E+05	↑	0.097	1	1	0.776
111	516.9384462	0.00E+00	1.90E+05	0.00E+00	5.83E+05	↑	0.097	1	1	0.776
107	518.9356053	1.88E+04	2.55E+05	1.84E+05	6.63E+05	↑	0.129	1	1	0.782
154	522.9048788	2.26E+05	5.33E+05	7.87E+05	1.01E+06	↑	0.226	0.918	0.467	0.788
157	528.8603526	7.67E+05	9.13E+05	1.26E+06	1.19E+06	↑	0.387	0.711	0.3	0.784

184	529.3057046	3.61E+05	5.48E+05	1.18E+06	1.19E+06	↑	0.194	0.907	0.4	0.779
231	530.9524307	4.26E+05	6.31E+05	8.90E+05	9.97E+05	↑	0.161	0.948	0.5	0.78
192	536.7413236	8.26E+04	2.57E+05	4.00E+05	6.69E+05	↑	0.129	0.959	0.5	0.775
217	548.8663091	1.34E+06	1.70E+06	1.26E+06	1.13E+06	↑	0.677	0.546	0.323	0.841
86	552.9342862	1.70E+05	5.11E+05	5.69E+05	8.70E+05	↑	0.258	0.928	0.533	0.796
210	554.8502367	1.97E+06	2.32E+06	1.21E+06	1.13E+06	↑	0.774	0.412	0.296	0.851
125	558.8352111	7.89E+04	3.24E+05	3.81E+05	7.40E+05	↑	0.161	0.959	0.556	0.782
188	572.8423337	3.86E+05	6.36E+05	9.08E+05	1.10E+06	↑	0.161	0.969	0.625	0.783
224	586.7681721	6.32E+05	1.01E+06	1.29E+06	1.50E+06	↑	0.323	0.804	0.345	0.788
42	590.5696214	2.36E+06	1.73E+06	2.28E+06	2.08E+06	↓	0.032	0.979	0.333	0.76
99	596.8721179	8.20E+05	1.28E+06	1.24E+06	1.19E+06	↑	0.548	0.701	0.37	0.829
26	598.5936294	9.94E+05	7.19E+05	1.25E+06	1.14E+06	↓	0.129	0.918	0.333	0.767
1	614.5999789	1.86E+06	1.06E+06	1.29E+06	1.19E+06	↓	-	-	-	0.758
71	619.5490379	2.83E+06	2.13E+06	3.16E+06	2.79E+06	↓	0.161	0.856	0.263	0.761
70	621.5460465	1.73E+06	8.17E+05	2.22E+06	1.60E+06	↓	-	-	-	0.758
28	622.6013334	3.06E+06	2.22E+06	1.61E+06	1.21E+06	↓	-	-	-	0.758
207	630.8664939	2.42E+06	2.85E+06	1.68E+06	1.57E+06	↑	0.452	0.763	0.378	0.813
72	631.5609641	2.01E+06	1.42E+06	1.56E+06	1.43E+06	↓	-	-	-	0.758
160	631.603771	4.40E+04	2.70E+05	3.03E+05	7.04E+05	↑	0.129	0.979	0.667	0.779
88	633.6677544	1.26E+05	5.35E+05	4.95E+05	1.00E+06	↑	0.194	0.99	0.857	0.793
170	635.5767742	4.37E+05	6.05E+05	8.96E+05	9.47E+05	↑	0.29	0.814	0.333	0.782
228	638.8327411	2.45E+06	2.77E+06	1.43E+06	1.26E+06	↑	0.806	0.381	0.294	0.86
41	639.5694495	1.26E+06	8.91E+05	1.21E+06	1.15E+06	↓	0.065	0.979	0.5	0.766
193	640.6051548	2.36E+04	1.99E+05	2.31E+05	6.09E+05	↑	0.097	0.99	0.75	0.774
11	641.542341	3.15E+06	2.55E+06	1.62E+06	1.62E+06	↓	0.29	0.722	0.25	0.761
12	647.5296153	2.30E+06	1.18E+06	2.26E+06	2.10E+06	↓	0.032	0.979	0.333	0.76
54	656.6363595	1.50E+06	8.60E+05	1.39E+06	1.19E+06	↓	-	-	-	0.758
22	666.574381	1.59E+06	1.31E+06	1.34E+06	1.30E+06	↓	0.129	0.897	0.286	0.763
46	668.5245926	1.67E+06	9.38E+05	1.76E+06	1.41E+06	↓	0.065	0.938	0.25	0.758

156

119	674.6366835	1.95E+05	4.08E+05	7.33E+05	8.34E+05	↑	0.194	0.928	0.462	0.783
61	680.5834632	1.65E+06	9.73E+05	1.61E+06	1.26E+06	↓	0.032	0.979	0.333	0.76
151	681.5583726	6.80E+05	8.85E+05	1.17E+06	1.12E+06	↑	0.387	0.732	0.316	0.789
29	682.6136219	3.15E+06	2.82E+06	1.26E+06	1.44E+06	↓	0.387	0.794	0.375	0.802
109	685.5492731	8.54E+04	3.56E+05	4.99E+05	8.12E+05	↑	0.161	0.979	0.714	0.785
176	688.8250512	1.72E+06	2.08E+06	1.53E+06	1.50E+06	↑	0.226	0.928	0.5	0.789
14	690.6922866	1.82E+06	9.84E+05	1.63E+06	1.55E+06	↓	0.032	1	1	0.764
53	692.6430023	1.69E+06	1.50E+06	1.15E+06	1.21E+06	↓	0.484	0.629	0.294	0.792
121	699.6329933	1.50E+05	3.33E+05	5.98E+05	7.61E+05	↑	0.161	0.938	0.455	0.778
194	700.5879877	1.16E+05	2.82E+05	5.02E+05	7.36E+05	↑	0.129	0.948	0.444	0.773
117	700.6849543	3.86E+05	7.00E+05	8.77E+05	1.13E+06	↑	0.29	0.835	0.36	0.786
5	706.5667028	2.31E+06	1.85E+06	1.44E+06	1.37E+06	↓	0.032	0.969	0.25	0.758
24	706.6140143	2.31E+06	1.98E+06	1.06E+06	1.23E+06	↓	0.613	0.402	0.247	0.765
47	706.6611412	1.11E+06	4.48E+05	1.49E+06	1.03E+06	↓	-	-	-	0.758
10	709.5625148	1.45E+06	6.95E+05	1.38E+06	1.10E+06	↓	-	-	-	0.758
23	710.6088148	1.80E+06	1.22E+06	1.52E+06	1.39E+06	↓	-	-	-	0.758
31	712.5603074	2.03E+06	1.65E+06	1.29E+06	1.25E+06	↓	0.645	0.412	0.26	0.784
62	714.5571559	2.35E+06	2.09E+06	1.31E+06	1.45E+06	↓	0.323	0.784	0.323	0.784
215	714.6420935	2.12E+06	2.31E+06	1.56E+06	1.41E+06	↑	0.742	0.371	0.274	0.818
195	716.5550866	1.21E+06	1.46E+06	1.33E+06	1.27E+06	↑	0.581	0.598	0.316	0.817
37	720.6564579	2.30E+06	1.91E+06	1.32E+06	1.36E+06	↓	0.613	0.433	0.257	0.778
15	724.6968331	1.41E+06	1.13E+06	1.31E+06	1.28E+06	↓	0.226	0.835	0.304	0.771
91	734.5808827	1.93E+05	4.39E+05	6.51E+05	8.99E+05	↑	0.194	0.938	0.5	0.784
85	739.6726098	1.72E+05	5.05E+05	6.17E+05	9.41E+05	↑	0.226	0.928	0.5	0.789
112	744.6141806	5.32E+05	8.33E+05	9.88E+05	1.13E+06	↑	0.323	0.825	0.37	0.792
4	746.6065017	1.58E+06	1.09E+06	1.29E+06	1.22E+06	↓	-	-	-	0.758
21	757.5398145	1.90E+06	1.29E+06	1.45E+06	1.29E+06	↓	-	-	-	0.758
20	765.5240229	1.93E+06	1.21E+06	1.53E+06	1.37E+06	↓	-	-	-	0.758
179	770.6039593	1.59E+06	2.05E+06	1.54E+06	1.39E+06	↑	0.581	0.619	0.327	0.822

64	774.5075332	4.59E+06	3.44E+06	2.65E+06	1.82E+06	↓	-	-	-	0.758
40	776.5615014	6.52E+05	3.81E+05	1.17E+06	8.72E+05	↓	-	-	-	0.758
168	786.4794632	1.95E+05	3.93E+05	6.69E+05	9.05E+05	↑	0.161	0.959	0.556	0.782
35	794.6308365	3.38E+06	2.73E+06	1.57E+06	1.37E+06	↓	0.032	0.969	0.25	0.758
32	814.5468959	5.45E+06	4.09E+06	2.65E+06	1.95E+06	↓	-	-	-	0.758
60	818.700604	3.44E+06	3.15E+06	1.78E+06	1.72E+06	↓	0.71	0.412	0.278	0.816
177	822.593624	9.18E+05	1.20E+06	1.44E+06	1.26E+06	↑	0.419	0.773	0.371	0.806
25	826.518497	1.58E+06	1.10E+06	1.33E+06	1.34E+06	↓	0.032	1	1	0.764
2	828.5154065	3.73E+06	3.04E+06	1.19E+06	1.52E+06	↓	0.032	0.979	0.333	0.76
6	832.5099989	2.29E+06	1.83E+06	1.31E+06	1.36E+06	↓	0.032	0.99	0.5	0.762
13	838.6176053	1.82E+06	9.89E+05	1.39E+06	1.27E+06	↓	-	-	-	0.758
9	844.4925207	1.88E+06	1.36E+06	1.72E+06	1.65E+06	↓	0.065	0.948	0.286	0.76
65	846.4821352	1.73E+06	1.47E+06	1.58E+06	1.61E+06	↓	0.065	0.969	0.4	0.764
130	848.4754866	0.00E+00	2.67E+05	0.00E+00	8.27E+05	↑	0.097	1	1	0.776
197	848.4794415	2.46E+06	2.79E+06	1.67E+06	1.24E+06	↑	0.903	0.247	0.277	0.889
138	858.8514895	4.00E+05	1.01E+06	1.78E+06	2.87E+06	↑	0.097	0.99	0.75	0.774
17	880.4944595	2.29E+06	1.75E+06	1.53E+06	1.34E+06	↓	-	-	-	0.758
82	898.5465822	2.52E+04	2.92E+05	2.47E+05	7.59E+05	↑	0.129	0.99	0.8	0.78
203	912.5555415	3.97E+05	7.89E+05	1.14E+06	1.72E+06	↑	0.194	0.897	0.375	0.777
133	916.5499487	4.65E+05	6.59E+05	1.03E+06	1.13E+06	↑	0.258	0.856	0.364	0.783

6.2 Instruments and Materials

Name	Manufacturer
12 T superconducting magnet	Magnex scientific Inc., Varian Inc., Oxford, UK
AchE fluorescence activity Kit	Arbor Assays, Michigan, USA
Acquity UPLC system	Waters, Milford, USA
AminoPac PA10 Analytical (2x250 mm)	Thermo Fisher Scientific, Ulm, Germany
AminoPac PA10 Guard (2x50 mm)	Thermo Fisher Scientific, Ulm, Germany
AS-11 (4x250 mm)	Thermo Fisher Scientific, Ulm, Germany
Apollo II (ESI source)	Bruker Daltonics, Bremen, Germany
BEH C18-column (1x150 mm)	Waters, Milford, Germany
Capillary (85 cm x 50 µm ID)	CS-Chromatographie Service GmbH, Langerwehe, Germany
Centrifuge 5702R	Eppendorf AG, Hamburg, Germany
ECOLab glass column (10x750 mm)	YMC Europe GmbH, Dinslaken, Germany
Element2 (ICP-sf-MS)	Thermo Fisher Scientific, Ulm, Germany
ESI-FAST system (SC-E2 DXS PC^3)	Elemental Scientific, Omaha, USA
hSyn total ELISA	Analytik Jena, Jena, Germany
Dionex ICS 5000 equipped with: VWD detector, AS AP autosampler,	Thermo Fisher Scientific, Ulm, Germany

DP pump system	
MaXis (QqTof-MS)	Bruker Daltonics, Bremen, Germany
NexIon 300D (ICP-MS)	Perkin Elmer, Rodgau, Germany
Smartline 1100 inert series equipped with: pump 1000, manager 5000, dynamic mixing chamber, manual injection port, UV detector 2600	Knauer, Berlin, Germany
solariX (FT-ICR-MS)	Bruker Daltonics GmbH, Bremen, Germany
Sonic bath	Bandelin Sonorex
PEEK column (8x250 mm)	Dionex, Idstein, Germany
Plate reader Safire2	Tecan, Crailsheim, Germany
PrinCE 706	Prince Technologies B.V., Emmen, Netherlands
Toyopearl HW 40/55 S (SEC material)	TasoHaas, Stuttgart, Germany
Vortex Genie 2	Scientific Industry

6.3 Chemicals

Name	Manufacturer
Acetic acid (100%)	Carl Roth, Karlsruhe, Germany
Acetonitrile (Chromasolv)	Sigma-Aldrich, Steinheim, Germany

Alanine (L-form, > 99.5%)	Fluka Analytical, Steinheim, Germany
(D/L-form)	Sigma-Aldrich, Steinheim, Germany
Ammonia (25%)	Merck, Darmstadt, Germany
Ammonium acetate (HPLC-grade, 99%)	Fisher Scientific, Loughborough, UK
Arginase (≥ 70%)	Sigma-Aldrich, Steinheim, Germany
Arginine (L-form, ≥ 99.5%)	Fluka Analytical, Steinheim, Germany
(D-form)	Sigma-Aldrich, Steinheim, Germany
Argon (liquid)	Air Liquide, Düsseldorf, Germany
Asparagine (D/L-form)	Sigma-Aldrich, Steinheim, Germany
Aspartic acid (D/L-form)	Sigma-Aldrich, Steinheim, Germany
β-Lactoglobulin (90%)	Sigma-Aldrich, Steinheim, Germany
Boric acid	Sigma-Aldrich, Steinheim, Germany
Citric acid (monohydrate)	AppliChem, Darmstadt, Germany
Cu-standard solution (1000 mg/L)	Perkin Elmer Pure Plus, Rodgau, Germany
Cysteine	Sigma-Aldrich, Steinheim, Germany
Fe-standard solution (1000 µg/mL)	Perkin Elmer Pure Plus, Rodgau, Germany
FeCl2 · 4 H_2O	AppliChem, Darmstadt, Germany
FeCl$_3$ (98%)	Merck, Darmstadt, Germany
Ferritin	Sigma-Aldrich, Steinheim, Germany

γ-Globulin	SERVA Electrophoresis, Heidelberg, Germany
Glutamic acid (L-form, ≥ 98.5%) **(D/L-form)**	Sigma-Aldrich, Steinheim, Germany
Glutamine (L-form, ≥ 99.5%) **(D-form)**	Fluka Analytical, Steinheim, Germany Sigma-Aldrich, Steinheim, Germany
Glycine (> 99%)	Sigma-Aldrich, Steinheim, Germany
GSH (98%)	Sigma-Aldrich, Steinheim, Germany
GSSG	
HCl (37%)	AppliChem, Darmstadt, Germany
Histidine (D/L-form, > 99%)	Sigma-Aldrich, Steinheim, Germany
HSA (96-99%)	Sigma-Aldrich, Steinheim, Germany
IBDC	Sigma-Aldrich, Steinheim, Germany
Isoleucine (D/L-form, ≥ 98.5%)	Sigma-Aldrich, Steinheim, Germany
Leucine (L-form, ≥ 99.5%) **(D-form)**	Fluka Analytical, Steinheim, Germany Sigma-Aldrich, Steinheim, Germany
Lysine (L-form, ≥ 98%) **(D-form)**	Sigma-Aldrich, Steinheim, Germany
MeOH (99.9%)	Merck, Darmstadt, Germany
MeOH (Chromasolv)	Sigma-Aldrich, Steinheim, Germany
Methionine (L-form, 99.5%) **(D-form)**	Sigma-Aldrich, Steinheim, Germany

Mg-standard solution (10,000 µg/mL)	Perkin Elmer Pure Plus, Rodgau, Germany
Milli-Q-water (18.2 mΩcm)	Merck-Millipore, Darmstadt, Germany
Mn-standard solution (1000 mg/L)	Perkin Elmer Pure Plus, Rodgau, Germany
NaAc (99.9%)	Fisher Scientific, Loughborough, UK
NaOH (50%)	Merck, Darmstadt, Germany
Ni-standard solution (1000 mg/L)	Perkin Elmer Pure Plus, Rodgau, Germany
Norleucine	Sigma-Aldrich, Steinheim, Germany
o-phthalaldehyde	Sigma-Aldrich, Steinheim, Germany
Phenylalanine (L-form, ≥ 98.5%) **(D-form)**	Sigma-Aldrich, Steinheim, Germany
Proline (L-form, ≥ 98.5%)	Sigma-Aldrich, Steinheim, Germany
Rh-standard solution (10 µg/mL)	Perkin Elmer Pure Plus, Rodgau, Germany
Sec (D/L-form)	Sigma-Aldrich, Steinheim, Germany
SeM (D/L-form)	Sigma-Aldrich, Steinheim, Germany
Serine (L-form, ≥ 99.5%) **(D/L-form)**	Fluka Analytical, Steinheim, Germany Sigma-Aldrich, Steinheim, Germany
Sr-standard solution (1000 mg/L)	Perkin Elmer Pure Plus, Rodgau, Germany

Threonine (L-form, ≥ 99%)	Fluka Analytical, Steinheim, Germany
(D-form)	Sigma-Aldrich, Steinheim, Germany
Tetramethylammonium hydroxide (TMAH, 25%)	Fisher Scientific, Loughborough, UK
Transferrin (98%)	Sigma-Aldrich, Steinheim, Germany
Tris(hydroxymethyl)aminomethane (Tris, 99.9%)	Carl Roth, Karlsruhe, Germany
Tryptophan (L-form)	Sigma-Aldrich, Steinheim, Germany
(D-form)	
Tyrosine (L-form, ≥ 99%)	Fluka Analytical, Steinheim, Germany
(D-form)	Sigma-Aldrich, Steinheim, Germany
Valine (L-form, ≥ 99.5%)	Fluka Analytical, Steinheim, Germany
(D/L-form)	Sigma-Aldrich, Steinheim, Germany
Zn-standard solution (1000 mg/L)	Perkin Elmer Pure Plus, Rodgau, Germany

Eidesstaatliche Erklärung

Ich erkläre an Eides statt, dass ich die bei der promotionsführenden Einrichtung TUM School of Life Sciences der Technischen Universität München zur Promotionsprüfung vorgelegte Arbeit mit dem Titel:

Investigations of changes of the metallome and metabolome as a cause for neurodegeneration: Application of combines speciation and metabolomics techniques

In Chemie am Lehrstuhl für Analytische Lebensmittelchemie unter der Anleitung und Betreuung durch apl.-Prof. Dr. Philippe Schmitt-Kopplin ohne sonstige Hilfe erstellt und bei der Abfassung nur die gemäß § 6 Abs. 6 und 7 Satz 2 angegebenen Hilfsmittel benutzt habe.

(x) Ich habe keine Organisation eingeschaltet, die gegen Entgelt Betreuerinnen und Betreuer für die Anfertigung von Dissertationen sucht, oder die mir obliegenden Pflichten hinsichtlich der Prüfungsleistungen für mich ganz oder teilweise erledigt.

(x) Ich habe die Dissertation in dieser oder ähnlicher Form in keinem anderen Prüfungsverfahren als Prüfungsleistung vorgelegt.

(x) Ich habe den angestrebten Doktorgrad noch nicht erworben und bin nicht in einem früheren Promotionsverfahren für den angestrebten Doktorgrad endgültig gescheitert.

Die öffentlich zugängliche Promotionsordnung der TUM ist mir bekannt, insbesondere habe ich die Bedeutung von § 28 (Nichtigkeit der Promotion) und § 29 (Entzug des Doktorgrades) zur Kenntnis genommen. Ich bin mir der Konsequenzen einer falschen Eidesstattlichen Erklärung bewusst.

Mit der Aufnahme meiner personenbezogenen Daten in die Alumni-Datei bei der TUM bin ich nicht einverstanden.